

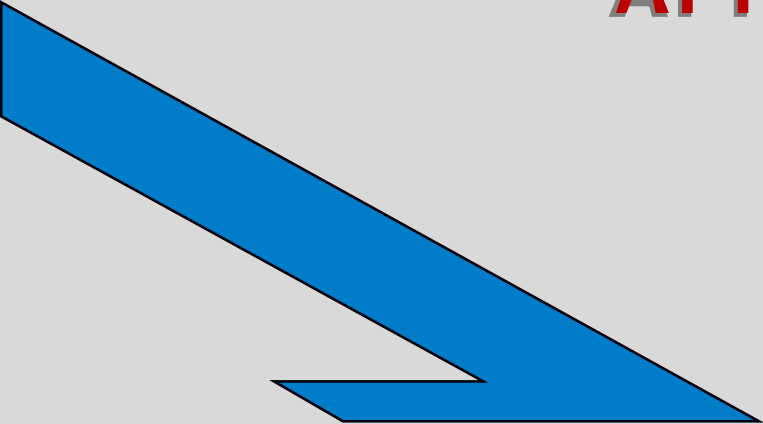


I T H E A



International Journal

**INFORMATION THEORIES
&
APPLICATIONS**



2010 Volume 17 Number 1



International Journal
INFORMATION THEORIES & APPLICATIONS
Volume 17 / 2010, Number 1

Editor in chief: Krassimir Markov (Bulgaria)

International Editorial Staff

Chairman: Victor Gladun (Ukraine)

Adil Timofeev	(Russia)	Koen Vanhoof	(Belgium)
Aleksey Voloshin	(Ukraine)	Krassimira Ivanova	(Bulgaria)
Alexander Eremeev	(Russia)	Levon Aslanyan	(Armenia)
Alexander Kleshchev	(Russia)	Luis F. de Mingo	(Spain)
Alexander Palagin	(Ukraine)	Martin P. Mintchev	(Canada)
Alfredo Milani	(Italy)	Nikolay Zagoruiko	(Russia)
Anatoliy Shevchenko	(Ukraine)	Peter Stanchev	(Bulgaria)
Arkadij Zakrevskij	(Belarus)	Plamen Mateev	(Bulgaria)
Avram Eskenazi	(Bulgaria)	Rumyana Kirkova	(Bulgaria)
Boris Fedunov	(Russia)	Stefan Dodunekov	(Bulgaria)
Constantine Gaindric	(Moldavia)	Tatyana Gavrilova	(Russia)
Eugenia Velikova-Bandova	(Bulgaria)	Vasil Sgurev	(Bulgaria)
Frank Brown	(USA)	Vitaliy Lozovskiy	(Ukraine)
Galina Rybina	(Russia)	Vitaliy Velichko	(Ukraine)
Georgi Gluhchev	(Bulgaria)	Vladimir Donchenko	(Ukraine)
Ilia Mitov	(Bulgaria)	Vladimir Jotsov	(Bulgaria)
Juan Castellanos	(Spain)	Vladimir Lovitskii	(GB)

International Journal "INFORMATION THEORIES & APPLICATIONS" (IJ ITA)
is official publisher of the scientific papers of the members of
the ITHEA International Scientific Society

IJ ITA welcomes scientific papers connected with any information theory or its application.

IJ ITA rules for preparing the manuscripts are compulsory.

The rules for the papers for IJ ITA as well as the subscription fees are given on www.foibg.com/ijita.

Responsibility for papers published in IJ ITA belongs to authors.

General Sponsor of IJ ITA is the Consortium FOI Bulgaria (www.foibg.com).

International Journal "INFORMATION THEORIES & APPLICATIONS" Vol. 17, Number 1, 2010

Printed in Bulgaria

Edited by the Institute of Information Theories and Applications FOI ITHEA, Bulgaria, in collaboration with:

V.M.Glushkov Institute of Cybernetics of NAS, Ukraine,
Institute of Mathematics and Informatics, BAS, Bulgaria,
Universidad Politécnica de Madrid, Spain.

Publisher: ITHEA

Sofia, 1000, P.O.B. 775, Bulgaria. www.ithea.org, www.foibg.com, e-mail: info@foibg.com

Copyright © 1993-2010 All rights reserved for the publisher and all authors.

© 1993-2010 "Information Theories and Applications" is a trademark of Krassimir Markov

ISSN 1310-0513 (printed)

ISSN 1313-0463 (online)

ISSN 1313-0498 (CD/DVD)

ON STRUCTURAL RECOGNITION WITH LOGIC AND DISCRETE ANALYSIS

Levon Aslanyan, Hasmik Sahakyan

Abstract: *The paper addresses issues of special style structuring of learning set in pattern recognition area. Above the regular means of ranking of objects and properties, which also use the structure of learning set, the logic separation hypotheses is treated over the multi value features area, which structures the learning set and tries to recover more valuable relations for better recognition. Algorithmically the model is equivalent to constructing the reduced disjunctive normal form of Boolean functions. The multi valued case which is considered is as harder as the binary case but it uses approximately the same structures.*

Keywords: *Learning, Boolean function, logic separation.*

ACM Classification Keywords: *F.2.2 Nonnumerical Algorithms and Problems: Computations on discrete structures*

Introduction

Pattern recognition undergoes an important developing for many years. As a research area this is not uni-modular like classic mathematical sciences, it has a long history of establishment. Inside the theory there are a number of sub disciplines such as – feature selection, object and feature ranking, analogy measures, supervised and unsupervised classification, etc. The same time pattern recognition is indeed an integrated theory studying object descriptions and their classification models. This is a collection of mathematical, statistical, heuristic and inductive techniques of fundamental role in executing the intellectual tasks, typical for a human being, – but on computers.

In many applied problems with multidimensional experimental data the object description is often non-classical, that is, - not exclusively in terms of only numerical or only categorical features, but simultaneously by both kinds of values. Sometimes, the missing value is introduced so that finally we deal with *mixed and incomplete* descriptions of objects as elements of Cartesian product of feature values, without any algebraic, logical or topological properties assumed in applied area. How then, do we select in these cases the most informative features, classify a new object given a (*training*) sample or find the relationships between all objects based on a certain measure of similarity? Logic Combinatorial Algebraic Pattern Recognition is a research area formed since 70's, that uses a mix of discrete descriptors – and similarities, separation, frequencies, integration and corrections, optimization, and solves the whole spectrum of pattern recognition tasks.

This approach is originated by the work [Dmitriev et al, 1966] that transfers the engineering domain technique of tests for electrical schemes [Chegis, Yablonskii, 1958] to the feature selection and object classification area. The applied task of [Dmitriev et al, 1966] is prognosis for mineral resources. In a basic model authors consider that all features are Boolean. Later formal extensions with different kinds of features appeared, as we do it below for the logic separation analysis. Consider the general form of learning set data, L :

FEATURES					
OBJECTS	x_1	x_2	...	x_n	CLASSES
\tilde{a}_1^1	a_{11}^1	a_{12}^1	...	a_{1n}^1	C_1
\tilde{a}_2^1	a_{21}^1	a_{22}^1	...	a_{2n}^1	
...					
$\tilde{a}_{l_1}^1$	$a_{l_1 1}^1$	$a_{l_1 2}^1$...	$a_{l_1 n}^1$	
...					C_m
\tilde{a}_1^m	a_{11}^m	a_{12}^m	...	a_{1n}^m	
\tilde{a}_2^m	a_{21}^m	a_{22}^m	...	a_{2n}^m	
...					
$\tilde{a}_{l_m}^m$	$a_{l_m 1}^m$	$a_{l_m 2}^m$...	$a_{l_m n}^m$	

Features x_1, x_2, \dots, x_n are categorical or numerical properties represented by their domains of values M_1, M_2, \dots, M_n . Categorical feature takes values from a set $H_t^s = \{s_1, s_2, \dots, s_t\}$. Numerical features are from metric spaces assuming the following two types:

- $H_{k,r}^z \equiv \{k, k+1, \dots, r\}$, where k, r are nonnegative integers, and $k < r$,
- $H_{k,r}^r \equiv \{\alpha : \alpha \in (k, r)\}$, where (k, r) is an interval on the real number line, and $k < r$.

Distances between the space elements are usual (numerical). This choice of primary/elementary attribute spaces reflects the common/usual situation that exists in application areas of pattern recognition and classification tasks. A space M in which metric spaces $M_i, i = 1, \dots, n$, are of H_t^s , $H_{k,r}^z$ and/or $H_{k,r}^r$ types, we call n dimensional attribute space.

Test (testor) theory [Dmitriev et al, 1966] is based on a restriction of feature sets and learning elements - with preservation of the basic learning set property - preservation of membership to different classes. A features subset $T = \{x_{i_1}, x_{i_2}, \dots, x_{i_k}\}$ is called a testor of L , if projection of L on T keeps the classes nonintersecting (learning set property). The testor is irreducible when no one x_{i_j} feature may be eliminated with conservation of the learning set property. Further a feature ranking is made taking into consideration the frequency of belonging x_{i_j} to the testors (irreducible testors). Other measure is introduced taking into account frequency of testors on classes. Testor based supervised classification algorithms are constructed by use of frequency similarity measures. Which is the structural property used from the learning set? This is the pair wise difference of learning set elements from different classes (learning set property). We may suppose that this is part or consequence of the well accepted compactness hypothesis.

On formal basis testor technology is well visible on binary tables. Now it is known that constructing all irreducible testors is an NP hard problem. Approximations are studied as well. There is a high similarity with association rule mining models, especially in part of learning of monotone set structures - be it with frequent itemsets in associative rule mining or irreducible tests and testers in this theory.

Consider n -vector $\vec{\tau} = (\tau_1, \tau_2, \dots, \tau_n)$, that indicates the types of elementary attribute spaces of space M . In further consideration without loss of generality we may suppose that $\tau_j \in \{z, r\}$ (this may be coded by binary 0,1

values). Hence $M = H_{c_1, d_1}^{\tau_1} \times H_{c_2, d_2}^{\tau_2} \times \dots \times H_{c_n, d_n}^{\tau_n}$. Then the space M can be adjusted by a pair of n -vectors $\tilde{c} = (c_1, c_2, \dots, c_n)$ and $\tilde{d} = (d_1, d_2, \dots, d_n)$ above the $\tilde{\tau} = (\tau_1, \tau_2, \dots, \tau_n)$. n -dimensional attribute space \tilde{M} is called sub-space of M , if its each metric sub-space $\tilde{M}_i, i = 1, \dots, n$ is a sub-space of corresponding to it in M , metric space $M_i, i = 1, \dots, n$. Obviously such space \tilde{M} can be presented by a pair of vectors $\tilde{c}' = (c'_1, \dots, c'_n)$, $\tilde{d}' = (d'_1, \dots, d'_n)$, where $c'_i \geq c_i$ and $d'_i \leq d_i, i = 1, \dots, n$. We call the number of positions with $c'_i \neq d'_i$ the dimension of \tilde{M} .

[Vaitsvaig, 1973] formulated one of the basic concept in pattern recognition – the KORA algorithm. KORA is constructing elementary conjunctions that intersect with only one class C_i of learning set L . Contrary, [Aslanyan, 1975] considers all irreducible conjunction forms that intersects with only one class C_i of learning set L . This is not the generating idea of this work but is the consequence of the Logic Separation Principle. It is to think, that the Logic Separation Principle is some kind of completion of the well known Compactness hypotheses. The work [Aslanyan, 1975], factually for the first time, is considering learning set elements in a non separated/isolated manner. The concept is used that an element spreads its "similarity", reduced with distance measure of course, which interrupts facing the different class object. An extension may consider not only pairs of learning set elements – one spreading the similarity measure and the second interrupting that - but also arbitrary subsets/fragments of learning set. Several comments: logically, it is evident that the best learning algorithm must be suited best to the learning set itself (at least the learning set is reconstructable by the information on learning set used by algorithm). This also may use the recognition hypothesis when available. The same learning set fragments play a crucial role in estimating the choice of algorithm by the given learning data. The technical solution of Logical Separation (LS) is by Reduced Disjunctive Normal Forms (RDNF), which answers to all issues, - implementation, complexity, interpretation. Further is important to mention that advanced data mining technique IREP (Incremental Reduced Error Pruning) finds its theoretical interpretation in terms of LS framework mentioned above.

Sub-spaces of M we will also call intervals of M . Similarly to the testor theory the irreducible subspace cover technology is well visible on binary tables. The mentioned two visible formalisms, in addition to the basic principles by Yu. Zhuravlev [Dmitriev et al, 1966], that appeared in early 70's, present the basics of Logic Combinatorial Algebraic Pattern Recognition research area.

Formal extensions

This point considers the LS model with similarity spread and interruption by learning set elements. We try to extend the basic constructions to the case of complicated attribute spaces. Let us introduce partially defined characteristic functions $f_i(x_1, x_2, \dots, x_n), i = 1, \dots, m$, which separate some class L_i from the rest of classes, $L_j, j \neq i, j = 1, \dots, n$. The separation is based on the information about the classification given by subsets $L_i, i = 1, \dots, m$ in learning set.

$$\tilde{f}_i = f(\alpha_1, \alpha_2, \dots, \alpha_n) = \begin{cases} 1, & \text{if } \tilde{\alpha} \in L_i \\ 0, & \text{if } \tilde{\alpha} \in L \setminus L_i \\ \text{undefined}, & \text{if } \tilde{\alpha} \in M \setminus L \end{cases}$$

This system of m partly defined functions will be considered in an analogous way to the class of the algebra of logic (Boolean) functions. For system \tilde{f}_i , $i = 1, \dots, m$ we will use analogous constructions [Yablinskii, 1958], to the concepts that are well known for functions of the algebra of logic.

The subspace \tilde{M} of M we call an interval of the function $\tilde{f}_i(x_1, \dots, x_n)$ if

- 1) $\tilde{M} \subseteq M \setminus \bigcup_{j \neq i} L_j$
- 2) $\tilde{M} \cap L_i \neq \emptyset$

Let \tilde{U} be an interval of $\tilde{f}_i(x_1, \dots, x_n)$. Then \tilde{U} is called the maximal interval if there is no other interval \tilde{V} of $\tilde{f}_i(x_1, \dots, x_n)$, such that $\tilde{V} \supset \tilde{U}$.

We denote by U_i , $i = 1, \dots, p_i$ the set of all maximal intervals of $\tilde{f}_i(x_1, \dots, x_n)$. By analogy to the similar constructions of the algebra of logic, we call the set of U_i reduced interval normal form /or interval cover form/ of $\tilde{f}_i(x_1, \dots, x_n)$.

Further, for each function $\tilde{f}_i(x_1, \dots, x_n)$, $i = 1, \dots, m$ we need to construct U_i , - the set of its all maximal intervals. This question is addressed by [Aslanyan, 1975] in the particular case when $M_i \equiv H_{0,1}^z$, $i = 1, \dots, m$.

Other methods designed for the mentioned constructions in the class of the algebra of logic are given in [Yablinskii, 1958] /for k -valued logic/. But the learning set L in our tasks is very specific – it consists of a finite and very low number of points, and therefore growing type methods analogous to those given in [Yablinskii, 1958] for constructing reduced interval forms, are less efficient than the step by step constructions given by sets L_i , $i = 1, \dots, m$. Notice also that if among the metric spaces M_i there exists a space of the type $H_{k,r}^r$, then the direct use of methods from [Yablinskii, 1958] is simply impossible. Below we describe the geometric constructions that appear in step by step procedures for reduced interval covers of systems of partial separation functions. Our goal is to demonstrate that there is a high similarity with the binary case with additions, that constructed intervals are accompanied with small size descriptive data.

Reduced interval covers of systems of partial separation functions

Before starting to construct reduced interval forms U_i of $\tilde{f}_i(x_1, x_2, \dots, x_n)$ let us assume that intervals $\{k, r\}$ of individual directions defined above /specifically the real value case/ include their endpoints in a following way: point is inclusive iff it is a boarder point of corresponding M_i and doesn't match to one of the considered vertices of the learning set. Different coding is possible. For $H_{k,r}^z$ we may use the instant intervals, - all end points included. For $H_{k,r}^r$ we use the scheme that the end point is an exclusive real value. We need this for only internal point indication, and end points of M_i are always inclusive when doesn't match to one of the considered vertices of learning set. Algorithmically, exclusive end point is very easy to code – the use of negative value of corresponding coordinate may code this case.

Thus we consider functions $\tilde{f}_i(x_1, \dots, x_n)$ which separate the sets L_i from the complementary sets L_j , $j \neq i$, $j = 1, \dots, m$. Construct sets U_i - the sets that consist of corresponding maximal intervals. Let $\tilde{\beta}_1, \tilde{\beta}_2, \dots, \tilde{\beta}_k$ be points of M , that belong to L_j , $j \neq i$, $j = 1, \dots, m$, where $k_i = m - (m_i - m_{i-1})$. Let $\tilde{\gamma}_1, \tilde{\gamma}_2, \dots, \tilde{\gamma}_n$ be points

of L_i , where $r_i = m_i - m_{i-1}$ (m_i are defined by table of learning set given above as the last enumerated index in the class L_i).

In general we are given also the point $\tilde{\alpha} = (\alpha_1, \alpha_2, \dots, \alpha_n) \in M$ that is to be recognized/arranged into one of the classes $C_i, i = 1, \dots, m$.

Consider the first point $\tilde{\beta}_1 = (\beta_{11}, \beta_{12}, \dots, \beta_{1n})$. Then an interval \tilde{U} will be maximal out of $\{\tilde{\beta}_1\}$ if and only if at least one of its elementary intervals $\{c'_i, d'_i\}, i = 1, \dots, n$ has no intersection with the corresponding β_{1i} , and all these intervals are maximal in $\{c_i, d_i\}$ out of the corresponding β_{1i} . Besides, it is clear that all but one elementary intervals from $\{c'_i, d'_i\}, i = 1, \dots, n$ should be coincide with the corresponding $\{c_i, d_i\}$, and the presence of exactly one interval $\{c'_i, d'_i\}$ which does not contain β_{1i} , - is sufficient. Let s_1, \dots, s_k be the coordinates of $\tilde{\beta}_1$ such that the following relations take place simultaneously: $\beta_{1s_j} \neq c_{s_j}$ and $\beta_{1s_j} \neq d_{s_j}$ for $j = 1, \dots, k$. Let s_{k+1}, \dots, s_n - are the rest of coordinates of $\tilde{\beta}_1$. In accordance with the reasoning above, we make the following table for maximal intervals after $\tilde{\beta}_1$:

$$\begin{aligned} & \{c_{11}, d_{11}\}, \{c_{12}, d_{12}\}, \dots, \{c_{1n}, d_{1n}\} \\ & \dots \\ & \{c_{\nu 1}, d_{\nu 1}\}, \{c_{\nu 2}, d_{\nu 2}\}, \dots, \{c_{\nu n}, d_{\nu n}\} \end{aligned}$$

Here several cases are possible. $\nu = 1$ and $c_{1i} = c_i, d_{1i} = d_i, i = 1, \dots, n$ if $\tilde{\beta}_1$ doesn't prick interval \tilde{U} . This is when at least in one direction, β_{1i} is out of $\{c_i, d_i\}$ or when β_{1i} is the repeated (or boarder) point. This case is not possible in step 1 but can appear later in iterations. Other special cases appear when \tilde{U} became one dimensional. The general construction is as follows in supposition that \tilde{U} is of dimension n :

$$c_{tr} = \begin{cases} \begin{cases} c_{s_j} & \text{for } t = 2j - 1 \text{ and } r = s_j \text{ if } \tau_{s_j} = 0 \\ \beta_{1s_j} + 1 & \text{for } t = 2j \text{ and } r = s_j \text{ if } \tau_{s_j} = 0 \\ c_{s_j} & \text{for } t = 2j - 1 \text{ and } r = s_j \text{ if } \tau_{s_j} = 1 \\ \beta_{1s_j} & \text{for } t = 2j \text{ and } r = s_j \text{ if } \tau_{s_j} = 1 \end{cases} \\ j = 1, \dots, k \\ \begin{cases} c_{s_j} & \text{for } t = k + j \text{ and } r = s_j \text{ if } d_{s_j} = \beta_{1s_j} \\ c_{s_j} + 1 & \text{for } t = k + j \text{ and } r = s_j \text{ if } c_{s_j} = \beta_{1s_j} \end{cases} \\ j = k + 1, \dots, n \end{cases}$$

$$d_{tr} = \begin{cases} \begin{cases} \beta_{1s_j} - 1 & \text{for } t = 2j - 1 \text{ and } r = s_j \text{ if } \tau_{s_j} = 0 \\ d_{s_j} & \text{for } t = 2j \text{ and } r = s_j \text{ if } \tau_{s_j} = 0 \\ \beta_{1s_j} & \text{for } t = 2j - 1 \text{ and } r = s_j \text{ if } \tau_{s_j} = 1 \\ d_{s_j} & \text{for } t = 2j \text{ and } r = s_j \text{ if } \tau_{s_j} = 1 \end{cases} \\ j = 1, \dots, k \\ \begin{cases} d_{is_j} - 1 & \text{for } t = k + j \text{ and } r = s_j \text{ if } d_{s_j} = \beta_{1s_j} \\ d_{s_j} & \text{for } t = k + j \text{ and } r = s_j \text{ if } c_{s_j} = \beta_{1s_j} \end{cases} \\ j = k + 1, \dots, n \end{cases}$$

It is easy to check that the rows of the constructed above table are all maximal intervals in M out of the point $\tilde{\beta}_1$. For s_{k+1}, \dots, s_n just change of the code sign on positive coordinates is applied. Assume that we have constructed a table whose rows are all maximal intervals in M out of $\{\tilde{\beta}_1, \tilde{\beta}_2, \dots, \tilde{\beta}_{i-1}\}$. Then for constructing an analogous table specifying the set $S_{\{\tilde{\beta}_1, \tilde{\beta}_2, \dots, \tilde{\beta}_i\}}$, it is sufficient to do the following: for each row of constructed in the previous stage table that specifies the maximal intervals of M out of $\{\tilde{\beta}_1, \tilde{\beta}_2, \dots, \tilde{\beta}_{i-1}\}$, we construct the set of its maximal subintervals out of $\tilde{\beta}_i$, - and list them as strokes of corresponding tables. It is easy to check that among the maximal intervals out of $\{\tilde{\beta}_1, \tilde{\beta}_2, \dots, \tilde{\beta}_{i-1}\}$, those that have no intersection with $\tilde{\beta}_i$, will not be changed, and thus the construction of subintervals out of $\tilde{\beta}_i$ is similar to the construction of maximal intervals of M out of $\tilde{\beta}_1$ given in the first step, and because instead of M we can deal with an interval which is maximal out of $\{\tilde{\beta}_1, \tilde{\beta}_2, \dots, \tilde{\beta}_{i-1}\}$, and instead of $\tilde{\beta}_1$ we take $\tilde{\beta}_i$. We take into consideration the dimension and fixed coordinates of current interval to prick. It is worth to mention that all new intervals that we get in i th step, are pair wise different and are not contained in each other. Therefore for the final construction of $S_{\{\tilde{\beta}_1, \tilde{\beta}_2, \dots, \tilde{\beta}_i\}}$ all we have to do is to remove from the set of all constructed intervals, those intervals constructed in i th step, which are included in others. The algorithm is complete.

Further, for recognition, we will consider the sets $S_i(\tilde{\gamma}_i)$ and $S_i(\tilde{\alpha}, \tilde{\gamma}_i)$ of all maximal intervals of M out of $\{\tilde{\beta}_1, \tilde{\beta}_2, \dots, \tilde{\beta}_i\}$ passing trough the points $\tilde{\gamma}_i$ and $\tilde{\alpha}$ and $\tilde{\gamma}_i$ respectively. The construction of these sets $S_i(\tilde{\gamma}_i)$ and $S_i(\tilde{\alpha}, \tilde{\gamma}_i)$ can be done either in an analogue way as the construction of S_i , or they might be derived from S_i by choosing those maximal intervals that pass trough the points $\tilde{\gamma}_i$ and $\tilde{\alpha}$ and $\tilde{\gamma}_i$ respectively.

Let $\tilde{u} = (u_1, u_2, \dots, u_n)$ is a point from M , where each coordinate u_i is equal either to c_i or to d_i . There are 2^n such points assuming that $c_i \neq d_i, i = 1, \dots, n$. Let $\tilde{u}_1, \tilde{u}_2, \dots, \tilde{u}_{2^n}$ denote these points. We call them corner/angular points of M . Let $\tilde{\alpha} \in M$. We consider intervals of the form $\tilde{U}(\tilde{\alpha}, \tilde{u}_i)$, $i = 1, \dots, 2^n$ in M . We call them intervals of directions \tilde{u}_i , outgoing from the point $\tilde{\alpha}$. Such way we get in M a system of independent directions, - outgoing from $\tilde{\alpha}$, which simplifies the study of such point $\tilde{\alpha}$. This study is fallen into iterations, studying the corresponding pictures/situations in spaces $\tilde{U}(\tilde{\alpha}, \tilde{u}_i)$, $i = 1, \dots, 2^n$, where $\tilde{\alpha}$ itself is a corner point of these spaces.

Clearly the above constructions are valid for any subspace (intervals) of M . These are useful also for studying S_i sets of maximal intervals of the function \tilde{f}_i , $i = 1, \dots, m$, as well as for discovering interrelations of points of M and constructions given by the sets S_i .

Conclusion

The description above is an attempt to interlink several basic ideas of Logic Combinatorial pattern recognition. In the point of view given it appears that ideas are around the recovering more valid relations in the learning set. Learning set (plus the global hypotheses is there is one) is the only information about the classes and its best use is related to selecting its characteristic fragments and constructing the classification algorithms on this basis. Two examples considered are the testor scheme with pair of elements from different classes that are different, and logic separation with similarity spread – interruption fragment. These basic ideas were further initiated as the associated rule generation and incremental reduced error pruning schemes in Data Mining theory. After this

methodological discussion the paper gives the algorithm of constructing the reduced interval covers for systems of discrete functions that just demonstrate the complexity of tasks and the similarity with the binary case.

Bibliography

- [ChegisYablonskii, 1958] Chegis I. A. and Yablonskii S. V., Logical Methods for controlling electrical systems, Proceedings of Mathematical Institute after V. A. Steklov, 51: 270-360, Moscow (In Russian), 1958.
- [Dmitriev et al, 1966] Dmitriev A. N., Zhuravlev Yu. I. and Krendelev F.P. On mathematical principles of object and phenomena classification, Discrete Analysis, 7: 3-15, Novosibirsk (In Russian), 1966.
- [Bongard, 1967] Bongard M.M. The problem of cognition, Moscow, 1967.
- [Vaintsvaig, 1973] Vaintsvaig M.N. Pattern Recognition Learning Algorithm KORA, Pattern recognition learning algorithms, Moscow, Sovetskoe Radio, 1973, pp.110-116.
- [Yablonskii, 1958] Yablonskii S. V., Functional constructions in k-valued logic, Proceedings of Mathematical Institute after V. A. Steklov, 51: 5-142, Moscow (In Russian), 1958.
- [Zhuravlev, 1958] Zhuravlev Yu. I., On separating subsets of vertices of n-dimensional unit cube, Proceedings of Mathematical Institute after V. A. Steklov, 51: 143-157, 1958.
- [Baskakova, Zhuravlev, 1981] Baskakova L.V., Zhuravlev Yu.I. Model of recognition algorithms with representative and support sets, Journal of Comp. Math. and Math. Phys., 1981, Vol. 21, No.5, pp. 1264-1275.
- [Zhuravlev, 1978] Zhuravlev Yu.I. On an algebraic approach to the problems of pattern recognition and classification, Problemy Kibernetiki, Vol. 33, 1978, pp.5-68.
- [Zhuravlev, Nikiforov, 1971] Zhuravlev Yu.I., Nikiforov V.V. Recognition algorithms based on calculation of estimates. Cybernetics, Vol. 3, 1971, pp.1-11. [Aslanyan, 1975]
- Aslanyan L. H. On a pattern recognition method based on the separation by the disjunctive normal forms. Kibernetika, 5, (1975), 103 -110.
- [Zhuravlev, 1977] Zhuravlev Yu.I. Correct algebras over the sets of incorrect (heuristic) algorithms: I, Cybernetics, No.4, 1977, pp.5-17., II, Cybernetics, No.6, 1977., III, Cybernetics, No.2, 1978.
- [Aslanyan, Zhuravlev, 2001] Aslanyan L., Zhuravlev Yu., Logic Separation Principle, Computer Science & Information Technologies Conference, Yerevan, September 17-20, 2001, 151-156.
- [Zhuravlev, 1998] Zhuravlev Yu. I., Selected Scientific Works (in russian), Magistr, Moscow, 1998, 417 p.
- [Aslanyan, Castellanos, 2006] Aslanyan L. and Castellanos J., Logic based pattern recognition – ontology content (1), iTECH-06, 20-25 June 2006, Varna, Bulgaria, Proceedings, pp. 61-66.
- [Aslanyan, Ryazanov, 2006] Aslanyan L. and Ryazanov V., Logic based pattern recognition – ontology content (1), iTECH-06, 20-25 June 2006, Varna, Bulgaria, Proceedings, pp. 61-66.
- [Aslanyan, 1975] Aslanyan L. H. On a pattern recognition method based on the separation by the disjunctive normal forms. Kibernetika, 5: 103-110, 1975.
- Aslanyan L. H. The Discrete Isoperimetry Problem and Related Extremal Problems for Discrete Spaces, Problemy Kibernetiki, 36: 85-128, 1979.

Authors' Information



Levon Aslanyan – Head of Department, Institute for Informatics and Automation Problems, NAS RA, P.Sevak St. 1, Yerevan 14, Armenia, e-mail: lasl@sci.am



Hasmik Sahakyan – Leading Researcher, Institute for Informatics and Automation Problems, NAS RA, P.Sevak St. 1, Yerevan 14, Armenia, e-mail: hasmik@jpia.sci.am

REPRESENTING TREE STRUCTURES BY NATURAL NUMBERS

Carmen Luengo, Luis Fernández, Fernando Arroyo

Abstract: Transformation of data structures into natural numbers using the classical approach of gödelization process can be a very powerful tool in order to encode some properties of data structures. This paper presents some introductory ideas in order to study tree data structures under the prism of Gödel numbers, and presents a few examples of using this approach to trees.

Keywords: Data structures, Trees, Gödelization

ACM Classification Keywords: E.1 Data Structures - Trees

Introduction

In [Luengo, 2008] was introduced a very interesting method in order to describe a Transition P system as a natural number. The process is based on the classical and very well known gödelization method. That paper described the way to find out the corresponding Gödel number to a transition P systems. A very important part of the process is to represent the membrane systems, a tree structure, as a natural number. In that paper the membrane structure was represented in a very naïf way, which it has been demonstrated to be not enough in order to recover the tree structure from the natural number that represents it. Following with this idea, in this paper it is depicted a sketch for assigning natural numbers to tree structures, which permits recover the tree from the natural number.

Tree definitions

A tree is an undirected simple graph $T = (V, E)$ satisfying that it is connected and has no cycles.

A tree T is said to be directed if it is a directed graph which would be a tree if directions on edges are not considered.

A tree T is said to be rooted if one vertex is designed as root, in which case the edges have a natural orientation, towards or away from the root.

In rooted trees, the parent of a vertex is the vertex connected to it on the path to the root. Every vertex on the tree has a unique parent except for the root. A child of a vertex v is a vertex of which v is the parent. And finally, a leaf is a vertex without children.

Rooted trees are the key element to define tree data structure and, on this context, vertexes are usually denoted as node and edges are usually denoted as links.

In Membrane Systems literature, a membrane structure is defined by a language MS over the alphabet $\{[,]\}$, as follows:

1. $[] \in MS$
2. if $\mu_1, \dots, \mu_n \in MS$ for some $n \geq 1$, then $[\mu_1, \dots, \mu_n] \in MS$

Once the language is established, in order to properly define membrane structure is needed to consider the following relation over the elements of MS : $m_1 \sim m_2$ if and only if we can write the two strings in the form $m_1 = \mu_1 \mu_2 \mu_3 \mu_4$, $m_2 = \mu_1 \mu_3 \mu_2 \mu_4$, for $\mu_1 \mu_4 \in MS$ and $\mu_2, \mu_3 \in MS$. That is, if two neighbouring pairs of parentheses are

interchanged, together with their contents, then we obtain the same membrane structure. If we represent by \sim^* the transitive and reflexive closure of the relation \sim . Clearly we have defined an equivalence relation over MS and membrane structures are equivalence classes.

It is very easy to translate this concept into graph theory. A membrane structure is a rooted tree, where the nodes are called membranes, the root is called skin and the leaves are called elementary membranes.

Finally, a recursive definition of membrane structure coming from graph theory is given:

A membrane structure is:

1. $\mu_0 = []_0 \in MS$
2. $([]_0, \mu_1, \dots, \mu_n)$ where $\mu_1, \dots, \mu_n \in MS$ for some $n \geq 1$

That is a membrane –the external one or skin- encloses a set of membrane structures. It is considered the same membrane structure every permutation of the different μ_i belonging to MS . Moreover, there is a unique link v_i connecting the membrane $[]_0$ with the membrane structure $\mu_i = ([]_i, \mu^i_1, \dots, \mu^i_n)$ where $\mu^i_1, \dots, \mu^i_n \in MS$ for some $n \geq 0$.

Now μ_0 is the ancestor of μ_1, \dots, μ_n and each one of them are connected by the link v_i . Obviously, the definition is extended to the other internal membrane structures in a natural way.

Let us say that every membrane system considered here has a finite number of membranes, $m \geq 1$.

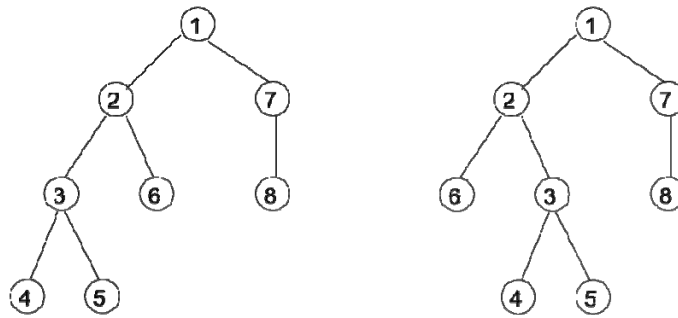


Figure 1: Two equivalent membrane structures

Tree Numbering Process

The purpose of the numbering process is to assign a natural number to each one of the different trees with m nodes or membranes and given a natural number associated to a tree with m nodes to recover the tree structure.

In [Luengo, 2008] we defined in a very simple way to assign natural numbers to membrane structure. The process was the following:

Let $T = (N, E)$ be a tree data structure with m nodes labelled in $L = \{1, 2, \dots, m\}$, and let $P_m = \{p_1, p_2, \dots, p_m\}$ be the set of the m first natural number starting in 2.

For the set of nodes of the tree T , it is defined the following map:

$$\begin{aligned}
 G_m : N &\rightarrow P_m \\
 n_k &\rightarrow p_k, \forall k \in L
 \end{aligned}
 \tag{1}$$

From this map it was defined the number associated to a tree T with labels in L as follows:

$$G_m(T) = \prod_{k=1}^m G_m(n_k), \forall k \in L \quad (2)$$

It is very easy to see that the process is not useful to extract the tree structure. In fact, it is possible to have several trees to which the map G_m gives the same natural number.

If we want to recover the tree structure from a natural number provide by a G_m map, it is needed to consider some particularities of the tree structure such as: number of branches, depth of each one of the branches, etc. Following with these ideas, we are going to consider branches and depth in order to assign natural number to nodes of the tree.

First of all we are going to map links instead of nodes as follows:

Let $T = (N, E)$ be a tree data structure with m nodes labelled in $L = \{1, 2, \dots, m\}$, and let $P_{m-1} = \{p_1, p_2, \dots, p_{m-1}\}$ be the set of the $m-1$ first natural number starting in 2. Every edge or link is numbered in pre-order starting from left to right in depth. This process is shown in figure 2.

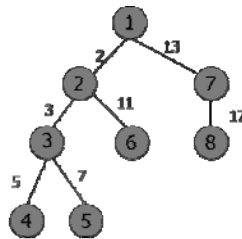


Figure 2: Numbering vertexes

As we did before, for the set of vertexes of the tree T , we define the map:

$$\begin{aligned} G_m : E &\rightarrow P_{m-1} \\ e_k &\rightarrow p_k, \forall k \in L - \{m\} \end{aligned} \quad (3)$$

And then, for the set of nodes of the tree T , it is defined the following map:

$$\begin{aligned} G_m : N &\rightarrow P_{m-1} \\ n_k &\rightarrow G(n_k), \quad \forall k \in L \text{ where :} \\ G_m(n_k) &= \begin{cases} p_k & \text{if } n_k \text{ is a direct descendent of the skin or root node} \\ p_k p_i G_m(n_j) & \text{if } n_k \text{ is a direct descendent of } n_j \text{ by the link } e_k \\ & \text{and } n_k \text{ is a node of the subtree } \mu_i \end{cases} \end{aligned} \quad (4)$$

Figure 3 shows this process.

This process permits to embedded information about tree structure into each one of the number associated to nodes, in particular, each one of the leaves of the tree have encoded the information corresponding to the branch to which they belong and the depth of each one of them.

Finally, it is possible to assign a natural number to the tree taking into account the leaves nodes of the tree as follows:

Let $T=(N, V)$ be a tree with m nodes and the set of leaves $L_{leaves} = \{l_1, l_2, \dots, l_s\}$, $1 \leq s \leq m$ then the natural number associated to T is defined by the expression:

$$G_m(T) = \prod_{l_k \in L_{leaves}} G_k(l_k) \tag{5}$$

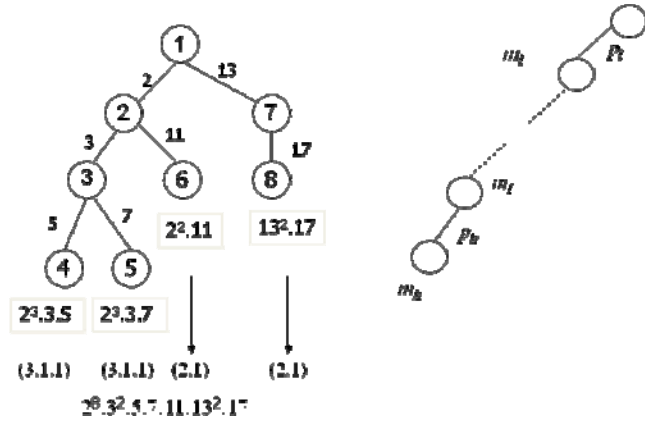


Figure 3: numbering nodes

This process permits to have some information about the tree structure, that is:

- For each one of the leaf nodes, the last prime factor is the label corresponding to the link which connects the node with its father.
- The exponent of the minimum prime corresponds to the depth of the leaf in the tree.
- Two equivalent trees have different natural number associated, which permits recover tree information independent of the equivalent relation defined before.

However when all the information is collected into only one unique natural number for the tree, there is some lost of information which is necessary in order to recover tree structure in the inverse process. In particular it is needed not only the number of branches the tree has, but also it is needed to know the depth of each one of them.

Figure 4 show different trees with four leaves with different structures depending on the number of nodes and branches.

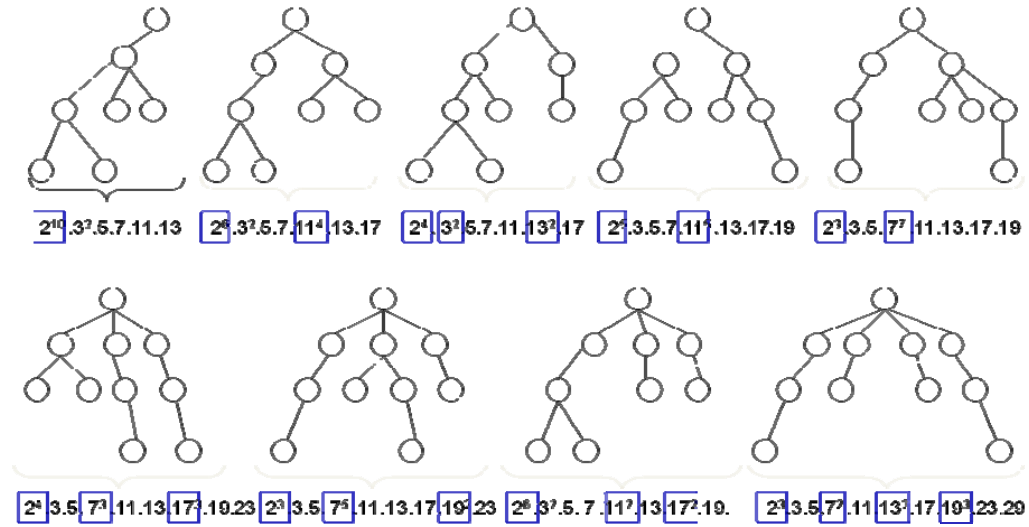


Figure 4: Trees with 4 leaves

As it was said before, what is important for recovering tree structure information is the number of leave nodes on the tree and, also, the depth of each one of them. If we incorporate these two data into the natural number associated to the tree, then it is possible to recover the tree structure from that number; and it is not very difficult.

Incorporating the information of number of leaves and their corresponding depth into expression (5), we have:

Let $T=(N, E)$ be a tree with m nodes, let $L=\{l_1, l_2, \dots, l_s\}$, $1 \leq s \leq m$ be the set of leaves, let $D=\{d_1, \dots, d_s\}$ be the corresponding depth for each one of the branches of the tree T , let P_m the set of the $m-1$ first prime number, and let p_0 a prime number such as $p_0 \notin P_{m-1}$; then the natural number associated to T is defined by the expression:

$$G^{p_0}_m(T) = p_0^{p_1^{d_1} \dots p_s^{d_s}} \prod_{l_k \in L} G_m(l_k) \tag{6}$$

Where G_m for nodes is defined by expression (4)

Recovering tree structure

In order to build a tree from a natural number, there is needed that the number satisfied some constrains, that is:

- Its factorization into prime numbers has to have m different prime factors
- p_0 has to be known

Let $G^{p_0}_m$ be a natural number which encodes a tree T with $m-1$ vertexes and m nodes, let p_0 be the prime which define the tree structure and let P_{m-1} be the rest of primes appearing in the factorization of $G^{p_0}_m$; then this number can be also expressed by:

$$G^{p_0}_m(T) = p_0^{p_1^{d_1} \dots p_s^{d_s}} \prod_{i \in \{1, \dots, m-1\}} p_i^{e_i} \tag{7}$$

From this prime factorization, it is possible to recover the tree structure as follows:

- Primes $\{p_i \mid 1 \leq i \leq m-1\}$, are ordered in an increasing way.
- Exponent of the p_0 factor encodes the number of leaves in the tree and the depth of each one of them.
- For each one of the rest of prime factor the exponent of the factor tell us about its position on the tree, factors having exponent equals to one are links to leaves nodes on the tree, or links to intermediate nodes without branches, because they appear only once; the rest of factor tell us the number of times the link is counted in order to encode the tree structure.

Let us to show some examples about these facts, for instance, considering the following number:

$$G_6^{13}(T) = 13^{2^3 3^3} \cdot 2^6 \cdot 3 \cdot 5 \cdot 7 \cdot 11$$

The number establish the tree structure as follows: the prime factor 13 determines that the tree has 2 leaves with 3 nodes each one. The rest of prime factors explicit the rest of the tree structure as follows:

- The root node is connected directly by a link labelled with the prime number 2 to the next node by the left. This is the first step in order to form the first path from the node to the leaf which is two more levels below. In order to build the path it is needed two more nodes connected by one more link labelled with the prime 5. This path consumes 3 times the number 2, 1 time the number 3 and 1 time the number 5. Hence we have now 3 times prime number 2, 0 times numbers 3 and 5 and 1 time numbers 7 and 11 in order to build the second path from the root to the second leaf of the tree.
- The second path starts in the root node and how we have 3 times the number 2, so the path has also to pass by the node connected to the root by the link labelled with 2 in order to consume the rest of 2's we

have. Now, the path cannot pass by the link labelled with number 3, we have no more 3's, so we need to open a second way and we consume one new prime, the next one in the factorization which is 7, and finally, we arrive to the last node of the tree trough a new link labelled with the 11 prime number. On this process we have consumed the rest of primes we have in the factorization, ending the building process of the tree.

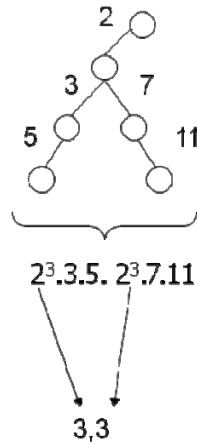


Figure 5: The built tree associated to G6 13(T)

Next figure shows some other examples of this process of recovering tree structures from a given natural number. In that figure it is considered that there are three leaves which are at depth of 4, 4 and 2 from the root node. In that figure is possible to see how important the multiplicity of the prime factors is in order to recover tree structures.

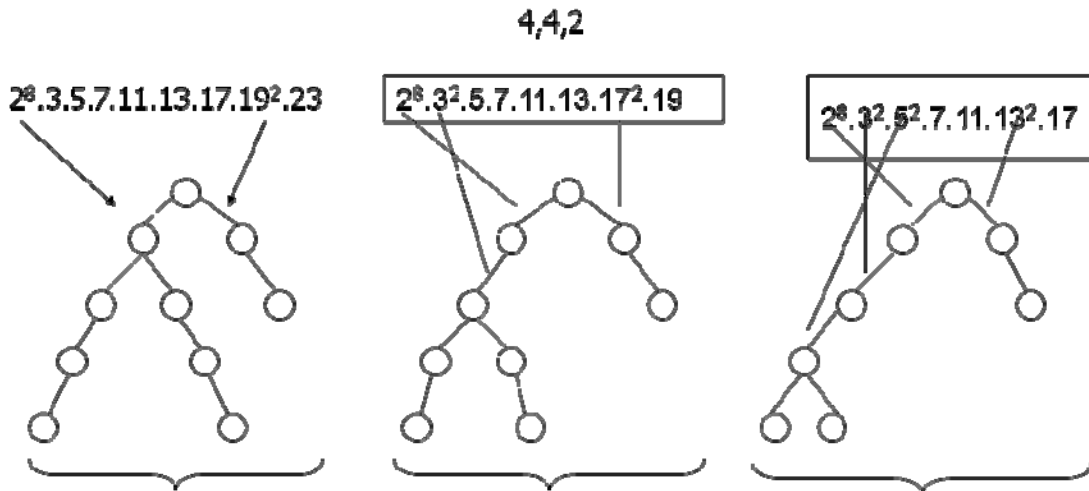


Figure 6: Several tree structures with 3 leaves and same depth

In terms of determining the general process for building a tree from a given natural number G^{p0}_m like in (7) we propose the following algorithmic description:

$G^{p^0}_m$ provides the following data:

- s = number of leaves in the tree.
- $D = \{d_1, \dots, d_s\}$ the set of number determining the depth for each one of the leaves.
- $P = \{(p_1, e_1), \dots, (p_{m-1}, e_{m-1})\}$ the set of prime factor with their multiplicities ordered in an increasing way.

Then we consider the initial tree T to be built defined by:

$$T = (N=\{1\}, L=\{\})$$

The idea is to add nodes linked by edges labelled by paired of natural number, the corresponding to the initial node and the final node as it is shows in Figure 7.

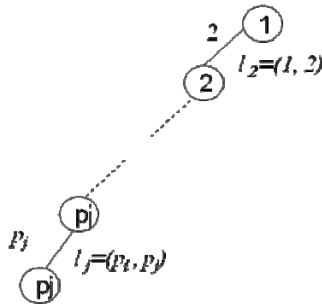


Figure 7: labeling nodes and links in the building process

The algorithm for building the tree from the natural number $G^{p^0}_m$ is the following:

```

for (i=1; i ≤ s; i++) {
  n_pos = 1;
  for (j=1; j ≤ d_s; j++) {
    take (p_j, e_j) ∈ P;
    if ( (n_pos, p_j) ∉ L)
      then {
        N = N ∪ {p_j};
        L = L ∪ {(n_pos, p_j)};
      }
    e_j --;
    n_pos = p_j;
  } //end for_j
  P_{m-1} = P_{m-1} - {(p_i, 0) | 1 ≤ m-1};
} //end for_i

```

Conclusions

This paper describes a way in order to transform tree structures into natural number. The process is based on the very well known gödelization process. Moreover, the process can be inverted in order to generate a tree from a natural number accomplishing several constrains. However, the paper is only introductory in this field; it is needed to follow up with the study in order to determine the real power of this approach in the study of tree structures. There are several open questions such as:

- Is it possible to determine that two trees are equivalent when they are represented by natural numbers?
- What happens with insertion / deletion of nodes on the tree on the natural number?
- Etc.

One more problem comes from dealing with big natural numbers. We are aware that the whole process is supported by natural number with a big digit number, and that is a problem itself in many cases.

This paper is only one preliminary study of coding tree by numbers, and we hope to continue our work with significant results and to apply to membrane computing and other natural computing fields in which such data structures are relevant.

Bibliography

[Luengo 2008] Carmen Luengo, Luís Fernández, Fernando Arroyo; P systems Gödelization, International Book Series Number 1, pp 29 -34, ISSN 1313-0455, Bulgaria

[Păun 2002] Gh. Păun, Membrane Computing. An Introduction, Springer-Verlag, Berlin, 2002

[Suzuki 2000] Y. Suzuki, H. Tanaka, On a LISP Implementation of a Class of P Systems, Romanian J. of Information Science and Technology, 3, 2 (2000), 173-186.

[Turing 1936] A.M. Turing, On computable numbers, with an application to the Entscheidungsproblem. Proceedings of the London Mathematical Society, 2-42, (1936-7), 230-265

[P system Web page] <http://ppage.psystems.eu/> (july 2010)

Authors' Information

Carmen Luengo Velasco – Dpto. Lenguajes, Proyectos y Sistemas Informáticos de la Escuela Universitaria de Informática de la Universidad Politécnica de Madrid; Ctra. Valencia, km. 7, 28031 Madrid (Spain); e-mail: cluengo@eui.upm.es

Luis Fernández Muñoz – Dpto. Lenguajes, Proyectos y Sistemas Informáticos de la Escuela Universitaria de Informática de la Universidad Politécnica de Madrid; Ctra. Valencia, km. 7, 28031 Madrid (Spain); e-mail: setillo@eui.upm.es

Fernando Arroyo Montoro - Dpto. Lenguajes, Proyectos y Sistemas Informáticos de la Escuela Universitaria de Informática de la Universidad Politécnica de Madrid, Ctra. Valencia, km. 7, 28031 Madrid (Spain); e-mail: farroyo@eui.upm.es

MATHEMATICAL MODEL OF THE CLOUD FOR RAY TRACING

Andrii Ostroushko, Nataliya Bilous, Andrii Bugriy, Yaroslav Chagovets

Abstract: *The three-dimensional computer graphics claimed today in many fields of the person activity: producing of computer games, TV, animation, advertise production, visualization systems of out-of-cockpit environment for transport simulators, CAD systems, scientific visualization, computer tomography etc. Especially high are requirements for realism of generated images. Realism rising leads to image detail increasing, necessity of shadows and light sources processing, the account of an environment transparency, generation of various special effects. Therefore in the field of a computer graphics researches are intensively conducted for the purpose of development of as much as possible effective models for three-dimensional scenes and fast methods of realistic image synthesis on their basis. One of the most promising methods is a ray tracing. The method provides possibility of synthesis of high realistic images; however it demands the large computational cost for the realization. The cloud synthesis model for a ray tracing is described. The model is directed to a real time graphics and allows raising realism of the synthesized image. Advantages of proposed model are the ability of working with cloud on different levels of detail, availability of bounding surfaces inside of cloud structure that allows to increase efficiency of an image synthesis algorithm, ease of cloud animation. Due to the great flexibility of a cloud model and high performance of its visualization algorithm these results can be used in real time visualization systems.*

Keywords: *cloud, procedural modeling, ray tracing, sphere, visualization algorithm.*

ACM Classification Keywords: *I.3.5 Computational Geometry and Object Modeling.*

Conference topic: *Information Retrieval.*

Introduction

One of the problems of computer graphics is generation of images in real time. Thus one of the major parameters of the graphic system providing synthesis of a three-dimensional scene is realism of the resulting image.

In recent years active works are conducted on development of ray tracing, which provides possibility of synthesis for high realistic images of three-dimensional scenes. The idea of a method consists in carrying out of mathematical modeling of propagation of a ray in a direction from the observer to scene objects and further to light sources. Number of traced rays is proportional to resolution of display system [Yan, 1985]. Despite the big computing complexity demanded for processing a scene, this method possesses a number of advantages in comparison with everywhere widespread rasterization, namely: realization simplicity of inter-object reflection effects, shadow generation, possibility of processing for analytically described surfaces (rasterization requires a pre-triangulation of all scene objects), the account of anisotropic properties of objects and environment. However the main advantage of this method is possibility of wide parallelization of calculations that allows using multicore processors and systems on their basis for carrying out of calculations.

Emergence of hardware and software (ATI Stream, NVIDIA CUDA, Intel OpenMP etc.) for the organization of multithreaded calculations gives the opportunity to solve right now a number of the problems related to generation of highly realistic images of three-dimensional objects in real time. Thus, development of mathematical models of objects and fast algorithms for a ray tracing is an actual problem.

One of possible applications of a ray tracing is the solution of a synthesis problem of the realistic cloud images in real time that is especially important for visualization systems of various vehicle simulators, tasks of meteorological data processing and image recognition.

Problem

Existing methods of clouds creation models can be divided on two groups. The first group includes methods based on modeling of physical processes occurring during the formation of clouds [Bouthors, 2008; Stam, 1995]. These methods require the assignment of a large number of input data, as well as a considerable amount of computing cost. The second group includes methods of procedural modeling of cloud shapes [Schpok, 2003; Harris, 2001; Voss, 1983]. Such methods are used when necessary to obtain an image of an arbitrary clouds or similar to the original, given in any way. They usually have more simple algorithms, but also let you create realistic three-dimensional image of the cloud.

The possibility of ray tracing to process analytically described objects can greatly simplify the cloud model and reduce the amount of data for presentation. One of the most simple and at the same time realistic cloud models are models based on the use of spheres and ellipsoids. However, in [Dobashi, 1999] due to lack of bounding surfaces need to cross the ray with all spheres of clouds, which leads to large computational cost. Model [Ostroushko, 2000] requires finding a smaller number of crossings through the use of the bounding surfaces. However, the use of ellipsoids as the basic building blocks leads to a more complicated calculation of the intersection points, which increases the computational costs.

Thus, it is necessary to develop a mathematical model based on the methods of procedural modeling of cloud shapes, which combines advantages of the models described in the sources [Bouthors, 2008; Stam, 1995], as well as the basic building blocks to use spheres and bounding surfaces.

Solution of the Task

Mathematical model of the cloud. The model is based on the model described in [Ostroushko, 2000]. The inputs in this model are the desired level of detail K and sizes of the cloud a, b, c . Based on this data sphere of the base level is formed with a radius r^0 and coordinates of the center x^0, y^0, z^0 :

$$r^0 = \begin{cases} \min(a, b, c)/2, & K = 0, \\ \max(a, b, c)/2, & K > 0, \end{cases}$$

$$x^0 = 0, \quad y^0 = 0, \quad z^0 = 0.$$

In case $K = 0$ the cloud consists of a single sphere of radius r^0 . If $K > 0$, then (a) deformation coefficients d_x, d_y, d_z for each axis are determined that allow to fit the cloud into the required dimensions, (b) the iterative process starts. The deformation coefficients for the first iteration step are calculated according to the following expressions:

$$d_x^0 = a/(2r^0), \quad d_y^0 = b/(2r^0), \quad d_z^0 = c/(2r^0).$$

For all following iteration steps $d_x^i = 1, \quad d_y^i = 1, \quad d_z^i = 1$.

At each iteration step the sphere obtained at the previous step is divided into five similar figures, forming the data to a new level of detail. The radii of the spheres in the new level are determined according to the expression:

$$r_j^{k+1} = I_j r^k,$$

where $k \in \{0, \dots, K-1\}$ – iteration number;

$j \in \{1, 2, 3, 4, 5\}$ – figure number;

I_j – random variable ranging from 0 to 1.

Coordinates of the centers of obtained spheres are defined as follows:

$$\begin{aligned} x_1^{k+1} &= x^k + (r^k - r_1^{k+1})s_1 d_x^k, & y_1^{k+1} &= y^k, & z_1^{k+1} &= z^k + \xi_1 f_\Delta((r^k - r_1^{k+1})s_1, r^k - r_1^{k+1}), \\ x_2^{k+1} &= x^k - (r^k - r_2^{k+1})s_2 d_x^k, & y_2^{k+1} &= y^k, & z_2^{k+1} &= z^k + \xi_2 f_\Delta((r^k - r_2^{k+1})s_2, r^k - r_2^{k+1}), \\ x_3^{k+1} &= x^k + \xi_3 f_\Delta((r^k - r_3^{k+1})s_3, r^k - r_3^{k+1}), & y_3^{k+1} &= y^k, & z_3^{k+1} &= z^k + (r^k - r_3^{k+1})s_3 d_z^k, \\ x_4^{k+1} &= x^k + \xi_4 f_\Delta((r^k - r_4^{k+1})s_4, r^k - r_4^{k+1}), & y_4^{k+1} &= y^k, & z_4^{k+1} &= z^k - (r^k - r_4^{k+1})s_4 d_z^k, \end{aligned}$$

$$\begin{aligned} x_5^{k+1} &= \begin{cases} x^k + \xi_5 f_\Delta(s_5, r^k - r_5^{k+1}), \xi_5 = -1, \\ x^k, \xi_5 = 1, \end{cases} \\ y_5^{k+1} &= y^k - (r^k - r_5^{k+1})s_5 d_y^k, \\ z_5^{k+1} &= \begin{cases} z^k + \xi_5 f_\Delta(s_5, r^k - r_5^{k+1}), \xi_5 = 1, \\ z^k, \xi_5 = -1. \end{cases} \end{aligned}$$

here s_j is a value which is chosen randomly in the range of 0.5 to 1;

ξ_j is a value randomly chosen from $\{+1, -1\}$;

$f_\Delta(C, R) = R^2 - C^2$ – function calculating one of the coordinates from the known values of radius R and other coordinate C . It allows to fit a new sphere into the sphere of previous level.

The use of randomly chosen values on each iteration allows eliminating periodicity of the structure of clouds. The iterative process continues until specified level of detail is reached. An example of generation of the next level of cloud description is shown in Figure 1.

The choice of the distribution of random variables used to construct the cloud model largely influences the results obtained and allows receiving various types of cloud formations. Thus, it was experimentally found that the best results when building a model of cumulus clouds can be obtained if I_j is in the range from 0.26 to 0.76, and s_j ranged from 0.9 to 1. Great influence on the obtained result has a number of figures into which the sphere is subdivided at each iteration step.

Transparency of the medium inside the cloud is determined by the meteorological optical range (MOR) S_m which is also an input parameter of the model. MOR determines the range of visibility of a black object and uniquely characterizes the weakening of the radiation by the environment.

For practical calculations of visibility the medium transmittance T is used, which for an optically homogeneous layer of medium with thickness equal to the unit length is called the specific transparency t . Knowing the specific transparency and thickness of the layer of the medium, we can determine the transmittance [McCartney, 1976]:

$$T = t^l. \quad (1)$$

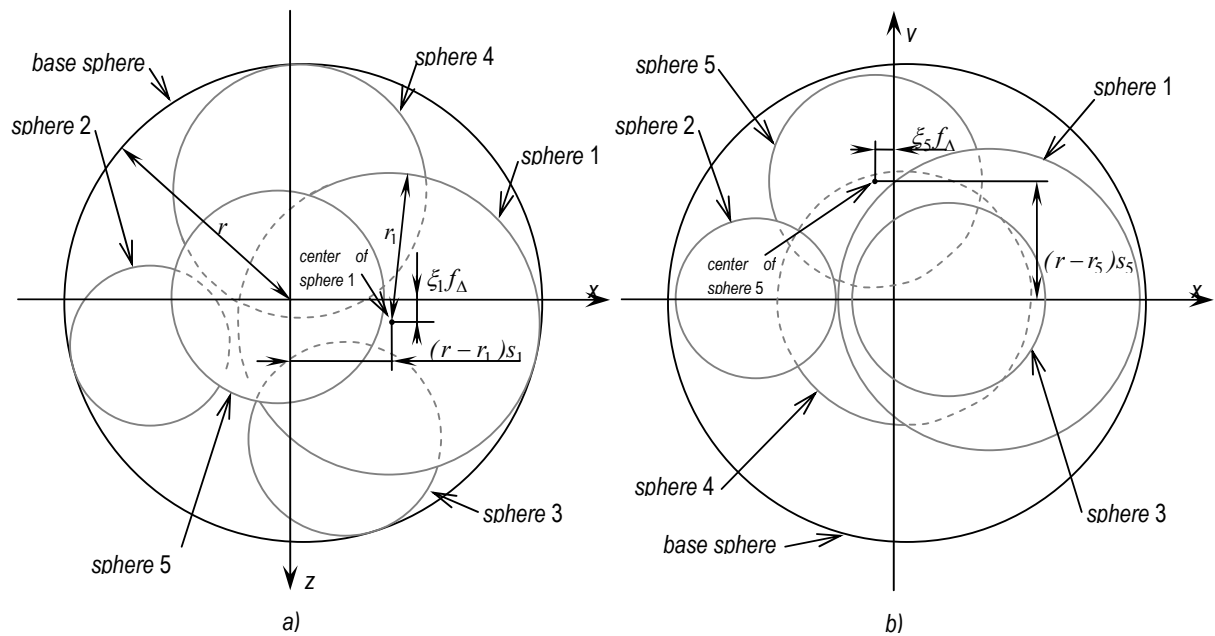


Figure 1. An example of subdivision of sphere when creating the next level of cloud description:
 a) projection on the XZ plane, b) projection on the XY plane.

Specific transparency and MOR are related as follows:

$$S_M = \ln 0.02 / \ln t.$$

Thus, knowing the MOR and calculating the length of the path of the projection ray inside the sphere, we easily obtain the transmittance.

To reduce the sphericity of cloud the specific transparency should grow from the center to the periphery, which requires an additional function $f(d_i, r_i)$ that takes into account such variation. We propose to use the following function:

$$f(d, r) = \begin{cases} 1 - \frac{d}{r}, & d \leq r, \\ 0, & d > r. \end{cases} \quad (2)$$

Then the transmittance of the i -th sphere, taking into account (1) and (2) is given by

$$T = T_i f(d_i, r_i) + 1 - f(d_i, r_i). \quad (3)$$

In addition, we propose to use the bump mapping technology, which will create a sense of surface irregularities [Blinn, 1978]. The apparent change in surface shape is achieved by changing the direction of normal in the point of intersection of the projection ray with the sphere and allows hiding the spherical structure of the cloud even more (Figure 2):

$$\bar{\mathbf{n}}' = f(u, v, \bar{\mathbf{n}}), \quad (4)$$

where $\bar{\mathbf{n}}$ – original normal to the sphere surface,

$f(u, v, \bar{\mathbf{n}})$ – parametric function of the normal variation,

u, v – parameters defining the position of the intersection point on the sphere surface.

Since the variations relate only to the normal direction (the coordinates of the intersection point do not change), then the amount of computation increases insignificantly. Function f can be represented analytically or, alternatively, it can use sampling from the texture map.

The use of bump mapping technology and variations in the specific transparency within the sphere allows obtaining a significant increase in realism of the generated images of clouds.

One of important features of this model is the easiness of cloud animation. It is carried out by changing parameters of spheres in the cloud model, specifically the radii of spheres and the coordinates of their centers. To animate the cloud the sequence is formed consisting of several implementations of cloud models, obtained by the method described above using the same number of iterations for all implementations. Since the sphere numbers in one implementation correspond to numbers in other implementations, it is easy to obtain correspondence between the two implementations. Through linear interpolation of parameters between the two consecutive implementations of models it is easy to achieve the modification of cloud shape in time. Using affine transformations - rotation, shift, scaling - in addition will allow to even more change the shape of cloud.

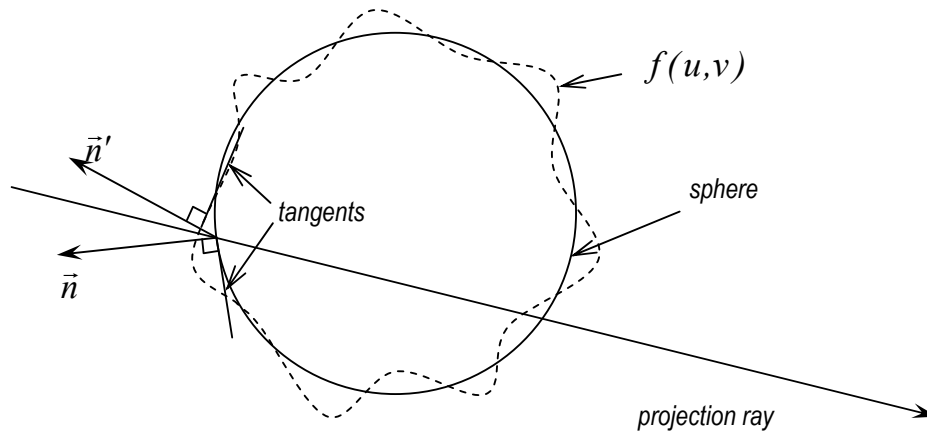


Figure 2 – Changing the direction of normal in the point of intersection of the projection ray with the sphere

The classical algorithm for the visualization of clouds. Currently, the main approach in the implementation of ray tracing is the solution of equations of the projection ray given in parametric form and the equations of the surface in an implicit form [Hill, 2001]. Let us consider it briefly.

Assume that the ray emanates from the point \mathbf{S} in the direction \vec{c} . Then the ray equation has the form:

$$r(t) = \mathbf{S} + \vec{c}t. \quad (5)$$

The condition of coincidence of the ray with a point on the surface of the base sphere, given by the equation $x^2 + y^2 + z^2 - 1 = 0$, has the form

$$|\vec{c}|^2 t^2 + 2(\mathbf{S} \cdot \vec{c})t + (|\mathbf{S}|^2 - 1) = 0.$$

This is a quadratic equation in t of the form $At^2 + 2Bt + C = 0$, where

$$A = |\vec{c}|^2, \quad B = \mathbf{S} \cdot \vec{c}, \quad C = |\mathbf{S}|^2 - 1.$$

The roots of the equation:

$$t_{1,2} = -\frac{B}{A} \mp \frac{\sqrt{B^2 - AC}}{A}. \quad (6)$$

If the discriminant $B^2 - AC$ is negative, a solution is absent, and the ray passes the sphere. If the discriminant is equal to zero, then the ray touches the sphere in a single point. If the discriminant is positive then two intersection points t_1 and t_2 exist that correspond to plus and minus signs in equation (6).

Consider now the case when sphere center does not coincide with the beginning of coordinate system or radius of sphere is not equal to 1, which corresponds to applying affine transformation \mathbf{M} to the sphere. Then before computation of (6) it is necessary to convert vector (5) into sphere coordinate system by multiplying it to the inverse matrix of sphere:

$$r'(t) = \mathbf{M}^{-1}r(t).$$

Then, using equation (6), the intersection points t_1 and t_2 are determined. The values without any conversion are directly used in equation (5) to determine the coordinates x , y , and z of the intersection points of projection ray with the sphere in the observer coordinate system.

To reduce the amount of computation in time of visualization of scene objects often the bounding primitives are used to easily allow a preliminary check on the possibility of a ray intersections with the object [Hill, 2001]. In the proposed clouds model as such bounding primitives can be used by the spheres of previous levels of detail, because each sphere of the previous level covers 5 spheres of the next level. Thus, if there is no intersection of the projection ray with a base sphere of clouds, it clearly points to the fact that any sphere of the next level of detail does not intersect with the ray. This property of the model allows to exclude from further work the rays which do not have intersections with the cloud and thereby reduce the amount of computing for visualization.

Results

The proposed model allowed obtaining a realistic cloud image, which requires for its description only a small amount of data. Thus, storage of cloud containing six levels of detail requires less than 50 KB. The images are presented in Figure 3. Also using this model, the cloud animation visualization has been conducted, results of which can be seen on the following link: <http://rtsquare.com/videos/clmorf.avi>. There you can also find other examples of the proposed model usage.

Table 1 shows the visualization time of model. Calculation of cloud image with resolution 800x600 pixels was performed on a workstation with a processor Intel CoreDuo E6600, 2 GB of RAM using one processor core.

Table 1 – Model visualization time

The number of spheres in the last level	Visualization time, ms
15625	4750
390625	9203
9765625	22116



a)



b)

Figure 3 - Images of clouds on the basis of the proposed model:
a) cirrus; b) cumulus clouds.

Conclusion

The developed model based on the methods of procedural modeling of cloud shape can generate realistic images of various cloud types (cumulus, cirrus, etc.) by controlling the probability distribution of random variables at the time of the model creation. A feature of this model is the fact that each sphere of any particular level is a bounding volume for the spheres of the next level. Firstly, this makes it easy to classify the projection rays by the presence of intersection with the cloud, and thus significantly reduce the amount of computation. Secondly, the use of identical elements at each level makes it possible to use adaptive algorithms for working with the model, choosing the desired level of detail, taking into account the angular resolution of graphics system. Thus, the farther away the cloud is from the observer, the lower the level number which provides the desired angular resolution, and, consequently, the less the amount of computation. Thirdly, the proposed model makes it easy to make animation of cloud. It should also be noted that the analytical descriptions can substantially reduce the amount of computation when geometric transformations are performed, since the rotation and translation require only to recalculate the coordinates of spheres center, and scaling will require an additional conversion of radii. The proposed model of the cloud is focused on the ray tracing and the ability to perform processing in real time.

Bibliography

- [Blinn, 1978] Blinn, James F. Simulation of Wrinkled Surfaces. Computer Graphics, Vol. 12 (3), pp. 286-292 SIGGRAPH-ACM, August 1978.
- [Bouthors, 2008] Antoine Bouthors, Fabrice Neyret, Nelson Max, Eric Bruneton, Cyril Crassin. Interactive multiple anisotropic scattering in clouds ACM Symposium on Interactive 3D Graphics and Games (I3D) – 2008.
- [Dobashi, 1999] Dobashi Y., Nishita T., Yamashita H., Okita T. Using metaballs to modeling and animate clouds from satellite images. Comput Graph Forum 15. 1999:471–482.
- [Harris, 2001] Mark J. Harris and Anselmo Lastra, Real-Time Cloud Rendering. Computer Graphics Forum (Eurographics 2001 Proceedings), 20(3):76-84, September 2001.
- [Hill, 2001] Fransis S. Hill Computer Graphics Using OpenGL (c) Prentice Hall 2001.
- [McCartney, 1976] E. J. McCartney, Optics of the Atmosphere Scattering by Molecules and Particles. Wiley, New York, 1976, 176–261
- [Ostroushko, 2000] Остроушко А.П., Gusyatin V.M. Synthesis of images of individual cloud formations // Radioelectronics and Computer Science. – 2000. – №2. – С. 79-81.(Russian language).
- [Schpok, 2003] Joshua Schpok, Joseph Simons, David S. Ebert, and Charles Hansen. A Real-Time Cloud Modeling, Rendering, and Animation System. Eurographics/SIGGRAPH Symposium on Computer Animation (2003)
- [Stam, 1995] Stam J, Fiume E (1995) Depicting fire and other gaseous phenomena using diffusion processes. Proceedings of SIG-GRAPH '95, Los Angeles, California 129–136.
- [Voss, 1983] Voss R. Fourier synthesis of Gaussian fractals: 1/f noises, landscapes, and flakes. In SIGGRAPH '83: Tutorial on State of the Art Image Synthesis, vol 10, ACM SIG-GRAPH.
- [Yan, 1985] Yan J.K. Advances in computer-generated imagery for flight simulation // IEEE Comp. Graph. - 1985. - 5, № 2.

Authors' Information



Andrii Ostroushko – Ph.D., Associate Professor, Kharkiv National University of Radio Electronics (KhNURE), Lenin Prospect 14, Kharkiv 61166, Ukraine; e-mail:

osa@kture.kharkov.ua

Major Fields of Scientific Research: computer graphics, ray tracing, digital visualization systems.



Nataliya Bilous – Ph.D., head of ITLCVS laboratory, professor of Kharkov National University of Radio Electronics, Lenin Prospect 14, Kharkiv 61166, Ukraine; e-mail:

belous@kture.kharkov.ua

Major Fields of Scientific Research: image processing, segmentation and recognition, building of computer vision system, computer testing and learning systems.



Andrii Bugriy – Ph.D., Senior Lecturer, Kharkiv National University of Radio Electronics (KhNURE), Lenin Prospect 14, Kharkiv 61166, Ukraine; e-mail:

abugriy@kture.kharkov.ua

Major Fields of Scientific Research: models, methods and algorithms of 3D image synthesis, structures of the digital visualization systems.



Yaroslav Chagovets – Ph.D., Associate Professor, Kharkiv National University of Radio Electronics (KhNURE), Lenin Prospect 14, Kharkiv 61166, Ukraine; e-mail:

yshagovets@kture.kharkov.ua

Major Fields of Scientific Research: ray tracing, terrain visualization, implementation of visualization systems using Graphics Processing Units.

THE ALGORITHM BASED ON METRIC REGULARITIES

Maria Dedovets, Oleg Senko

Abstract: *The new pattern recognition method is represented that is based on collective solutions by systems of metric regularities. Unlike previous methods based on voting by regularities discussed technique does not include any constraints on geometric shape of regularities. Metric regularities searching is reduced to connected components calculating in special contiguity graph. Methods incorporate statistical validation of found metric regularities with the help of permutation test.*

.Keywords: *pattern recognition, metric regularities, permutation test*

ACM Classification Keywords: *1.5 Pattern Recognition; 1.5.2 Design Methodology – Classifier design and evaluation*

Conference topic: *Pattern recognition and Forecasting, Machine Learning*

Introduction

Family of pattern recognition tools exist that are based on searching of regularities that are subregions of features space containing objects of one class only (complete regularity) or predominantly of one class (partial regularity). Usually in these methods subregions geometric shapes correspond to some sub predetermined model. The most frequently used model is the model of regularities, where the desired subregions of features space have the form of hyperparallelepiped. Logical regularities ([Yu. I. Zhuravlev et al.,2006], [V.V. Ryazanov,2007], [A. A. Ivachnenko and K. V. Vorontsov]) and «syndromes» concept ([Yu. I. Zhuravlev et al.,2006], [V.A. Kuznetsov et al., 1996], [O.V. Senko and A. V. Kuznetsova]) may be mentioned. Besides approaches exists where regularities are formed with the help of hyperplanes in features space ([A.A. Dokukin and O.V.Senko], [O.V. Senko and A. V. Kuznetsova]). However a priori specification of the geometric shape is a significant limitation hampering detection of some regularities actually existing in data, but not satisfying constraints that are put on by used model. In this work a new type of regularities (metric regularities) is discussed. Metric-type regularities allow to find the feature space subregions containing representative groups of connected objects of some class with minimal inclusion of other classes. We use a concept of a generalized connectivity between the same class objects (contiguity relationship \diamond_k) to define metric-type regularities. It must be noted that no suppositions about regularity shape are made.

Metric (generalized) regularities.

The standard problem of pattern recognition is considered. Let Ω is general set of recognized objects. Let $\tilde{S} = \{S_1, \dots, S_q\} \subset \Omega$ - a training sample, $\tilde{K} = \{K_1, \dots, K_l\}$ - a set of classes, the class $K_j, j = \overline{1, l}$ for each training set object $S_i, i \in \overline{1, q}$ is a priori known. Thus description of object $S_i \in \tilde{S}$ consists class indicator and future description that is used for recognition. Our goal is to find a correct class $K_j, j = \overline{1, l}$ for every arbitrary object $S \in \Omega$. It is supposed that metric $\rho(s', s'')$ are defined at Cartesian product $\Omega \times \Omega$. Correct metric choice is a significant issue in problems of classification, clustering, and nonparametric regression. Metric

is a mathematical model of the similarity of objects, and its choice in many cases is not unique. In recent years increasingly used methods where the metric is adjusted to the training set. We use a weighted Minkowski metric

for each fixed set of features: $\rho(S', S'') = \left(\sum_{j=1}^n w_j |f_j(S') - f_j(S'')|^p \right)^{\frac{1}{p}}$, where $f_j(S)$ is object S feature j

value, w_j - feature j weight. The weights of features are specified by reasons of normalization:

$$M_j = \max_{i=1, \dots, q} |f_j(S_i)|, w_j = M_j^{-p}$$

Definition 1. Two objects S_1 and S_2 are connected by class K or are in contiguity relation ship ($S_1 \diamond_K S_2$), if there are not in the training set \tilde{S} such object $S \in CK$ (CK is addition of class K to full train set), that both following inequalities will be correct:

- 1) $\rho(S_1, S_2) < \rho(S, S_1)$
- 2) $\rho(S_1, S_2) < \rho(S, S_2)$, where ρ is a metric in feature space.

The relation \diamond_K defines an indirected contiguity graph $G_{K\tilde{S}}$ such that there is one to one correspondence between vertices of $G_{K\tilde{S}}$ and objects from $\tilde{S} \cap K$. There is an edge between to vertices v' and v'' if an only if corresponding them objects S' and S'' .

Definition 2. We call a set $F \subseteq K \cap \tilde{S}$ a regularity by metric ρ (or connectivity field) of class K , if: $\forall S', S'' \in F \exists S_1, \dots, S_n \in F : S' \diamond_K S_1 \diamond_K \dots \diamond_K S_n \diamond_K S''$.

In other words any regularity by metric ρ correspond connected component of graph $G_{K\tilde{S}}$. Intuitively regularity by metric regularity by metric ρ corresponds compact in terms of metric regularity by metric ρ region of feature space with minimal inclusion of objects that do not belong to class K

Definition 3 (Regularity quality definition)

. A set F' is called a closure by training set \tilde{S} of a class K regularity F if: $F' = F \cup \{S \in CK \cap \tilde{S} \mid \exists S' \in F : S' \diamond_K S\}$.

Thus closure F' is union of F and objects from \tilde{S} that do not belong to class K but are connected to class objects from F . It is naturally to define regularity F quality as fraction of objects from class K in closure F' :

$$val(F) = \frac{|F|}{|F'|}$$

Closure F' may be calculated using reference objects concept.

Reference objects

A minimal set $\tilde{S}_{ref}(F)$ of objects from F such that any object from F is connected to at least one object from $\tilde{S}_{ref}(F)$ will call reference patterns:

Let F is a regularity. Then $\tilde{S}_{ref}(F) = \arg \min_{A \subseteq F} (|A| \mid \forall S' \in F, \exists S \in A : S \diamond_K S')$ is a reference

objects set.

Closure F' now is defined union of F and objects from \tilde{S} that do not belong to class K but are connected to class objects from $\tilde{S}_{ref}(F)$. At that regularity quality is define in the same way. Using reference objects concept allows to decrease significantly amount of information that is need for regularity description. Instead of storage of description of all objects from F it is sufficient to store descriptions of objects from $\tilde{S}_{ref}(F)$.

Regularities validation

Parameter $val(F)$ describe regularity quality but it does not allow to answer a question if discovered regularity is statistically valid? However statistical validity of regularity may be evaluated with the help of permutation test that is based on generating of set $\{\tilde{S}_{rand}\}$ of randomized data sets. To receive randomized data set \tilde{S}_{rand} positions of class indicators in initial data set \tilde{S} are randomly permuted. Then they are newly put in correspondence to fixed positions of features descriptions. The metrics regularities are found for each \tilde{S}_{rand} . Let $val_{max}(\tilde{S}_{rand})$ is maximal value of quality parameter $val(F)$ for regularities revealed at \tilde{S}_{rand} . Measure of statistical validity of regularity F found at true initial data set (p-value) is defined as ratio $p = \frac{|\{\tilde{S}_{rand} | val_{max}(\tilde{S}_{rand}) > val(F)\}|}{|\{\tilde{S}_{rand}\}|}$. It is evident that statistical validity is greater if p-value is less.

Possibility of statistical validation with the help of permutation test allows to use metric regularities searching as a tool for evaluating if there is an effect of explanatory variables X_1, \dots, X_n on outcome categorical variable. It is sufficiently to define metrics in X space, to find regularities and to evaluate their validity.

Training

At initial stage contiguity graph $G_{K\tilde{S}}$ is constructed for each class K and connected components of these graphs are calculated. Closures are found for corresponding regularities and quality parameters $val(F)$ are calculated. At the second stage permutation test is used to evaluate statistical validity of regularities found at the first stage. At the third stage final set \tilde{F}_{final} of regularities is formed. At that only regularities with high statistical validity or with evaluated p-values less some threshold are joined \tilde{F}_{final} . Usually threshold equal 0.1 was used.

Often there are outlying objects in data sets that deviate significantly from main part of data set. These outliers may significantly affect relationships \diamond_k between objects of the same class and decrease method efficiency. So procedure was suggested that allow to reveal outliers. It is assumed that the fraction of outliers in a class can be no more than X% of objects. Outlying objects $\tilde{S}_{outliers}$ are stored, analyzed and removed or not removed at the end of the learning.

Recognition

Let S - arbitrary recognized legitimate object. Estimates for class K are calculated as fraction of reference sets of class K metric regularities, connected to S , among full set of class K metric regularities. Object S is put into the class with maximal estimate.

Experiments

The program version of algorithm based on metric regularities was realized. In this version regularities are searched for each pair of features and estimates are calculated by set of all found regularities. Performance of the version was evaluated in variety of tasks including tasks from UCI Machine Learning Repository. At that its recognition ability was compared with recognition abilities of standard statistical methods, neural networks, support vectors machine and algorithm based on voting by systems of regularities. Experiments demonstrated sufficiently high generalization ability of method. Inclusion of algorithm in RECOGNITION system ([Yu. I. Zhuravlev et al., 2006]) and in the set of algorithms for resource Poligon.MachineLearning.ru for further study is planned.

Acknowledgment

The authors would like to thank ITHEA -XXI for support of these researches:

Bibliography

- [Yu. I. Zhuravlev et al., 2006] Yu. I. Zhuravlev, V.V. Ryazanov, O.V. Senko. *RECOGNITION. Mathematical methods. Program system. Applications* (in Russian). - Fuzis, Moscow, 2006. p.176.
- [V.V. Ryazanov, 2007] Ryazanov V.V. Logical regularities in recognition tasks (nonparametrical approach). *ЖБМ и МФ*, №10, 2007, с.1793-1808.
- [V.A. Kuznetsov et al., 1996] V.A. Kuznetsov, O.V. Senko, A.V. Kuznetsova et al. Recognition of fuzzy systems by method of statistically weighed syndromes and its use for immune and hematologic norm and chronic pathology. *Chemical Physics*, 15 (1) (1996), p.81-100
- [Yu. I. Zhuravlev et al., 2008] Zhuravlev Yu.I., Kuznetsova A.V., Ryazanov V.V., Senko O.V., Botvin M.A. The Use of Pattern Recognition Methods in Tasks of Biomedical Diagnostics and Forecasting // *Pattern Recognition and Image Analysis*, MAIK Nauka/Interperiodica. 2008, Vol. 18, No. 2, pp. 195-200.
- [O.V. Senko and A. V. Kuznetsova] O. Senko, A. Kuznetsova A recognition method based on collective decision making using systems of regularities of various types. *Pattern Recognition and Image Analysis*, Vol. 20, No. 2. (1 June 2010), pp. 152-162.
- [A. A. Ivachnenko and K. V. Vorontsov] Ivachnenko A. A., Vorontsov K. V. Upper boundaries of overfitting and variety profiles for logical // *Mathematical methods of pattern recognition-13*. — M.: MAKS Press, 2007. — p. 33–37.
- [A.A. Dokukin and O.V.Senko] Dokukin A.A. Senko O.V. About new pattern recognition method for the universal program system Recognition. *Proceedings of the International Conference I.Tech-2004*, Varna (Bulgaria), 14-24 June 2004, pp. 54-58.

Authors' Information

Oleg Senko – Leading researcher in Dorodnicyn Computer Center of Russian Academy of Sciences, Russia, 119991, Moscow, Vavilova, 40, e-mail: senkoov@mail.ru

Dedovets Maria – postgraduate student in Dorodnicyn Computer Center of Russian Academy of Sciences, Russia, 119991, Moscow, Vavilova, 40, e-mail: dedovets_m@mail.ru

ADAPTIVE CODING SCHEME FOR RAPIDLY CHANGING COMMUNICATION CHANNELS

Gurgen Khachatryan

Abstract: *In this paper we investigate the problem of reliable and efficient data transmission over rapidly changing communication channels. A typical example of such channel would be high-speed free space optical communication channel under various adverse atmospheric conditions, such as turbulence. We propose a new concept of developing an error correcting coding scheme in order to achieve an extremely reliable communication through atmospheric turbulence. The method is based on applying adaptive error correcting codes to recover lost information symbols caused by fading due to turbulent channel.*

Keywords: *error correcting codes.*

ACM Classification Keywords: *E.4 CODING AND INFORMATION THEORY.*

Conference topic: *Information Retrieval.*

Introduction

We propose an entirely new concept of developing an error correcting coding scheme in order to achieve an extremely high reliable communication through atmospheric turbulence. The method is based on applying *adaptive* error correcting codes to recover lost information symbols caused by fading due to turbulent channel. *To the best of our knowledge, this solution based on our adaptive-controlled approach does not exist.*

The reason of proposing channel coding is to be able to detect or even to correct transmission errors if we append additional information (so called redundant information) to the information sequence. In order to find effective codes, we must first characterize the transmission channel. The atmosphere causes very slow fading (compared to the high communication rates) which significantly degrade transmission quality. Usually, the fading time-constant is much higher than the bit-duration. The fading process can be described by the "mean number of fades per second (NOF), "mean duration of fades"(DOF), and the "probability of fades"(POF). Using the binary intensity modulation the receiver performance, described by the receiver sensitivity and the noise processes of the detector is very important to calculate the error probability. The noise for a 1 and 0 level is different if we are using an avalanche photo-detector (APD). Additionally, the noise depends on the current mean received power. Due to these noise effects, *we can minimize the error probability by using an **adaptive** decision-threshold, optimized for the current mean received power.*

Note that since the transmitter laser power and receiver sensitivity are limited by the available technology, fading imposes a severe problem that can be solved by the use of forward error correction schemes (FEC) in order to improve system performance. Block coding can improve the bit error rate (BER) if the received power is rather high. Using block codes there is a threshold after which the coded transmission is better than the transmission without coding. This is because of the redundant bits which must additionally be transmitted using codes. The fade time caused by randomly varying communication channel is usually much shorter than the duration of a code block, so that the code should correct as much as possible errors which occur during a fade. With block codes we can improve the BER significantly.

Code Construction

The proposed work is based on the construction of special linear $(N+m, N)$ block codes [1] which will correct any single burst of erasures up to the length m . This section explains briefly the code construction and states the two prepositions about a code. The generator matrix of the code has a very simple construction, that can be represented as follows. Let D_n denote an $n \times n$ binary matrix where all elements on or above a diagonal are 1's and all other elements are 0's. For an example D_3 will be a matrix

$$D_3 = \begin{array}{|c|c|c|} \hline 1 & 1 & 1 \\ \hline 0 & 1 & 1 \\ \hline 0 & 0 & 1 \\ \hline \end{array}$$

Then the generator matrix G of an $(N+m, N)$ code will be

$$G = I_N \mid \begin{array}{|c|} \hline D_r \\ \hline D_r \\ \hline \dots \\ \hline D_r \\ \hline D_r \\ \hline \end{array}$$

Where I_N is an identity matrix of the dimension N and $r = \lfloor N/m \rfloor$.

The following prepositions can be proofed:

Preposition 1. A linear code $(N+m, N)$ represented with the generator matrix G will be able to recover burst of erasures up to the length m in one block of the length $N+m$. (this is a guaranteed combination of erasures, in fact the given code can recover much more combinations).

The proof of preposition 1 is omitted and can be found in [1].

Preposition 2. Linear $(N+m, N)$ codes described above are optimal in the sense that : a)they have a minimum number of redundant symbols if a linear code is used and, b) they meet Shannon bound when we consider the model of the channel where most probable errors are bust of erasures up to the some length.

Proof of preposition 2: a) If the number of check(redundant) symbols is less than m and the number of erased symbols is at least m , then we will have less than N symbols which remain uncorrupted. Since the code is a linear in order to recover uniquely erased symbols at least N symbols(where N is the number of information symbols of the code) are needed which we do not have in this case.

b) If the probability of erasure per symbol is P it is well known that the Capacity of the channel is $C=1-P$. According to the model of the channel the most probable erasure pattern would be of the length $N \times P$ per block of N symbols. The corresponding parameter of our code from the preposition 1 will be a linear $(N, N-NP)$ code that corrects the burst of errors up to the length NP . The Rate of a given code will be $N(1-P)/N=1-P$ which is just equal to C -the channel capacity.

How the adaptive coding works in presence of fading channel

The performance of free-space optical communication systems can be degraded by many factors, such as fog, obstruction of line-of-sight path, atmosphere turbulence etc. These factors in turn will cause a channel fading an intensity of which will depend on the real conditions of the channel. In many situations it would be possible to estimate the intensity of fading in the channel and apply appropriate error correcting codes to recover loosed information symbols caused by fading. In order to facilitate this adaptive coding concept we will make some assumptions. At first we assume that on-off keying (OOK) modulation is used, i.e. we have a binary channel. Secondly the information is divided into blocks (packets) of the length N , and as a result of fading some symbols may be erasure or loosen, however the locations of such symbols in the whole packet will be known at the receiver end. We assume also that before transmission a transmitter (sender) knows the intensity of fading of the channel, which will allow him to estimate the maximum number of consecutive symbols m corrupted (erased) as a result of that fading. These m symbols will form a burst of erasure of the length m . Finally we will assume that there will be not more than one burst of length m per each block of the length N . In the case if there is more than one burst of error such packets should be simply retransmitted.

We have developed linear $(N+m, N)$ codes which will correct any single burst of erasures up to the length m . The parameter m actually determines the number of redundant symbols that should be attached to N information symbols in each packet. m in fact determines the intensity of fading in the channel, so it can be adjusted before transmission. Thus the number of redundant symbols that will determine the information transmission rate will depend on the conditions of the channel. Note that proposed $(N+m, N)$ codes have very simple structure and as a result can be effectively implemented on DSP-based hardware devices.

Let's consider some numerical example. Suppose $N=500$ and $m=50$. Let's denote by

$P(N,r)$ the probability that in the block of N symbols exactly r consecutive symbols will be corrupted. $P(N,0)$ will denote the probability that none of the N symbols will be corrupted. Lets consider the case when $P(N,0) = 0.05$,

$\sum_{i=1}^{50} P(500, i) = 0.9$, $\sum_{i>50} P(500, i) = 0.05$. This means that with the probability 0.95 the length of the burst of

corrupted symbols will not exceed 50. In order to keep the same rate 0.95 for the probability, that the number of erasures will not exceed the level which will be recovered by our code construction, we will need to put $m=55$, which means that actual block length would be $N=555$. We can then approximate that $P(555,0)$ will be $(500/555) * 0.05 = 0.045$ and $\sum_{i>50} P(555, i)$ will be equal to 0.055.

Now let's compare the number for retransmissions per 1000 blocks needed before and after our encoding scheme. Since before encoding our system cannot tolerate any erasures the number of retransmissions per 1000 blocks would be 950, since the probability that there is no error in block with 500 symbols is 0.05. After encoding when we have 555 symbols we will need only in average 55 retransmission per 1000 blocks, since the probability that errors will not tolerated by our system is equal to 0.055. As a result of our coding scheme, for this example we achieve more that 17 times reduction in retransmission rate which greatly enhances the efficiency of our communication system.

Also note that we can adjust the variable rate coding scheme (adaptive coding), depending on the probability of fade at certain time (which we can measure or probe) and adjust the redundant scheme accordingly. This is because of the redundant bits that must additionally be transmitted using codes. The threshold depends on the used code. *The "fade time" is usually much shorter than the duration of a code block, so that the code should correct as much as possible errors that occur during a fade.* We wanted to illustrate the coding gain in dB, with or without coding, at least qualitatively.

We now explain how the coding gain curves should be drafted. For the future curves we will have $BER(P)$ (in our case actually P will denote the probability for the burst of erasure which will be transferred into the length of the burst equal to $N \times P$): this $BER(P)$ is a function of SNR and σ_R (the turbulence strength variance parameter). Thus we will have 3 parameters: SNR , σ_R and P (P determines the Capacity and $C = 1 - P$). For a given σ_R , we will have pairs (SNR, P) and a coding gain will be determined as $(SNR_1 - SNR_2)$ if we go from (SNR_1, P_1) to (SNR_2, P_2) where $SNR_1 > SNR_2$ and $P_1 < P_2$. As a result of coding we can achieve the same BER for less SNR .

How the code parameters are related to the most probable fading time and the most probable idle time between fades are explained below. Code parameters we have developed will depend on the most probable duration of fade (FD) and the most probable duration of idle time (IT) between fades. For example, if information speed is 10 Gbit/sec (= 107 bits/sec), FD is 5×10^{-4} sec (= 0.5 msec), and (IT) is 2 msec an average 5000 consecutive bits will be corrupted followed by in average 15000 uncorrupted bits. According to our construction a linear code (20000, 15000) will take care for 5000 corrupted bits. Actually the rate of the linear code will be equal to $1 - FD/IT$.

Conclusion

In this paper we have introduced an idea of adaptive coding scheme for rapidly changing communication channels. We have suggested an optimal fade – tolerant

linear code construction and showed how they can be used to achieve high reliability and efficiency of information transmission when the channel model can be represented as fading channel with variable fading rate.

Bibliography

[KHACH, 1988] G. Khachatrian, "Code Constructions for Binary Switching Two-User Channel"- Proceedings of Second Intern. Joint Colloquium On Coding Theory between Osaka University and Academy of Sciences of Armenia, June 24-28, Osaka, Japan (1988), 175-184

Authors' Information

Gurgen Khachatryan – *American University of Armenia*; e-mail: gurgenk@aua.am

Major Fields of Scientific Research: Coding theory, Cryptography.

A MAMDANI-TYPE FUZZY INFERENCE SYSTEM TO AUTOMATICALLY ASSESS DIJKSTRA'S ALGORITHM SIMULATION

Gloria Sánchez-Torrubia, Carmen Torres-Blanc

Abstract: *In education it is very important for both users and teachers to know how much the student has learned. To accomplish this task, GRAPHS (the eMathTeacher-compliant tool that will be used to simulate Dijkstra's algorithm) generates an interaction log that will be used to assess the student's learning outcomes. This poses an additional problem: the assessment of the interactions between the user and the machine is a time-consuming and tiresome task, as it involves processing a lot of data. Additionally, one of the most useful features for a learner is the immediacy provided by an automatic assessment. On the other hand, a sound assessment of learning cannot be confined to merely counting the errors; it should also take into account their type. In this sense, fuzzy reasoning offers a simple and versatile tool for simulating the expert teacher's knowledge. This paper presents the design and implementation of three fuzzy inference systems (FIS) based on Mamdani's method for automatically assessing Dijkstra's algorithm learning by processing the interaction log provided by GRAPHS.*

Keywords: *Algorithm Simulation, Algorithm Visualization, Active and Autonomous Learning, Automatic Assessment, Fuzzy Assessment, Graph Algorithms.*

ACM Classification Keywords: *1.2.3 [Artificial Intelligence]: Deduction and Theorem Proving - Answer/reason extraction; Deduction (e.g., natural, rule-based); Inference engines; Uncertainty, "fuzzy," and probabilistic reasoning. K.3.2 [Computers and Education]: Computer and Information Science Education – computer science education, self-assessment. G.2.2 [Discrete Mathematics]: Graph Theory – graph algorithms, path and circuit problems.*

Conference topic: *Decision Making and Decision Support Systems.*

Introduction and preliminaries

Since the late 1990s, we have developed several web applications for graph algorithm learning based on visualization and aimed at promoting active and autonomous learning [Sánchez-Torrubia, Lozano-Terrazas 2001], [Sánchez-Torrubia et al. 2009 (a)] and [Sánchez-Torrubia et al. 2009 (b)].

When designed and used under the appropriate conditions, visualization technologies have proved to be a very positive aid for learning [Hundhausen et al. 2002]. Learners who were actively involved in visualization consistently outperformed other learners who viewed the algorithms passively. Thus, when using an e-learning tool, the program should request a continuous user-side interaction to rule out laziness and force learners to predict the following step.

All the applications we develop are designed on the basis of the philosophy underlying the eMathTeacher concept. An e-learning tool is eMathTeacher compliant [Sánchez-Torrubia et al. 2008] and [Sánchez-Torrubia et al. 2009 (a)] if it works as a virtual math trainer. In other words, it has to be an on-line self-assessment tool that helps students (users) to actively learn math concepts or algorithms independently, correcting their mistakes and providing them with clues to find the right answer. To culminate all these years of research, we have created an environment called GRAPHS, integrating several graph algorithms, where Dijkstra's algorithm will be simulated.

When using e-learning as a teaching aid, it is very important for both users and teachers to know how much the student has learned. To accomplish this task, GRAPHS generates an interaction log that will be used to assess the student's learning outcomes. This poses an additional problem: the assessment of the interactions between the user and the machine is a time-consuming and tiresome task, as it involves processing a lot of data. Additionally, one of the most useful features for a learner is the immediacy provided by an automatic assessment. On the other hand, a sound assessment of learning cannot be confined to merely counting the errors; it should also take into account their type. As is common knowledge, to grade a student, an instructor takes into account the quality of the errors and does not just add up the number of mistakes.

Our goal then is to design an automatic assessment system that emulates the instructor's reasoning when grading a Dijkstra's algorithm simulation within GRAPHS environment. The automatic assessment will be performed by means of a Mamdani-type fuzzy inference system.

Dijkstra's algorithm

Dijkstra's Algorithm [Dijkstra 1959] is one of the most popular algorithms in computer science. It is a graph search algorithm that solves the problem of finding the shortest path between a source node and every other node in a connected weighted graph with non-negative weights. It can also be used to find the shortest path between a source node and a fixed target node by stopping the algorithm when the target node has been fixed.

Dijkstra's algorithm (with target node) pseudocode might be described as follows:

Input: A connected weighted graph with non-negative weights $G = (V, E)$, where V is the set of nodes and E is the set of edges. A source node $O \in V$ and a target node $T \in V$.

Output: A list of nodes O, \dots, T , representing the shortest path from O to T .

Initialize Variables

```

S ← V           # non-fixed nodes
Vf ← ∅
D ← [0, ∞, ..., ∞] # distances vector (n components) corresponding to [O, v1, ..., vn-1] nodes in V
P ← [-1, 0, ..., 0] # predecessors vector (n components) corresponding to [O, v1, ..., vn-1]
target node found ← false

```

Procedure:

```

While not (target node found) do
  v ← node in S with minimum distance D(v)           # D(v) = value in D corresponding to v
  S ← S - {v}, Va ← Va ∪ {v}
  If (v ≠ T)
    Adjacents ← {nodes in S that are adjacent to v}
    For (u ∈ Adjacents) do
      If (D(u) > D(v) + w(u,v)) then:           # w(u,v) = weight of the edge uv
        P(u) ← v
        D(u) ← D(v) + d(u,v)
      endif
    endfor
  else
    target node found ← true
  endif
end while
return shortest path = O, ..., P(P(T)), P(T), T and D(T)

```

Dijkstra's algorithm constitutes a successive approximation procedure and was inspired by *Bellman's Principle of Optimality* [Sniedovich 2006]. This principle states that "An optimal policy has the property that whatever the initial state and initial decision are, the remaining decisions must constitute an optimal policy with regard to the state resulting from the first decision" [Bellman 1957]. The central idea behind the algorithm is that each subpath of the minimal path is also a minimum cost path. In Dijkstra's words "We use the fact that, if R is a node on the minimal path from P to Q, knowledge of the latter implies the knowledge of the minimal path from P to R" [Dijkstra 1959], which is a formulation of Bellman's Principle of Optimality in the context of shortest path problems.

GRAPHS environment

GRAPHS is an environment conceived to improve active and autonomous learning of graph algorithms by visually simulating an algorithm running on a graph. This environment has been designed to integrate eMathTeacher-compliant tools [Sánchez-Torrubia et al. 2008] and [Sánchez-Torrubia et al. 2009 (a)]. It launches in Java Web Start, features a language selector (with English and Spanish available at the present time) and is an extendible system, including a kernel and series of algorithms that will exploit its functionalities.

To ensure that algorithm learning is progressive, GRAPHS provides different algorithm simulation difficulty levels. At the lower levels, mouse-driven node or edge selection together with pop-up windows asking basic questions about the current step are the key tools used to simulate algorithms. At the more advanced levels, students will have to modify all the algorithm structures. Dijkstra's algorithm (see Figure 1), with and without final node and also with the option of selecting any starting node, is implemented at three levels (low, medium and high).

The screenshot shows the GRAPHS software interface. The main canvas displays a graph with nodes A, B, C, D, E, and F. The edges and their weights are: A-B (7.0), A-C (9.0), A-F (14.0), B-D (15.0), C-D (11.0), C-E (2.0), D-E (6.0), and F-E (9.0). Node C is highlighted in green. Below the canvas is a dialog box with the text "Update the distance and the predecessor of the adjacent node" and an "OK" button.

The "Data Structures" table is as follows:

Q	S	dA	dB	dC	dD	dE	dF	pA	pB	pC	pD	pE	pF
{}	{A, B, C, D, E, F}	∞?	∞?	∞?	∞?	∞?	∞?	-	-	-	-	-	-
{}	{A, B, C, D, E, F}	∞?	∞?	∞?	∞?	0.0	-	-	-	-	-	-	-1
{F}	{A, B, C, D, E}	14.0	∞?	2.0	∞?	9.0	0.0	F	-	F	-	F	-1
{F, C}	{A, B, D, E}	14.0	12.0	2.0	∞?	9.0	0.0	F	C	F	-	F	-1

The "Dijkstra Algorithm" window shows the following code:

```

Q = {} --Initializing set nodes list
S = {graph nodes} --Initializing not set nodes list
D = {inf,inf,...} --Initializing distances
P = {-,-,...} --Initializing predecessors
Select initial node
Select final node (or without final node)
While (final node not find) do
  ActiveNode (v) = node in S with lowest cost
  S <- S - {v}
  Q <- Q + {v}
  If (v = final node)
    For (u adjacent node) do
      If (D(u) > D(v) + d(u,v)) then
        D(u) = D(v) + d(u,v) --Update distances
        P(u) = v --Update predecessors
      End If
    End For
  Else
    node found
  End If
End While
RETURN Ppath
  
```

Figure 1. GRAPHS being used to simulate Dijkstra's algorithm.

During algorithm simulation GRAPHS creates an XML-based interaction log that is able to record both user errors and correct actions and the time taken to complete the simulation. Each tag in this file is associated with a specific action characterized by the error or hint message provided by the tool.

Fuzzy inference and automatic assessment

Mamdani's direct method [Mamdani 1974] has proved to be very apt for simulating human reasoning as it formalizes the expert's knowledge by synthesizing a set of linguistic if-then rules. We chose this method because of its simple structure of min-max operations, and its flexibility and simplicity, being based, as it is, on natural language. Since 1996 several authors have applied fuzzy reasoning to determine the question assessment criterion depending on the results achieved by the student group for that question. This is usually denoted as "grading on a curve" methods [Bai, Chen 2008] and [Law 1996]. However, our goal is to model the reasoning of an expert teacher with regard to assessment, while, at the same time, outputting results automatically. Therefore, the goal of this paper is to design and implement a system capable of automatically assessing user interaction simulating Dijkstra's graph algorithm. Students will use the GRAPHS environment (which we designed, see Figure 1) for the simulation.

Input data for the automatic fuzzy assessment system are taken from the interaction log that is generated by GRAPHS. This log records both user errors and correct actions during the simulation and the time taken to complete the simulation. GRAPHS has been designed subject to eMathTeacher specifications, that is, the learner simulates algorithm execution using the respective inputs. It is also important to highlight that, in an eMathTeacher-compliant tool, algorithm simulation does not continue unless the user enters the correct answer.

Description of the input data for the system

When simulating Dijkstra's algorithm execution, users have to manipulate several data structures depending on the algorithm step that they are executing: fixed and unfixed nodes, selection of the active node and updating of distances and predecessors among the set of (unfixed) nodes adjacent to the active node.

In the following we describe the structure of the interaction log file, showing the different types of user input to the application and their error codes. Depending on these codes we will define the errors that are to be taken into account in the assessment, which we will normalize for use as system input data.

Interaction log file

The GRAPHS implementation of Dijkstra's algorithm offers users a choice of three execution levels: low, medium and high. Depending on the selected level, the pseudo code is run step by step (low), by blocks (medium) or executing just the key points (high). When the user completes the simulation at the selected level, GRAPHS generates an XML file containing each and every application input. These inputs are described by the request message identifier tag if they are correct or by the identifier tag of the error message that they generate if they are incorrect (see Figure 2). In this paper we present a system that automatically assesses the interaction log of a medium-level Dijkstra's algorithm simulation. As the automatic assessment system depends on the error codes and they are different at each interaction level, each level will have its own fuzzy inference system (FIS) in the future.

As Figure 2 shows, each of the correct and incorrect actions in the interaction is characterized by a tag that corresponds to its identifier tag in the properties file, enabling the internationalization of a Java application. For example, the <ALERT_ADJACENT_ERR> and <ALERT_MORE_ADJACENTS_ERR> tags correspond to C₂₋₁ (adjacent checking) errors and the <ALERT_ADJACENT_MSG> and <ALERT_MORE_ADJACENTS_MSG> tags correspond to correct C₂₋₁ actions (see Table 1).

```

<?xml version="1.0" encoding="UTF-8" ?>
<Algorithm Execution="22" Finished="03/02/2010 11:50:56" Level="Medium" Name="Dijkstra" Started="03/02/2010 11:28:49">
... (selection of initial and final nodes)...
<Step>
  <Number>2</Number>
  <Iteration>0</Iteration>
  <ALERT_FINISH_ERR>YES instead of NO, Algorithm not finished</ALERT_FINISH_ERR>
  <ALERT_FINISH_MSG>Algorithm not finished</ALERT_FINISH_MSG>
</Step>
<Step>
  <Number>3</Number>
  <Iteration>0</Iteration>
  <MSG_SEL_ACTIVE_NODE_MSG>Active Node: F</MSG_SEL_ACTIVE_NODE_MSG>
</Step>
<Step>
  <Number>5</Number>
  <Iteration>0</Iteration>
  <ALERT_ADJACENT_MSG>Adjacent exists</ALERT_ADJACENT_MSG>
</Step>
<Step>
  <Number>6</Number>
  <Iteration>0</Iteration>
  <MSG_SEL_ADJACENT_NODE_MSG>Adjacent Node: E</MSG_SEL_ADJACENT_NODE_MSG>
</Step>
<Step>
  <Number>7</Number>
  <Iteration>0</Iteration>
  <MSG_SEL_UPDATE_MED_ERR>Update of E is incorrect</MSG_SEL_UPDATE_MED_ERR>
  <MSG_SEL_UPDATE_MED_MSG>Update of E is correct</MSG_SEL_UPDATE_MED_MSG>
</Step>
<Step>
  <Number>8</Number>
  <Iteration>0</Iteration>
  <ALERT_MORE_ADJACENTS_MSG>More adjacents exist</ALERT_MORE_ADJACENTS_MSG>
</Step>
<Step>
  <Number>9</Number>
  <Iteration>0</Iteration>
  <MSG_SEL_ADJACENT__NODE_MSG>Adjacent Node: A</MSG_SEL_ADJACENT__NODE_MSG>
</Step>
<Step>
  <Number>10</Number>
  <Iteration>0</Iteration>
  <MSG_SEL_UPDATE_MED_MSG>Update of A is correct</MSG_SEL_UPDATE_MED_MSG>
</Step>

```

Figure 2. Part of the medium-level interaction log from Dijkstra's algorithm with final node.

Input data

The data contained in the codes generated by the interaction log described in the previous subsection are transformed into valid FIS inputs. In order to simplify the rule set within the inference system, some errors in the assessment are grouped by similarity, leading to the following table.

Table 1. GRAPHS outputs and assessment system inputs (* is MSG or ERR, depending on if it corresponds to an error or a correct action).

Input data	Error code	Pseudo code action	XML tags
E ₁₋₁	C ₁₋₁	Selection of active node	<MSG_SEL_ACTIVE_NODE_*>
E ₁₋₂₃	C ₁₋₂	End of algorithm check (while condition)	<ALERT_FINISH_*>
	C ₁₋₃	Final node check (if condition)	<ALERT_ACTIVE_IS_FINAL_*>
E ₂₋₃	C ₂₋₃	Distance and predecessor update	<MSG_SEL_UPDATE_MED_*>
E ₂₋₁₂	C ₂₋₁	Set of adjacents check (for loop)	<ALERT_ADJACENT_*>
	C ₂₋₂	Selection of adjacent	<MSG_SEL_ADJACENT_NODE_*>
Time		Time taken	

E_i and T are normalized as follows:

$$E_{1-1} = \min \left\{ \frac{\text{Number of tags } C_{1-1} \text{ error } (<MSG_SEL_ACTIVE_NODE_ERR>)}{\text{Number of tags } C_{1-1} \text{ correct } (<MSG_SEL_ACTIVE_NODE_MSG>)}, 1 \right\} \quad (1)$$

$$E_{1-23} = \min \left\{ \frac{\text{No. of tags } C_{1-2} \text{ \& } C_{1-3} \text{ errors } (<ALERT_FINISH_ERR> \text{ \& } <ALERT_ACTIVE_IS_FINAL_ERR>)}{\text{No. of tags } C_{1-2} \text{ \& } C_{1-3} \text{ correct } (<ALERT_FINISH_MSG> \text{ \& } <ALERT_ACTIVE_IS_FINAL_MSG>)}, 1 \right\} \quad (2)$$

$$E_{2-3} = \min \left\{ \frac{\text{No. of tags } C_{2-3} \text{ error } (<MSG_SEL_UPDATE_MED_ERR>)}{\text{No. of tags } C_{2-3} \text{ correct } (<MSG_SEL_UPDATE_MED_MSG>)}, 1 \right\} \quad (3)$$

$$E_{2-12} = \min \left\{ \frac{\text{No. of tags } C_{2-1} \text{ \& } C_{2-2} \text{ errors } (<ALERT_ADJACENT_ERR> \text{ \& } <MSG_SEL_ADJACENT_NODE_ERR>)}{\text{No. of tags } C_{2-1} \text{ \& } C_{2-2} \text{ correct } (<ALERT_ADJACENT_MSG> \text{ \& } <MSG_SEL_ADJACENT_NODE_MSG>)}, 1 \right\} \quad (4)$$

$$T = \frac{\text{time taken}}{\text{maximum time}} \quad (5)$$

In an eMathTeacher-compliant tool, algorithm simulation does not continue unless the user enters the correct answer. For this reason, when the quotient in E_i (1), (2), (3) and (4) is greater than or equal to 1, the error rate indicates that the learner has no understanding of the algorithm step, and the data item is truncated at 1.

A Mamdani three-block assessment system

The design of the fuzzy inference system is based on Mamdani's direct method. This method was proposed by Ebrahim Mamdani [Mamdani 1974]. In an attempt to design a control system, he formalized the expert's knowledge by synthesizing a set of linguistic if-then rules. We chose this method because of its simple structure of min-max operations, and its flexibility and simplicity in that it is based on natural language. The fuzzy inference process comprises four successive steps: evaluate the antecedent for each rule, obtain a conclusion for each rule, aggregate all conclusions and, finally, defuzzify.

To better assess the different error types, we divided the FIS into three subsystems, each one implementing the direct Mamdani method, as below.

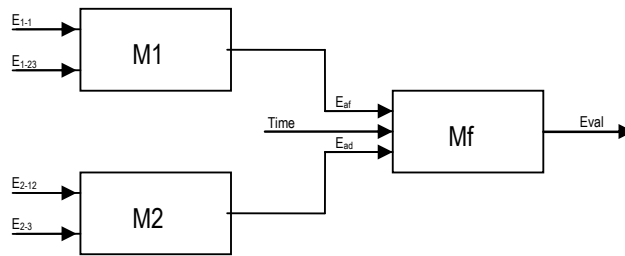


Figure 3. Diagram of FIS design.

In Figure 3, E_{af} , the output of block M1, represents the assessment of errors E_{1-1} and E_{1-23} . Block M2 deals with errors E_{2-12} and E_{2-3} outputting E_{ad} . The time variable T and variables E_{af} and E_{ad} , i.e. the outputs of M1 and M2, respectively, are the inputs for block Mf. Its output is the final assessment.

M1 subsystem

The M1 subsystem sets out to assess node activation and flow control by processing the errors made in the selection of the active node (E_{1-1}) and in the simulation of *while* and *if* statements (E_{1-23}). The result of the assessment will be given by the *activation* and *flow* error (E_{af}) variable, which is the subsystem output. Figure 4 illustrates the membership functions used for the linguistic labels of these variables.

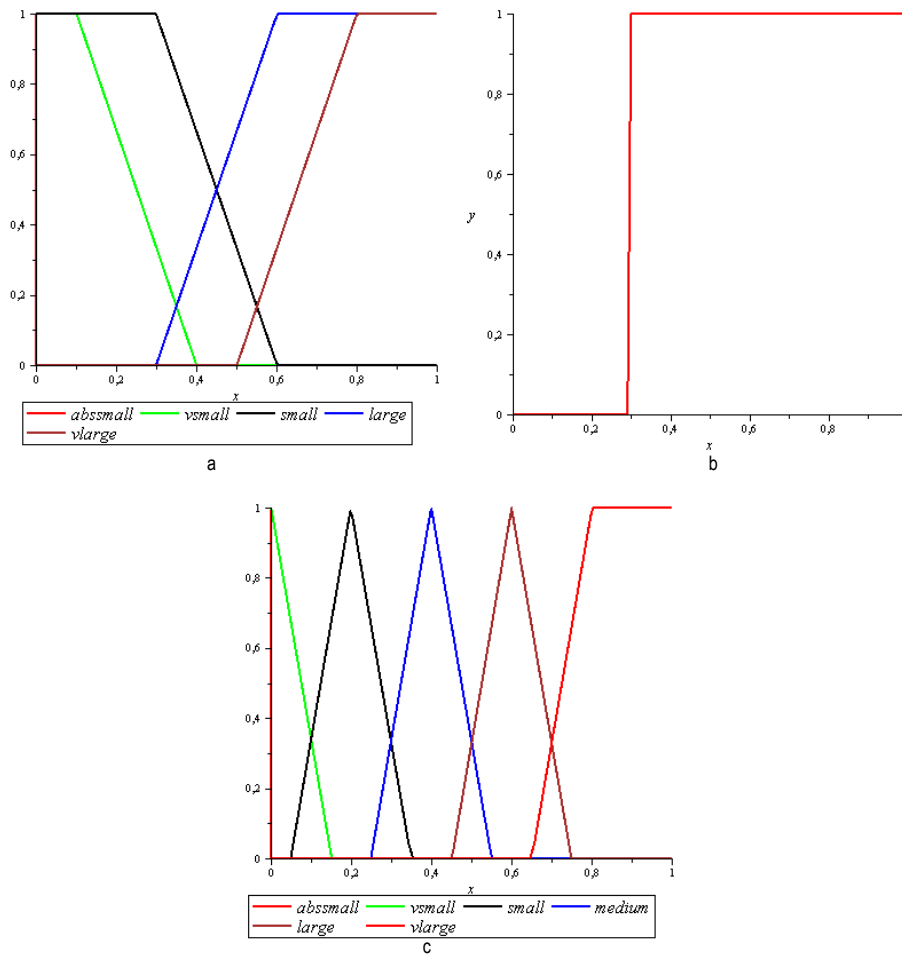


Figure 4. Membership functions for the linguistic labels of the variables E_{1-1} (a), E_{1-23} (b) and E_{af} (c).

The selection of the active node as the node in the unfixed nodes set (E_{1-1}) that is closest to the initial node is a key feature in Dijkstra's algorithm. For this reason, the non-commission of errors of this type is rated highly through the absolutely small label. On the other hand, variable E_{1-23} represents flow control errors. Errors in such actions can be due to either a minor slip or a complete misunderstanding of the algorithm instructions, for which reason only a very small number of errors is acceptable. Otherwise, the overall understanding of the algorithm will be considered to be insufficient. This leads to a very high E_{af} output for values of E_{1-23} strictly greater than 0.29. Additionally the errors are somehow accruable, and a build-up of either of the two types should be penalized.

All these features are reflected in the following rule set:

- IF E_{1-23} is large OR E_{1-1} is very large THEN E_{af} is very large
- IF E_{1-23} is not large AND E_{1-1} is large THEN E_{af} is large
- IF E_{1-23} is not large AND E_{1-1} is small AND E_{1-1} is not absolutely small THEN E_{af} is small
- IF E_{1-23} is not large AND E_{1-1} is very small AND E_{1-1} is not absolutely small THEN E_{af} is very small
- IF E_{1-23} is not large AND E_{1-1} is absolutely small THEN E_{af} is absolutely small

The AND and THEN operators have been implemented by means of the minimum t-norm, whereas the maximum t-conorm has been used for the OR operator and the aggregation method. The Mamdani method usually uses the centroid method to defuzzify the output. As discussed in the section describing Mf subsystem, this method generates information loss problems in the error endpoint values. For this reason, we have decided to use the fuzzy set resulting from the aggregation of the rule conclusions as the subsystem output. In Section "Examples of FIS outcomes", we compare the results of using the aggregation sets as input for the Mf subsystem with the use of the centroid method to calculate a numerical output for subsystems M1 and M2. Figure 5 shows the fuzzy sets resulting from the application of M1 to some values of E_{1-1} y E_{1-23} and their centroids.

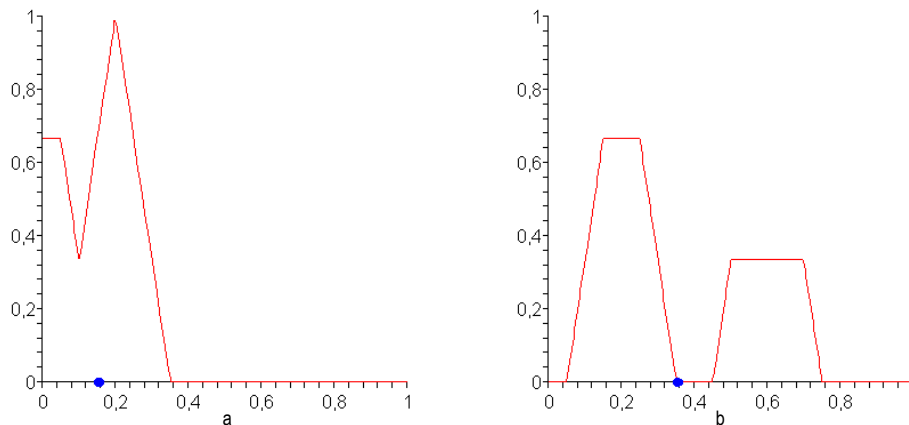


Figure 5. Fuzzy sets resulting from the aggregation in M1 setting $E_{1-1}=1/5$, $E_{1-23}=1/10$ (a) and $E_{1-1}=2/5$, $E_{1-23}=0$ (b) and their centroids.

M2 subsystem

Block M2 deals with error E_{2-12} (adjacent check and selection) and error E_{2-3} (distance and predecessor update), outputting E_{ad} (adjacent management). Figures 6 and 7 illustrate the membership functions used for the linguistic labels of these variables.

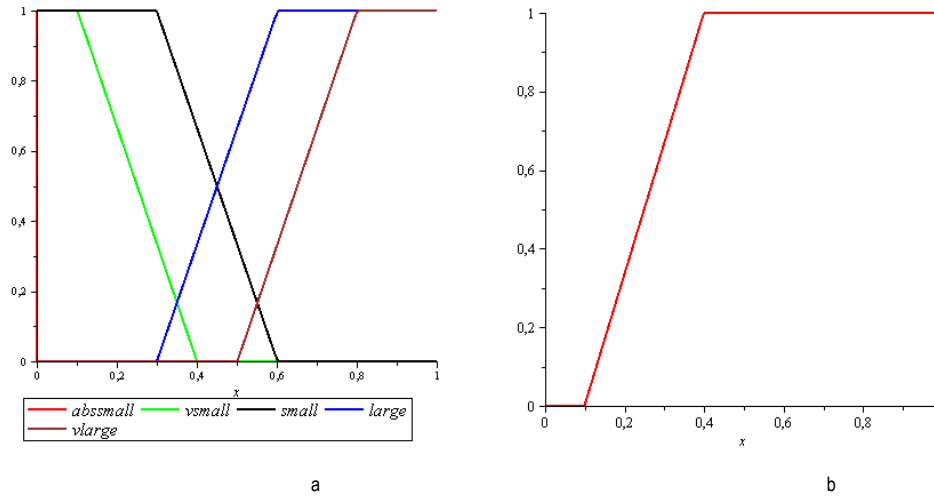


Figure 6. Membership functions for the linguistic labels of the variables E_{2-12} (a), E_{2-3} (b)

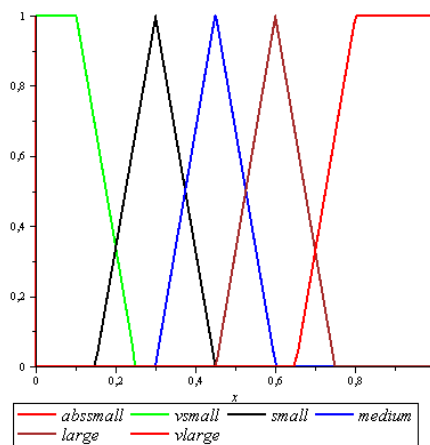


Figure 7. Membership functions for the linguistic labels of the variable E_{ad} .

Some of the rules used in this subsystem are:

- IF E_{2-12} is large THEN E_{ad} is very large
- IF (E_{2-12} is large OR E_{2-3} is very large) AND E_{2-3} is not very small THEN E_{ad} is very large
- IF E_{2-12} is not large AND E_{2-3} is large THEN E_{ad} is large
- IF E_{2-12} is not large AND E_{2-3} is small AND E_{2-3} is not absolutely small THEN E_{ad} is small
- IF E_{2-12} is not large AND E_{2-3} is very small AND E_{2-3} is not absolutely small THEN E_{ad} is very small
- IF E_{2-12} is not large AND E_{2-3} is absolutely small THEN E_{ad} is absolutely small

The AND, THEN and OR operators and the aggregation method are the same as in M1. Figure 8 illustrates the fuzzy sets resulting from the application of M2 to some values of E_{2-12} y E_{2-3} and their centroids.

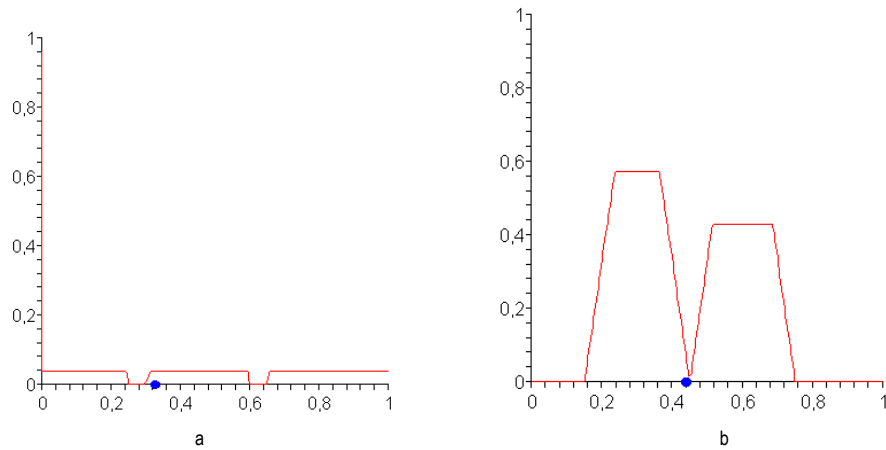


Figure 8. Fuzzy sets resulting from the aggregation in M2 setting $E_{2-12}=2/18$, $E_{2-3}=0$ (a) and $E_{2-12}=0$, $E_{2-3}=3/7$ (b) and their centroids.

Mf subsystem

The time variable T and variables E_{af} (activation and flow control) and E_{ad} (adjacent management), outputs of M1 and M2, respectively, are the inputs for block Mf. Its output is Eval, the final assessment.

Figure 9 illustrates the membership functions used for the linguistic labels of T, E_{af} , E_{ad} and Eval.

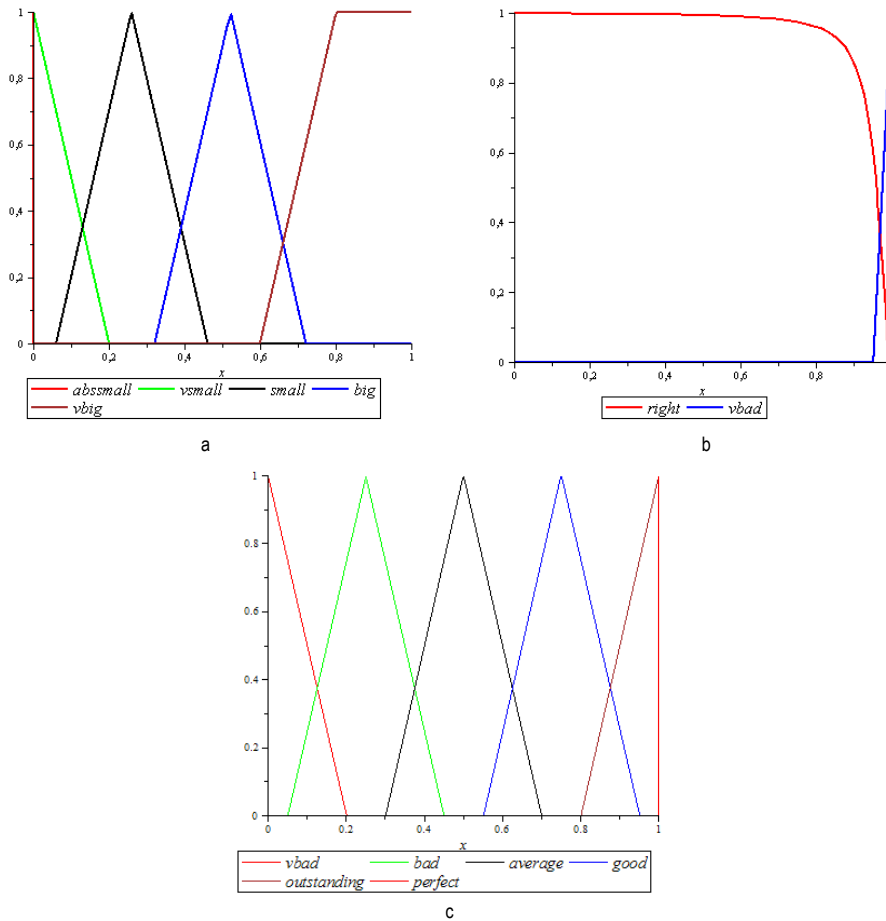


Figure 9. Membership functions for E_{af} (a), E_{ad} (a), Time (b) and Eval (c).

As is well known, Mamdani's direct method for FIS design uses the centroid defuzzification method. We found that this method causes problems with the endpoint values. The absolutely small function in the consequent of M1 and M2 generates a slight deviation from the centroid because its area is 0. When the aggregation contains the above function plus other consequents whose area is different from 0, there is a very sizeable deviation from the centroid, and the system output is disproportionately shifted away from the target value (see Figure 8(a)). To remedy this problem, we have decided to do away with defuzzification in subsystems M1 and M2, and use the fuzzy sets generated by the aggregation of the rules of the above subsystems, M1 and M2, as Mf subsystem inputs [Tanaka 1997]. This corrects the defuzzification-induced information loss in both systems.

This problem resurfaces in the output of Mf, as this output should be numerical, and, therefore, there is nothing for it but to apply defuzzification. As mentioned above, the membership functions of the consequent whose area is 0 lead to an information loss when the centroid method is used for defuzzification. The Mf subsystem has been designed using a crisp perfect function, which returns the output 10 (optimum result of the assessment in the 0-10 range). To remedy the information loss generated by the perfect function, whose area is 0, the centroid has been replaced by a new defuzzification method. This new method [Sánchez-Torrubia et al. 2010] involves implementing a weighted average given by the following equation:

$$Eval = \frac{\sum_i \omega_i c_i}{\sum_i \omega_i}, \text{ with } \omega_i = \max_j (r_{ji} (E_{af}, E_{ad}, T)) \quad (6)$$

where r_{ji} are the maximum heights obtained in the rule conclusions whose membership function in the consequent is f_i , and c_i are defined as follows: $c_{vbad} = 0$, $c_{bad} = 0.25$, $c_{average} = 0.5$, $c_{good} = 0.75$, $c_{outstanding} = 0.9$ and $c_{perfect} = 1$.

Some of the rules used in the final subsystem are:

- IF E_{af} is very large OR E_{ad} is very large THEN Eval is very bad.
- IF T is not right AND E_{af} AND E_{ad} are not very small THEN Eval is very bad.
- IF T is right AND E_{af} AND E_{ad} are large THEN Eval is very bad.
- IF T is right AND E_{af} is large AND E_{ad} is small THEN Eval is bad.
- IF T is right AND E_{af} is small AND E_{ad} is large THEN Eval is bad.
- IF T is right AND E_{af} AND E_{ad} are small THEN Eval is average.
- IF T is right AND E_{af} is very small AND E_{ad} is small AND E_{af} is not absolutely small THEN Eval is good.
- IF T is right AND E_{af} is small AND E_{ad} is very small AND E_{ad} is not absolutely small THEN Eval is good.
- IF T is right AND E_{af} is absolutely small AND E_{ad} is small THEN Eval is good.
- IF T is right AND E_{af} is small AND E_{ad} is absolutely small THEN Eval is good.
- IF T is not very bad AND E_{af} AND E_{ad} are very small AND E_{af} AND E_{ad} are not absolutely small THEN Eval is outstanding.
- IF T is not very bad AND E_{af} is absolutely small AND E_{ad} is very small AND E_{ad} is not absolutely small THEN Eval is outstanding.
- IF T is not very bad AND E_{af} is very small AND E_{ad} is absolutely small AND E_{af} is not absolutely small THEN Eval is outstanding.
- IF T is not very bad AND E_{af} AND E_{ad} are absolutely small THEN Eval is perfect.

Figures 10 and 11 illustrates the performance surfaces of the output of the inference systems. Evalc is output by taking the fuzzy sets resulting from the aggregation in M1 and M2 as inputs for the subsystem Mf, whereas Evalcc is output by taking the centroids of the above sets as inputs for the subsystem Mf and, in both cases by using the

centroid method for final defuzzification. Eval is output by taking the fuzzy sets resulting from the aggregation in M1 and M2 as inputs for the subsystem Mf and using a weighted average (see equation (6)) to defuzzify the output. The surface Evalcc shown in Figure 10 (a) was calculated taking variables E_{af} and E_{ad} and setting $T = 0.8$. The surfaces Evalc and Eval shown in Figures 10 (b) and 11 respectively, were calculated taking variables E_{1-1} and E_{2-3} and setting $E_{1-23} = E_{2-12} = 0.1$ and $T = 0.8$.

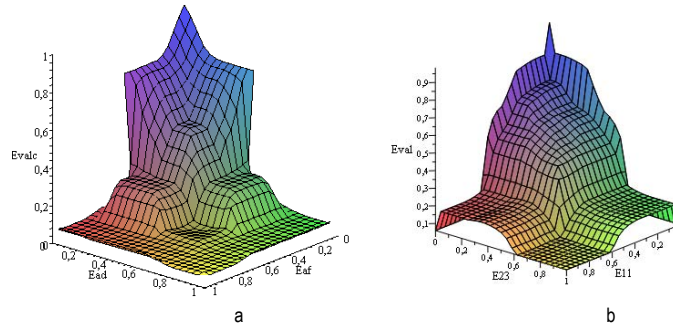


Figure 10. Performance surfaces for Evalcc ($T=0.8$) (a) and Evalc (b) ($E_{1-23}=0.1$, $E_{2-12}=0.1$ and $T=0.8$).

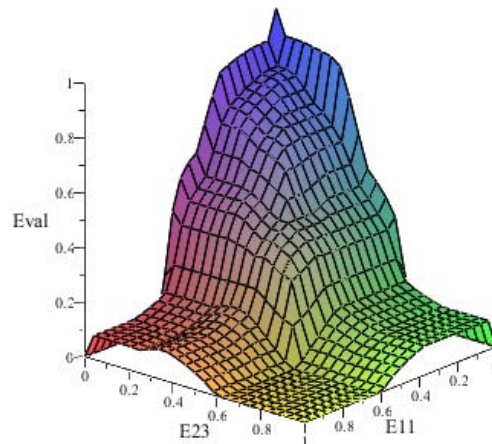


Figure 11. Performance surface for Eval ($E_{1-23}=0.1$, $E_{2-12}=0.1$ and $T=0.8$).

Examples of FIS outcomes

Table 2 shows the assessments that the implemented FIS would output. The last three columns list the outputs of the three implemented systems, Evalcc, Evalc and Eval. Dijkstra's algorithm was simulated by the students on several graphs to output these data.

When $E_{2-12} = 2/18$ and $E_{2-3} = 0$, the centroid returns a disproportionately high error value (see Figure 8 (a)), as, in subsystem M2, the area of the absolutely small function is 0 and other rules are triggered that do produce area. This causes assessment Evalcc (5.6) to be much lower than Evalc (7.6) while Eval returns 8.4, as shown in Table 2 (see row 5). Eval is the closest to the instructor's assessment, as there is only one big mistake.

Table 2. Error rates and assessment system outputs in a 0-10 range.

E_{1-1}	E_{1-23}	E_{2-12}	E_{2-3}	time	Evalcc	Evalc	Eval
0/7	0/15	0/28	0/11	0.8	10	10	10
0/9	0/19	1/40	0/16	0.6	10	10	10
0/9	0/19	2/40	3/16	0.8	7.7	8.1	8.9
1/5	1/10	2/18	0	0.8	5.6	7.6	8.4
1/9	1/19	0/40	1/16	0.7	7.1	6.8	8.1
2/9	0/19	0/40	1/16	0.7	7.1	6.7	7.8
1/7	0/15	0/28	3/11	0.8	5.9	5.7	6.7
3/7	0/15	0/28	0/11	0.8	7.5	6.1	5.7
3/7	0/15	0/28	1/11	0.8	5.9	5.1	5
2/5	0	0	3/7	0.8	2.8	4.6	4.2
4/9	0/19	0/40	6/16	0.8	3.3	4.6	4.1
5/9	1/19	1/40	1/16	0.7	2.5	3.6	3.3
5/7	0/15	0/28	3/11	0.8	0.6	1.9	1.1
2/7	0/15	0/28	11/11	0.8	0.6	1.9	1.1
7/7	0/15	0/28	3/11	0.8	0.6	1.8	0.9
6/7	2/15	7/28	8/11	0.7	0.6	0.6	0

Looking at row 11, both centroids, especially, the centroid of subsystem M2, return fairly high errors ($E_{af} = M1(2/5, 0) = 0.36$, see Figure 5 (b) and $E_{ad} = M2(0, 3/7) = 0.44$, see Figure 8 (b)). For this reason, they trigger the rules in Mf whose antecedent membership functions include not very small and small, but large. This has the effect of shifting the consequent to the left (as the consequent in the rules that are triggered is bad) and, therefore, lowers the assessment disproportionately.

Generally speaking, Eval is much closer to the instructor's assessment than the other two implemented systems and the distribution of the grades is also better. The defuzzification-induced information loss due to the centroid method has been corrected by using the fuzzy sets resulting from the aggregation in M1 and M2 as inputs for the subsystem Mf and the weighted average as final defuzzification method.

Conclusions and further work

In this paper, we presented the design and implementation of three fuzzy inference systems, based on Mamdani's direct method. These systems automatically assess the interaction log of students with the machine when simulating Dijkstra's algorithm (medium-level) in GRAPHS environment. After running several tests we are able to state that the results of the assessment obtained by the Eval system are quite similar to the grades that a teacher would award. We have also examined the problems caused by information losses due to the use of the centroid as the defuzzification method. These problems were resolved, in subsystems M1 and M2, by using the fuzzy sets output by aggregation and in subsystem Mf by using a weighted average as the final defuzzification method.

As the automatic assessment system depends on the error codes and they are different at each algorithm level, each one will have its own FIS in the future. Furthermore, in future research these systems will be integrated into the GRAPHS tool.

Acknowledgements

This work is partially supported by CICYT (Spain) under project TIN2008-06890-C02-01 and by UPM-CAM.

Bibliography

- [Bai, Chen 2008] S.M. Bai, S.M. Chen. Evaluating students' learning achievement using fuzzy membership functions and fuzzy rules. *Expert Syst. Appl.* 34, 399–410, 2008.
- [Bellman 1957] R.E. Bellman. *Dynamic Programming*. Princeton University Press, Princeton, NJ, 1957
- [Dijkstra 1959] E. Dijkstra. A note on two problems in connexion with graphs. *Numerische Mathematik*, 1, 269–271, 1959.
- [Hundhausen et al. 2002] C.D. Hundhausen, S.A. Douglas and J.T. Stasko. A Meta-Study of Algorithm Visualization Effectiveness. *J. Visual Lang. Comput.* 13(3), 259–290, 2002.
- [Law 1996] C.K. Law. Using fuzzy numbers in educational grading system. *Fuzzy Set Syst.* 83, 311–323, 1996
- [Mamdani 1974] E.H. Mamdani. Application of Fuzzy Algorithms for Control of Simple Dynamic Plant. *Proc. IEEE* 121(12), 1585–1588, 1974.
- [Sánchez-Torrubia, Lozano-Terrazas 2001] M.G. Sánchez-Torrubia and V.M. Lozano-Terrazas. Algoritmo de Dijkstra: Un tutorial interactivo. In *Proc. VII Jornadas de Enseñanza Universitaria de la Informática (Palma de Mallorca, Spain, July 16 – 18, 2001)*. 254-258, 2001.
- [Sánchez-Torrubia et al. 2010] M.G. Sánchez-Torrubia, C. Torres-Blanc and S. Cubillo. Design of a Fuzzy Inference system for automatic DFS & BFS algorithm learning assessment. In *Proc. 9th Int. FLINS Conf. on Found. and Appl. of Comp. Intell. (Chengdu, China, August 2 – 4, 2010)*, (in print), 2010.
- [Sánchez-Torrubia et al. 2008] M.G. Sánchez-Torrubia, C. Torres-Blanc and S. Krishnankutty. Mamdani's fuzzy inference eMathTeacher: a tutorial for active learning. *WSEAS Transactions on Computers*, 7(5), 363–374, 2008.
- [Sánchez-Torrubia et al. 2009 (a)] M.G. Sánchez-Torrubia, C. Torres-Blanc and M.A. López-Martínez. PathFinder: A Visualization eMathTeacher for Actively Learning Dijkstra's algorithm. *Electronic Notes in Theoretical Computer Science*, 224, 151–158, 2009.
- [Sánchez-Torrubia et al. 2009 (b)] M.G. Sánchez-Torrubia, C. Torres-Blanc and L. Navascués-Galante. EulerPathSolver: A new application for Fleury's algorithm simulation. In *New Trends in Intelligent Technologies*, L. Mingo, J. Castellanos, K. Markov, K. Ivanova, I. Mitov, Eds. *Information Science and Computing* 14, 111-117, 2009
- [Sniedovich 2006] M. Sniedovich. Dijkstra's algorithm revisited: the dynamic programming connection. *Control and Cybernetics*, 35 (3), 599–620, 2006
- [Tanaka 1997] K. Tanaka. *An introduction to fuzzy logic for practical applications*. Springer-Verlag, 1997.
-

Authors' Information

Gloria Sánchez-Torrubia – Facultad de Informática, Universidad Politécnica de Madrid, Campus de Montegancedo s.n., 28660 Boadilla del Monte, Madrid, Spain; e-mail: gsanchez@fi.upm.es

Carmen Torres-Blanc – Facultad de Informática, Universidad Politécnica de Madrid, Campus de Montegancedo s.n., 28660 Boadilla del Monte, Madrid, Spain; e-mail: ctorres@fi.upm.es

A SURVEY OF NONPARAMETRIC TESTS FOR THE STATISTICAL ANALYSIS OF EVOLUTIONARY COMPUTATIONAL EXPERIMENTS

Rafael Lahoz-Beltra, Carlos Perales-Gravan

Abstract: One of the main problems in the statistical analysis of Evolutionary Computation (EC) experiments is the 'statistical personality' of data. A main feature of EC algorithms is the sampling of solutions from one generation to the next. Sampling is based on Holland's schema theory, having a greater probability to be chosen those solutions with best-fitness (or evaluation) values. In consequence, simulation experiments result in biased samples with non-normal, highly skewed, and asymmetric distributions. Furthermore, the main problem arises with the noncompliance of one of the main premises of the central limit theorem, invalidating the statistical analysis based on the average fitness \bar{f} of the solutions. In this paper, we address a tutorial or 'How-to' explaining the basics of the statistical analysis of data in EC. The use of nonparametric tests for comparing two or more medians combined with Exploratory Data Analysis is a good option, bearing in mind that we are only considering two experimental situations that are common in EC practitioners: (i) the performance evaluation of an algorithm and (ii) the multiple experiments comparison. The different approaches are illustrated with different examples (see <http://bioinformatica.net/tests/survey.html>) selected from Evolutionary Computation and the related field of Artificial Life.

Keywords: Evolutionary Computation, Statistical Analysis and Simulation.

ACM Classification Keywords: G.3 PROBABILITY AND STATISTICS

Conference topic: Evolutionary Computation.

Introduction

Evolutionary Computation (EC) refers to a class of stochastic optimization algorithms inspired in the evolution of organisms in Nature by means of Darwinian natural selection [Lahoz-Beltra, 2004][Lahoz-Beltra, 2008]. Nowadays, this class of algorithms is applied in many diverse areas, such as scheduling, machine learning, optimization, electronic circuit design [Lahoz-Beltra, 2001][Perales-Gravan and Lahoz-Beltra, 2008], pattern evolution in biology (i.e. zebra skin pattern) [Perales-Gravan and Lahoz-Beltra, 2004], etc. All methods in EC are *bioinspired* in the fundamental principles of neo-Darwinism, evolving a set of potential solutions by a selection procedure to sort candidate solutions for breeding. At each generation, a new set of solutions is selected for reproduction, contributing with one or more copies of the selected individuals to the offspring representing the next generation. The selection is carried out according to the goodness or utility of the solutions x_i , thus calculating the values $f(x_i)$ which are known as fitness values. Once the selection has concluded, the next generation of solutions is transformed by the simulation of different genetic mechanisms (Fig. 1). The genetic mechanisms are mainly crossover or recombination (combination of two solutions) and/or mutation (random change of a solution). These kinds 'genetic procedures' evolve a set of solutions, generation after generation, until a set of solutions is obtained with one of them representing an optimum solution. Genetic algorithms, evolutive algorithms, genetic programming, etc. are different types of EC algorithms. However all of them share with some variations the following general steps:

1. Generate at random an initial set of solutions $x_i \in S(0)$.
2. Evaluate the fitness of each solution $f(x_i)$.
3. Select the best-fitness solutions to reproduce.
4. Breed a new generation ($t=t+1$) of solutions $S(t)$ through crossover and/or mutation and give birth to offspring.
5. Replace a part of solutions with offspring.
6. Repeat 2-5 steps until {terminating condition}.

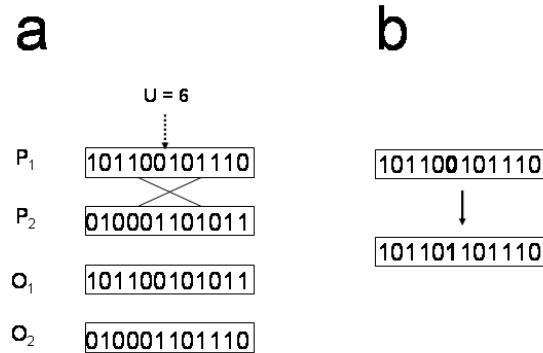


Figure 1.- Evolutionary Computation methods are based on genetic mechanisms simulation such as crossover and/or mutation. In (a) crossover two parental solutions represented in 1D-arrays called chromosomes (P_1 and P_2) exchange their segments (in this example, U is the one-point crossover randomly selected) obtaining two recombinant solutions, O_1 and O_2 , thus the offspring solutions. However, in (b) mutation a random 'genetic' change occurs in the solution, in this example replacing or inverting in position 6 a bit value 0 by 1.

However, at present EC methods lack of a general statistical framework to compare their performance [Czarn et al., 2004] and evaluate the convergence to the optimum solution. In fact, most EC practitioners are satisfied with obtaining a simple performance graph [Goldberg, 1989][Davis, 1991] displaying the x -axis the number of generation, simulation time or epoch and the y -axis the average fitness per generation (other such possibilities exist such as the maximum fitness per generation at that point in the run).

One of the main problems in the statistical analysis of EC experiments is the 'statistical personality' of data. The reason is that selection of the best-fitness solutions generation after generation leads to non-normal, highly skewed, and asymmetric distributions of data (Fig. 2). At present, there are many available techniques that are common in EC algorithms to select the solutions to be copied over into the next generation: fitness-proportionate selection, rank selection, roulette-wheel selection, tournament selection, etc. A main feature of selection methods is that all of them generate new random samples of solutions x_1, x_2, \dots, x_N but *biased* random samples. Thus, solutions are chosen at random but according to their fitness values $f(x_i)$, having a greater probability to be chosen those x_i solutions with the best-fitness values. The consequence is that EC algorithms select the solutions x_1, x_2, \dots, x_N (or sample) from one generation to the next based on Holland's schema theory [Holland, 1992]. This theorem – the most important theorem in EC- asserts the following: the number $m(H)$ of 'short' (distance between the first and last positions) and 'low-order' (number of fixed positions) solutions H (called *schema*) with above-average fitness $f(H)$ increase exponentially in successive generations:

$$m(H, t + 1) \geq \frac{m(H, t) \cdot f(H)}{\bar{f}(t)} [1 - p] \quad (1)$$

where $\bar{f}(t)$ is the average fitness of the set of solutions at time t , and p is the probability that crossover or mutation will destroy a solution H .

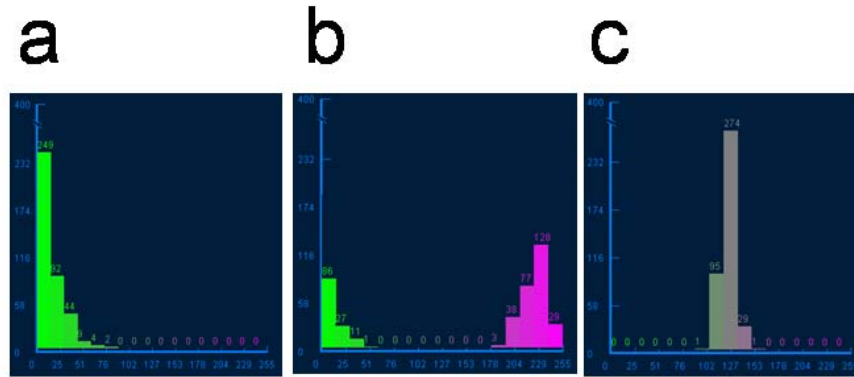


Figure 2.- Darwinian natural selection modes (see Manly, 1985). (a) Directional selection, (b) disruptive, and (c) stabilizing selection. Histograms were obtained with EvoTutor selection applet (see <http://www.evotutor.org/TutorA.html>).

The main statement and motivation of the present paper is as follows. EC practitioners frequently use parametric methods such as t -student, ANOVA, etc. assuming that x_1, x_2, \dots, x_N sample is a sequence of independent and identically distributed values (i.i.d.). In such cases, the non-compliance of one of the main premises of the central limit theorem (CLT), invalidate the statistical analysis based on the average fitness \bar{f} of the solutions x_1, x_2, \dots, x_N :

$$\bar{f} = \frac{f(x_1) + f(x_2) + \dots + f(x_N)}{N} \quad (2)$$

In consequence, there is no convergence of $\sqrt{N}(\bar{f} - \mu)$ towards the standard normal distribution $N(0, \sigma^2)$. We suggest that nonparametric tests for comparing two or more medians could provide a simple statistical tool for the statistical analysis of data in EC. Furthermore, since important assumptions about the underlying population are questionable and the fitness values of the solutions can be put in order, thus $f(x_1), f(x_2), \dots, f(x_N)$ are ranked data, then the statistical inference based on ranks [Hettmansperger, 1991] provide a useful approach to compare two or more populations.

In the present paper and according with the above considerations, we illustrate how the statistical analysis of data in EC experiments could be addressed using assorted study cases and general and simple statistical protocols. The protocols combine the Exploratory Data Analysis approach, in particular Box-and-Whisker Plots [Tukey, 1977], with simple nonparametric tests [Siegel and Castellan, 1988][Hollander and Wolfe, 1999][Gibbons and Chakraborti, 2003]. The different approaches are illustrated with different examples chosen from Evolutionary Computation and Artificial Life [Prata, 1993][Lahoz-Beltra, 2008].

Performance analysis and comparison of EC experiments

Most of the general research with EC algorithms usually addresses two type of statistical analysis (Table I).

Table I.- Statistical analysis protocols in Evolutionary Computation

Performance evaluation	Robust Performance Graph Statistical Summary Table		
Simulation experiments comparison	$K_e = 2 \text{ experiments}$	Multiple Notched Box-and-Whisker Plot	$\sigma_i = \sigma_j$ Mann-Whitney (Wilcoxon) test
		Statistical Summary Table	$\sigma_i \neq \sigma_j$ Studentized Wilcoxon test
	$K_e > 2 \text{ experiments}$	Multiple Notched Box-and-Whisker Plot Statistical Summary Table Kruskal-Wallis test Dunn's post-test	

The evaluation of the algorithm performance is one of the most common tasks in EC experiments. In such a case, the evaluation could be carried out combining a robust performance graph with a statistical summary table. A robust performance graph is as a plot with the x-axis displaying the number of generation, simulation time or epoch, depicting for each generation a Notched Box-and-Whisker Plot [McGill et al., 1978]. The Notched Box-and-Whisker Plot shows the distribution of the fitness values of the solutions, displaying the y-axis the scale of the batch of data, thus the fitness values of the solutions. The statistical summary table should include the following descriptive statistics: the average fitness or other evaluation measure (i.e. mean distance, some measure of error) computed per generation, the median and the variance of the fitness, as well as the minimum, maximum, Q_1 , Q_3 , the interquartile range (IQR), and the standardized skewness and standard kurtosis.

Comparative studies are common in simulation experiments with EC algorithms. In such a case researchers use to compare different experimental protocols, genetic operators (i.e. one-point crossover, two-points crossover, uniform crossover, arithmetic crossover, heuristic crossover, flip-a-bit mutation, boundary mutation, Gaussian mutation, roulette selection, tournament selection, etc.) and parameter values (i.e. population size, crossover probability, mutation probability). According to tradition, a common straightforward approach is the performance graph comparison. In this approach, practitioners have a quick look at the plot lines of different simulation experiments, without any statistical test to evaluate the significance or not of performance differences. In the case of two experiments ($k_e=2$) with non-normal data, the statistical comparison could be addressed resorting to a Multiple Notched Box-and-Whisker Plot, the statistical summary table and a Mann-Whitney (Wilcoxon) test [Mann and Whitney, 1947]. The statistical summary table (i.e. IQR or the box length in the Box-and-Whisker Plot) is important since differences in population medians are often accompanied by other differences in spread and shape, being not sufficient merely to report a p value [Hart, 2001]. Note that Mann-Whitney (Wilcoxon) test assumes two populations with continuous distributions and similar shape, although it does not specify the shape of the distributions. The Mann-Whitney test is less powerful than t -test because it converts data values into ranks, but more powerful than the median test [Mood, 1954] presented in many statistical textbooks and popular statistical software packages (SAS, SPSS, etc.). Freidlin and Gastwirth [Freidlin and Gastwirth, 2000] suggested that the median test should be "retired" from routine use, showing the loss of power of this test in the case of highly unbalanced samples. Nevertheless, EC simulation experiments are often designed with balanced samples. It is important to note that in this tutorial, we only consider the case of two EC experiments where distributions may differ only in medians. However, when testing two experiments ($k_e=2$) researchers should take care of the

statistical analysis under heteroscedasticity. For instance, Table XIII (see <http://bioinformatica.net/tests/survey.html>) shows three simulation experiments (*study case 5*) with significant differences among variances. In such a case, if our goal were for testing the significance or not of performance of two simulation experiments a studentized Wilcoxon test [Fung, 1980] should be used instead the Mann-Whitney test.

In the case of more than two experiments ($k_e > 2$) with non-normal data the Multiple Box-and-Whisker Plot and the statistical summary table can be completed making inferences with a Kruskal-Wallis test [Kruskal and Wallis, 1952]. This approach can be applied even when variances are not equal in the k simulation experiments. In such a case, thus under heteroscedasticity, medians comparisons also could be carried out using the studentized Brown and Mood test [Fung, 1980] as well as the S-PLUS and R functions introduced by Wilcox [Wilcox, 2005][Wilcox, 2006]. However, the loss of information involved in substituting ranks for the original values makes this a less powerful test than an ANOVA. Once again, the statistical summary table is important, since the Kruskal-Wallis test assumes a similar shape in the distributions, except for a possible difference in the population medians. Furthermore, it is well suited to analyzing data when outliers are suspected. For instance, solutions with fitness values laying more 3.0 times the IQR. If the Kruskal-Wallis test is significant then we should perform multiple comparisons [Hochberg and Tamhane, 1987] making detailed inferences on $\binom{k_e}{2}$ pairwise simulation experiments. One possible approach to making such multiple comparisons is the Dunn's post-test [Dunn, 1964].

The Box-and-Whisker plot

The Box-and-Whisker Plot, or boxplot, was introduced by Tukey [Tukey, 1977] as a simple but powerful tool for displaying the distribution of univariate batch of data. A boxplot is based on five number summary: minimum (Min), first quartile (Q_1), median (Me), third quartile (Q_3), and maximum (Max). One of the main features of a boxplot is that is based on robust statistics, being more resistant to the presence of outliers than the classical statistics based on the normal distribution. In a boxplot [Frigge et al., 1989; Benjamini, 1988] a central rectangle or box spans from the first quartile to the third, representing the interquartile range ($IQR = Q_3 - Q_1$, where $IQR = 1.35\sigma$ for data normally distributed), which covers the central half of a sample. In the simplest definition, a central line or segment inside the box shows the median, and a plus sign the location of the sample mean. The whiskers that extend above (upper whisker) and below (lower whisker) the box illustrate the locations of the maximum ($Q_3 + k(Q_3 - Q_1)$) and the minimum ($Q_1 - k(Q_3 - Q_1)$) values respectively, being usually $k = 1.5$. In consequence, small squares or circles (its depend on the statistical package) outside whiskers represent values that lie more than 1.5 times the IQR above or below the box, whereas those values that lie more 3.0 times the IQR are shown as small squares or circles sometimes including a plus sign. Usually, the values that are above or below $3 \times IQR$ are considered outliers whereas those above or below $1.5 \times IQR$ are suspected outliers. However, outlying data points can be displayed using a different criterion, i.e. unfilled for suspected outlier and filled circles for outliers, etc. Boxplots can be used to analyze data from one simulation experiment or to compare two or more samples from different simulation experiments, using medians and IQR during analysis without any statistical assumptions. It is important to note that a boxplot is a type of graph that shows information about: (a) location (displayed by the line showing the median), (b) shape (skewness by the deviation of the median line from box central position as well as by the length of the upper whisker in relation with length of the lower one), and (c) variability of a distribution (the length of the box, thus the IQR value, as well as the distance between the end of the whiskers).

A slightly different form boxplot is the Notched Box-and-Whisker Plot or notched boxplot [McGill et al., 1978]. A notched boxplot is a regular boxplot including a notch representing an approximate confidence interval for the

median of the batch of data. The endpoints of the notches are located at the median $\pm 1.5 \frac{IQR}{\sqrt{n}}$ such that the

medians of two boxplots are significantly different at approximately the 0.05 level if the corresponding notches do not overlap. It is important to note that sometimes a 'folding effect' is displayed at top or bottom of the notch. This folding can be observed when the endpoint of a notch is beyond its corresponding quartile, occurring when the sample size is small.

In the following site <http://bioinformatica.net/tests/survey.html> we describe how the statistical analysis of six selected study cases was accomplished using the statistical package STATGRAPHICS 5.1 (Statistical Graphics Corporation), excepting the Dunn test which was performed using Prisma® (Graph Pad Software, Inc.) software. In this web site we included the study cases explanation as well as the statistical summary Tables of this paper.

Hands-on statistical analysis

Statistical performance

The Fig. 3 shows a robust performance graph obtained with a simple genetic algorithm (*study case 1*). Note how the performance has been evaluated based on a sequential set of Notched Box-and-Whisker Plots, one boxplot per generation. The dispersion measured with the IQR of the fitness values decreases during optimization, being the average fitness per generation, thus the classical performance measure in genetic algorithms, greater or equal to the median values during the first six generations. After the sixth generation some chromosomes have an outlying fitness value. Maybe some of them, i.e. those represented in generations 8 and 10, would be representing optimal solutions. The Table IV summarizes the minimum and maximum fitness, the mean fitness, median fitness and the IQR values per generation.

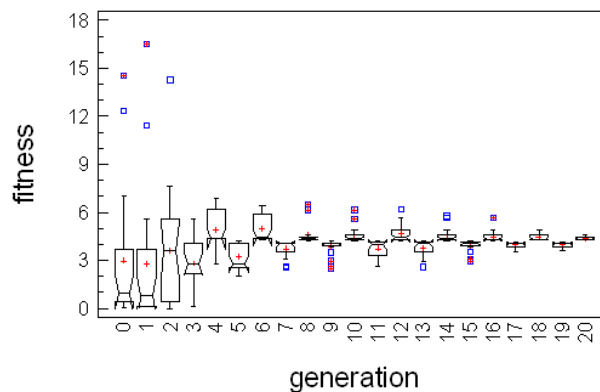


Figure 3.- Robust performance graph in a simple genetic algorithm showing the medians (notches) and means (crosses) of the fitness. Squares and squares including a plus sign indicate suspected outliers and outliers respectively.

The performance of the second and third study cases was evaluated using the Hamming and Euclidean distances. Such distances are useful when the individuals in the populations are defined by binary and integer chromosomes, respectively. In particular, in the *study case 2*, thus the experiment carried out with the ant population, since ants are defined by a 10 bits length chromosome, a robust performance graph (Fig. 4) is obtained based on the Hamming distance. The Kruskal-Wallis test (Table V) shows with a p -value equal to 0.0384 that there is a statistically significant difference among medians at the 95.0% confidence level. Note that the Multiple Box-and-Whisker Plot (Fig. 4) shows an overlapping among notches. At first glance, we perceive an

overlapping among the 0, 1, 2 and 3 sample times, and between 4 and 5 sample times. Table VI summarizes the genetic drift, thus the average Hamming distance per generation, the median and the variance of the Hamming distance, as well as the minimum, maximum, Q_1 , Q_3 , IQR and the standardized skewness and standard kurtosis. The special importance is how the genetic drift decreases with the sample time, illustrating the population evolution towards the target ant. Genetic drift values are related with the Hamming ball of radius r , such that with $r=2$ the number of ants with distance $d(a,t) \leq 2$ increases with sample time (Table VII). An important fact is the similar shapes of distributions, according to one of the main assumptions of the Kruskal-Wallis test. In particular, for any sample time the standard skewness (Table VI) is lesser than zero. Thus, the distributions are all asymmetrical showing the same class of skewed tail.

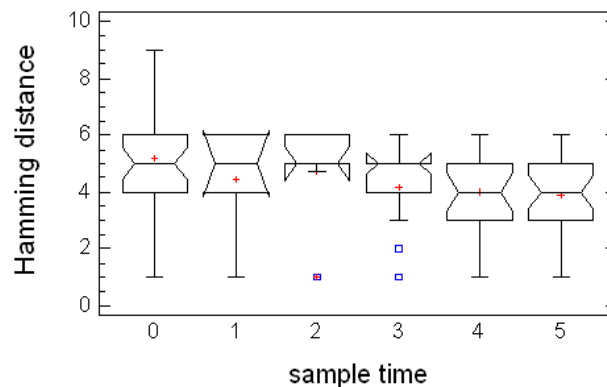


Figure 4.- Robust performance graph in the ant population evolution experiment showing the medians (notches) and means (crosses) of the Hamming distance. Squares and squares including a plus sign indicate suspected outliers and outliers respectively.

The Fig. 5 shows the robust performance graph obtained in the third *study case*, thus the simulation of evolution in Dawkin's biomorphs (Fig. 6).

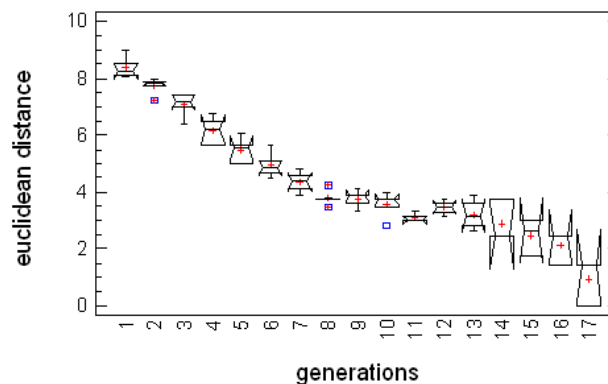


Figure 5.- Robust performance graph in the Dawkin's biomorphs evolution experiment showing the medians (notches) and means (crosses) of the Euclidean distance. Squares and squares including a plus sign indicate suspected outliers and outliers.

Since each biomorph is defined by a chromosome composed of 8 integer values, the performance graph is based on the Euclidean distance. The performance graph shows how the medians as well as the average of the Euclidean distances per generation (or genetic drift) become smaller as a consequence of the convergence of the population towards a target biomorph. Table VIII summarizes the genetic drift, thus the average of the Euclidean

distance computed per generation, the median and the variance of the Euclidean distance, as well as the minimum, maximum, Q_1 , Q_3 , IQR, and the standardized skewness and standard kurtosis. Note how in this case the different shape of the distributions, thus the different sign of the standardized skewness values, breaks one of the main assumptions in the Kruskal-Wallis test.

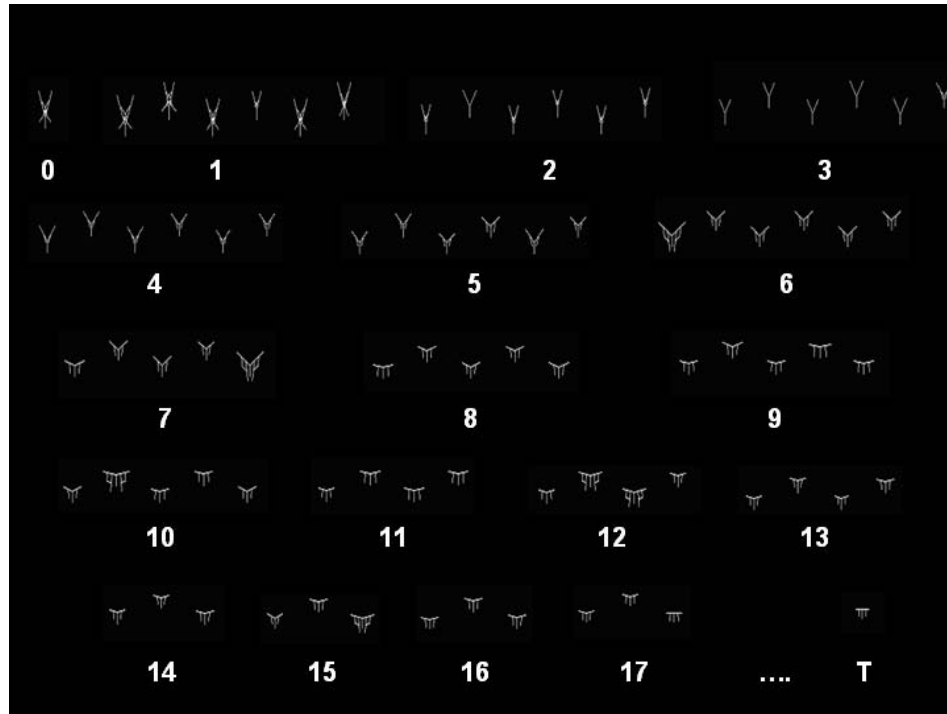


Figure 6.- Dawkin's biomorphs evolution during 17 generations showing T the target biomorph.

Statistical comparisons

Using the SGA program three simulation experiments were carried out (*study case 4*) representing in a Multiple Notched Box-and-Whisker Plot (Fig. 7) the obtained results.

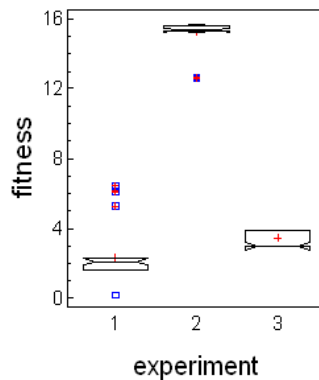


Figure 7.- Multiple Notched Box-and-Whisker Plot showing the medians (notches) and means (crosses) of the fitness in three different SGA experiments. Squares and squares including a plus sign indicate suspected outliers and outliers.

Table IX summarizes the mean, median and variance of the fitness, as well as the minimum, maximum, Q_1 , Q_3 , IQR, and the standardized skewness and standard kurtosis. A first statistical analysis compares the genetic algorithm experiment with crossover and mutation probabilities of 75% and 5% (first experiment) and the genetic algorithm without mutation and crossover with a probability of 75% (second experiment). Since the standardized skewness and standard kurtosis (Table IX) do not belong to the interval $[-2, 2]$ then it suggests that data do not come from a Normal distribution. In consequence, we carried out a Mann-Whitney (Wilcoxon) test to compare the medians of the two experiments. The Mann-Whitney test (Table X) shows with a p -value equal to zero that there is a statistically significant difference between the two medians at the 95.0% confidence level. Finally, we compared the three experiments together, thus the first and second simulation experiments together with a third one consisting in a genetic algorithm with only mutation with a probability equal to 5%. A Kruskal-Wallis test was carried out comparing the medians of the three experiments, with Dunn's post-test for comparison of all pairs. The Kruskal-Wallis test (Table XI) shows with a p -value equal to zero that there is a statistically significant difference among medians at the 95.0% confidence level. In agreement with the Dunn test (Table XII) all pairs of experiments were significant, considering the differences with the value $p < 0.05$ statistically significant. The statistical analysis results illustrate the importance and role of the crossover and mutation in an optimization problem.

The statistical analysis of the three TSP simulation experiments performed with ACO algorithm (*study case 5*), was similar to the protocol for the SGA experiments (*study case 4*). Fig. 8 shows the obtained results represented in a Multiple Notched Box-and-Whisker Plot, and Table XIII summarizes the mean, median and variance of the tour length, as well as the minimum, maximum, Q_1 , Q_3 , IQR, and the standardized skewness and standard kurtosis. In the case of the second experiment the standardized skewness and standard kurtosis do not belong to the interval $[-2, 2]$ suggesting that data do not come from a Normal distribution.

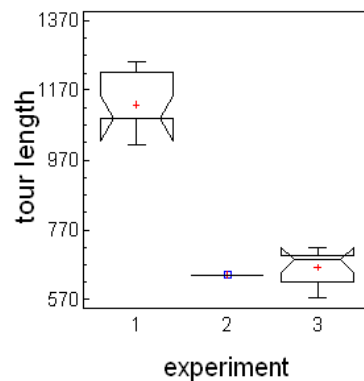


Figure 8.- Multiple Notched Box-and-Whisker Plot showing the medians (notches) and means (crosses) of the tour length in three different TSP experiments carried out with ACO algorithm.

Furthermore, in agreement with Table XIII and the statistical tests we carried out for determining homoscedasticity or variance homogeneity, thus whether significant differences exist among the variances σ_1^2 , σ_2^2 and σ_3^2 of the three ACO experiments (Fig. 9), we concluded that variances were very different. Since the p -values for Cochran's C test and Bartlett test were both lesser than 0.05, in particular 0.0016 and 0.0000 respectively, we concluded that variance differences were statistically significant. Once again, a Kruskal-Wallis test was carried out comparing the medians of the three experiments, with Dunn's post-test for comparison of all pairs. The Kruskal-Wallis test (Table XIV) shows with a p -value equal to zero that there is a statistically significant difference among medians at the 95.0% confidence level. In agreement with the Dunn test (Table XV) the first

TSP tour experiment significantly differs from the second and third TSP tours, whereas the differences observed between the second TSP tour and third one are not significant, considering the differences with the value $p < 0.05$ as statistically significant. No matter such differences, the best tour in the first, second and third simulation experiments were as follows: 5-4-3-2-1-0-9-8-7-6 with a tour length equal to 984.04, 7-5-4-3-0-1-9-2-8-6 with a tour length equal to 641.58, and 9-0-4-2-1-3-7-5-6-8 with a tour length equal to 576.79, respectively.

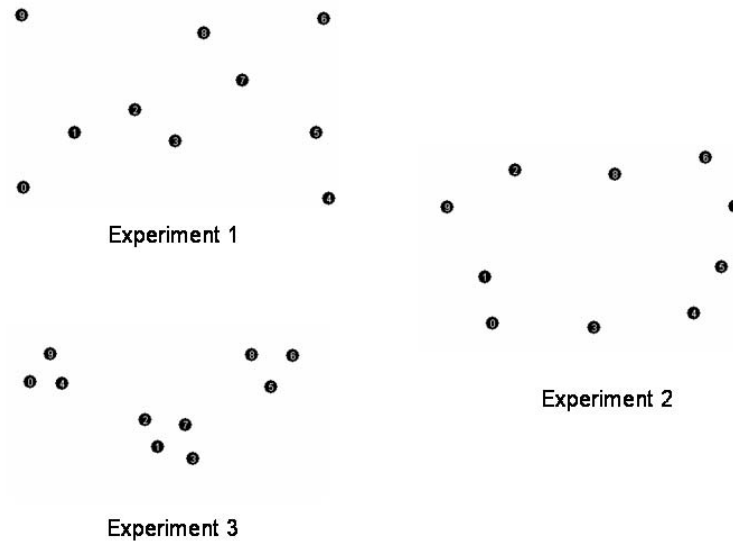


Figure 9.- Three different simulation experiments performed with ACO algorithm of the popular TSP experiment with ten cities labeled from 0 to 9.

The symbolic regression experiment (*study case 6*) illustrates once again the general protocol continued with the SGA and ACO experiments. The Fig. 10 shows the obtained results represented in a Multiple Notched Box-and-Whisker Plot, and Table XVI summarizes the mean, median and variance of the fitness –calculated using the error between the approximated and the target functions-, as well as the minimum, maximum, Q_1 , Q_3 , IQR, and the standardized skewness and standard kurtosis. Note that the best 'genetic protocol' is used in the first simulation experiment (Fig. 10).

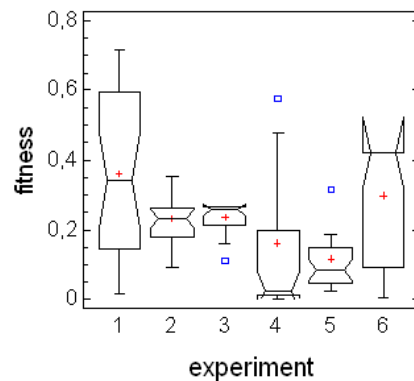


Figure 10.- Multiple Notched Box-and-Whisker Plot showing the medians (notches) and means (crosses) of the fitness in six different simulation experiments carried out with a symbolic regression problem. The problem consisted in the search of an approximation of $3x^4 - 3x + 1$ function. Squares indicates suspected outliers.

carried out with a crossover probability of 80%, the first experiment significantly differs of the other two simulations because in the experiments fourth and fifth the method of selection is the tournament approach instead the fitness proportionate. Surprisingly, when the method of selection is the tournament approach, the best performance is obtained when crossover has a low probability, only a 5% in the sixth simulation experiment, with a high mutation rate of 20% differing significantly from the fourth and fifth experiments where crossover had a high probability of 80%.

Conclusion

This tutorial shows how assuming that EC simulation experiments result in biased samples with non-normal, highly skewed, and asymmetric distributions, the statistical analysis of data could be carried out combining Exploratory Data Analysis with nonparametric tests for comparing two or more medians. In fact and except for the initial random population, the normality assumption was only fulfilled in two examples (see <http://bioinformatica.net/tests/survey.html>): in the symbolic regression problem (*study case 6*) and in the Darwin's biomorphs experiment (*study case 3*). Note that for *case 3* normality was accomplished once data were transformed with the logarithmic transformation. In both examples the Kolmogorov-Smirnov p -value was greater than 0.01. The use of nonparametric tests combined with a Multiple Notched Box-and-Whisker Plot is a good option, bearing in mind that we only considered two experimental situations that are common in EC practitioners: the performance evaluation of an algorithm and the multiple experiments comparison. The different approaches have been illustrated with different examples chosen from Evolutionary Computation and the related field of Artificial Life.

Bibliography

- [Benjamini, 1988] Y. Benjamini. 1988. Opening the box of a boxplot. *The American Statistician* 42: 257-262.
- [Czarn et al., 2004] A. Czarn, C. MacNish, K. Vijayan, B. Turlach, R. Gupta. 2004. Statistical exploratory analysis of genetic algorithms. *IEEE Transactions on Evolutionary Computation* 8: 405-421.
- [Davis, 1991] L. Davis (Ed.). 1991. *Handbook of Genetic Algorithms*. New York: Van Nostrand Reinhold.
- [Dawkins, 1986] R. Dawkins. 1986. *The Blind Watchmaker*. New York: W. W. Norton & Company.
- [Dorigo and Gambardella, 1997] M. Dorigo, L.M. Gambardella. 1997. Ant colonies for the travelling salesman problem. *BioSystems* 43: 73-81.
- [Draper and Smith, 1998] N.R. Draper, H. Smith. 1998. *Applied regression analysis (Third Edition)*. New York: Wiley.
- [Dunn, 1964] O.J. Dunn. 1964. Multiple comparisons using rank sums. *Technometrics* 6: 241-252.
- [Frederick et al., 1993] W.G. Frederick, R.L. Sedlmeyer, C.M. White. 1993. The Hamming metric in genetic algorithms and its application to two network problems. In: *Proceedings of the 1993 ACM/SIGAPP Symposium on Applied Computing: States of the Art and Practice*, Indianapolis, Indiana: 126-130.
- [Frigge et al., 1989] M. Frigge, D.C. Hoaglin, B. Iglewicz. 1989. Some implementations of the boxplot. *The American Statistician* 43: 50-54.
- [Gerber, 1998] H. Gerber. 1998. Simple Symbolic Regression Using Genetic Programming à la John Koza. <http://alphard.ethz.ch/gerber/approx/default.html>
- [Gibbons and Chakraborti, 2003] J.D. Gibbons, S. Chakraborti. 2003. *Nonparametric Statistical Inference*. New York: Marcel Dekker.
- [Goldberg, 1989] D.E. Goldberg. 1989. *Genetic Algorithms in Search, Optimization, and Machine Learning*. Reading, MA: Addison-Wesley.
- [Hart, 2001] A. Hart. 2001. Mann-Whitney test is not just a test of medians: differences in spread can be important. *BMJ* 323: 391-393.

- [Hochberg and Tamhane, 1987] Y. Hochberg, A.C. Tamhane. 1987. Multiple Comparison Procedures. New York: John Wiley & Sons.
- [Holland, 1992] J.H. Holland. 1992. Adaptation in Natural and Artificial Systems: An Introductory Analysis with Applications to Biology, Control, and Artificial Intelligence. Cambridge: The MIT Press. (Reprint edition 1992, originally published in 1975).
- [Hollander and Wolfe, 1999] M. Hollander, D.A. Wolfe. 1999. Nonparametric Statistical Methods. New York: Wiley.
- [Koza, 1992] J.R. Koza. 1992. Genetic Programming: On the Programming of Computers by Means of Natural Selection. Cambridge, MA: MIT Press.
- [Koza, 1994] J.R. Koza. 1994. Genetic Programming II: Automatic Discovery of Reusable Programs. Cambridge, MA: MIT Press.
- [Kruskal and Wallis, 1952] W.H. Kruskal, W.A. Wallis. 1952. Use of ranks in one-criterion variance analysis. J. Amer. Statist. Assoc. 47: 583-621.
- [Lahoz-Beltra, 2001] R. Lahoz-Beltra. 2001. Evolving hardware as model of enzyme evolution. BioSystems 61: 15-25.
- [Lahoz-Beltra, 2004] R. Lahoz-Beltra. 2004. Bioinformática: Simulación, Vida Artificial e Inteligencia Artificial. Madrid: Ediciones Diaz de Santos. (Transl.: Spanish).
- [Lahoz-Beltra, 2008] R. Lahoz-Beltra. 2008. ¿Juega Darwin a los Dados? Madrid: Editorial NIVOLA. (Transl.: Spanish).
- [Manly, 1985] B.F.J. Manly. 1985. The Statistics of Natural Selection on Animal Populations. London: Chapman and Hall.
- [Mann and Whitney, 1947] H.B. Mann, D.R. Whitney. 1947. On a test of whether one or two random variables is stochastically larger than the other. Annals of Mathematical Statistics 18: 50-60.
- [McGill et al., 1978] R. McGill, W.A. Larsen, J.W. Tukey. 1978. Variations of boxplots. The American Statistician 32: 12-16.
- [Mühlenbein and Schlierkamp-Voosen, 1993] H. Mühlenbein, D. Schlierkamp-Voosen. 1993. Predictive models for the breeder genetic algorithm I: Continuous parameter optimization. Evolutionary Computation 1: 25-49.
- [Perales-Gravan and Lahoz-Beltra, 2004] C. Perales-Gravan, R. Lahoz-Beltra. 2004. Evolving morphogenetic fields in the zebra skin pattern based on Turing's morphogen hypothesis. Int. J. Appl. Math. Comput. Sci. 14: 351-361.
- [Perales-Gravan and Lahoz-Beltra, 2008] C. Perales-Gravan, R. Lahoz-Beltra. 2008. An AM radio receiver designed with a genetic algorithm based on a bacterial conjugation operator. IEEE Transactions on Evolutionary Computation 12(2): 129-142.
- [Prata, 1993] Prata, S. (1993). Artificial Life Playhouse: Evolution at Your Fingertips (Disk included). Corte Madera, CA: Waite Group Press.
- [Siegel and Castellan, 1988] S. Siegel, N.J. Castellan. 1988. Nonparametric Statistics for the Behavioral Sciences. New York: McGraw-Hill.
- [Sinclair, 2006] M.C. Sinclair. 2006. Ant Colony Optimization. <http://uk.geocities.com/markcsinclair/aco.html>
- [Tukey, 1977] J.W. Tukey. 1977. Exploratory Data Analysis. Reading, MA: Addison-Wesley.

Authors' Information



Rafael Lahoz-Beltra –Chairman, Dept. of Applied Mathematics, Faculty of Biological Sciences, Complutense University of Madrid, 28040 Madrid, Spain ; e-mail: lahozraf@bio.ucm.es

Major Fields of Scientific Research: evolutionary computation, embryo development modeling and the design of bioinspired algorithms



Carlos Perales Gravan – Member at Bayes Forecast; e-mail: soyperales@gmail.com

Major Fields of Scientific Research: design and development of artificial intelligence methods and its application to decision making processes, optimization and forecasting as well as the modeling and simulation of biological systems

DECREASING VOLUME OF FACE IMAGES DATABASE AND EFFICIENT FACE DETECTION ALGORITHM

Grigor A. Poghosyan and Hakob G. Sarukhanyan

Abstract: *As one of the most successful applications of image analysis and understanding, face recognition has recently gained significant attention. Over the last ten years or so, it has become a popular area of research in computer vision and one of the most successful applications of image analysis and understanding. A facial recognition system is a computer application for automatically identifying or verifying a person from a digital image or a video frame from a video source. One of the ways to do this is by comparing selected facial features from the image and a facial database. Biometric face recognition, otherwise known as Automatic Face Recognition (AFR), is a particularly attractive biometric approach, since it focuses on the same identifier that humans use primarily to distinguish one person from another: their "faces". One of its main goals is the understanding of the complex human visual system and the knowledge of how humans represent faces in order to discriminate different identities with high accuracy.*

Human face and facial feature detection have attracted a lot of attention because of their wide applications, such as face recognition, face image database management and human-computer interaction. So it is of interest to develop a fast and robust algorithm to detect the human face and facial features. This paper describes a visual object detection framework that is capable of processing images extremely rapidly while achieving high detection rates.

Keywords: *Haar-like features, Integral Images, LEM of image- Line Edge Map, Mask $n \times n$ size*

Introduction

As the necessity for higher levels of security rises, technology is bound to swell to fulfill these needs. Any new creation, enterprise, or development should be uncomplicated and acceptable for end users in order to spread worldwide. This strong demand for user-friendly systems which can secure our assets and protect our privacy without losing our identity in a sea of numbers, grabbed the attention and studies of scientists toward what's called biometrics.

Biometrics is the emerging area of bioengineering; it is the automated method of recognizing person based on a physiological or behavioral characteristic. There exist several biometric systems such as signature, finger prints, voice, iris, retina, hand geometry, ear geometry, and face. Among these systems, facial recognition appears to be one of the most universal, collectable, and accessible systems.

Biometric face recognition, otherwise known as Automatic Face Recognition (AFR), is a particularly attractive biometric approach, since it focuses on the same identifier that humans use primarily to distinguish one person from another: their "faces". One of its main goals is the understanding of the complex human visual system and the knowledge of how humans represent faces in order to discriminate different identities with high accuracy.

The face recognition problem can be divided into two main stages:

- face verification (or authentication)
- face identification (or recognition)

The detection stage is the first stage; it includes identifying and locating a face in an image.

Face detection has been regarded as the most complex and challenging problem in the field of computer vision, due to the large intra-class variations caused by the changes in facial appearance, lighting, and expression. Such variations result in the face distribution to be highly nonlinear and complex in any space which is linear to the original image space. Moreover, in the applications of real life surveillance and biometric, the camera limitations and pose variations make the distribution of human faces in feature space more dispersed and complicated than that of frontal faces. It further complicates the problem of robust face detection.

Face detection techniques have been researched for years and much progress has been proposed in literature. Most of the face detection methods focus on detecting frontal faces with good lighting conditions. According to Yang's survey [Yang, 1996], these methods can be categorized into four types: knowledge-based, feature invariant, template matching and appearance-based.

Knowledge-based methods use human-coded rules to model facial features, such as two symmetric eyes, a nose in the middle and a mouth underneath the nose.

Feature invariant methods try to find facial features which are invariant to pose, lighting condition or rotation. Skin colors, edges and shapes fall into this category.

Template matching methods calculate the correlation between a test image and pre-selected facial templates.

Appearance-based, adopts machine learning techniques to extract discriminative features from a pre-labeled training set. The Eigenface method is the most fundamental method in this category. Recently proposed face detection algorithms such as support vector machines, neural networks [Raul, 1996] statistical classifiers and AdaBoost-based [Tolba, 2006] face detection also belong to this class.

Any of the methods can involve color segmentation, pattern matching, statistical analysis and complex transforms, where the common goal is classification with least amount of error. Bounds on the classification accuracy change from method to method yet the best techniques are found in areas where the models or rules for classification are dynamic and produced from machine

learning processes.

The recognition stage is the second stage; it includes feature extraction, where important information for discrimination is saved, and the matching, where the recognition result is given with the aid of a face database. Among the different biometric techniques facial recognition may not be the most reliable and efficient but it has several advantages over the others: it is natural, easy to use and does not require aid from the test subject.

Because the face detection and recognition database is a collection of images and automatic face recognition system should work with these images, which can hold large volumes of computer memory that is way it's necessary to investigate and develop a method / tool for optimal using volume of computer memory (that decrease image database volume) and implement quick face detection within database.

In this paper investigations and study of certain methods that helps us to develop and implemented method/tool, which decreases volume of face images database and use these database for face detection and recognition. To achieve the above mentioned goal we are using image LEM (Line Edge Map) [Tolba, 2006] of image and Viola Jones method [Viola and Jones, 2001]. As quantity of images in recognition database (n) is not infinite and we need define format for images (*.bmp, *.jpg), in this work we've selected $n=40$ and *.jpg format [Face Database]. As object detection and recognition algorithm we are using Haar-like features [Viola and Jones, 2001]. Haar-like features are digital image features used in object recognition. They owe their name to their intuitive similarity with Haar wavelets and were used in the first real-time face detector.

This paper is organized as follows. Section 2 and 3 presents the Line Edge Map (LEM) of image and Viola Jones method (Haar like features/ classifier cascades). Section 4 presents using image LEM in Viola Jones method as

input image, which will decrease volume of our face images database. Section 5 shows the experimental results of frontal face detection using constructed face images database (LEM) and Haar-like features and conclusions follows in Section 6.

Line Edge Map (LEM)

Edge information is a useful object representation feature that is insensitive to illumination changes to certain extent. Though the edge map is widely used in various patterns recognition fields, it has been neglected in face recognition except in recent work reported in [Takacs, 1998].

Edge images of objects could be used for object recognition and to achieve similar accuracy as gray-level pictures. In [Takacs, 1998] made use of edge maps to measure the similarity of face images and 92% accuracy was achieved. Takacs [Takacs, 1998] argued that process of face recognition might start at a much earlier stage and edge images can be used for the recognition of faces without the involvement of high-level cognitive functions.

A LEM approach, proposed by [Gao, 2002], extracts lines from a face edge map as features. This approach can be considered as a combination of template matching and geometrical feature matching. The LEM approach not only possesses the advantages of feature-based approaches, such as invariance to illumination and low memory requirement, but also has the advantage of high recognition performance of template matching. LEM integrates the structural information with spatial information of a face image by grouping pixels of face edge map to line segments. After thinning the edge map, a polygonal line fitting process [Leung, 1990] is applied to generate the LEM of a face. An example of LEM is illustrated in Fig. 1.

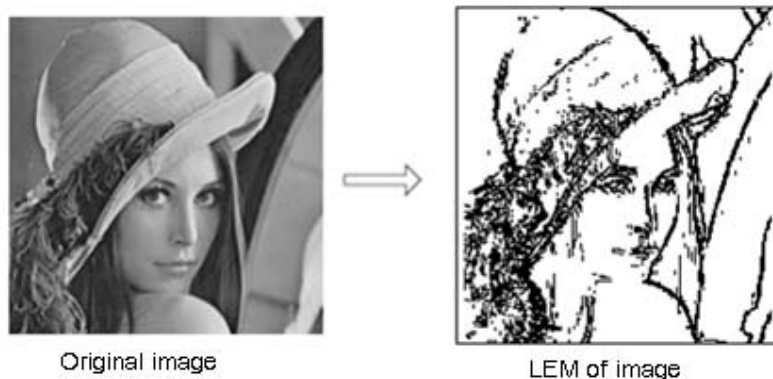


Figure 1. Used 8x8 mask for getting image LEM

Experiments on frontal faces under controlled /ideal conditions indicate that the proposed LEM is consistently superior to edge map. LEM correctly identify 100% and 96.43% of the input frontal faces on face databases [Bern, 2002, Purdue Univ. Face Database], respectively.

Viola Jones method (Haar like features/ classifier cascades)

Image sensors have become more significant in the information age with the advent of commodity multi-media capture devices such as digital cameras, webcams and camera phones. The data from these media sources (whether they are still images or video) is reaching the stage where manual processing and archiving is becoming impossible. It is now possible to process these images and videos for some applications in near real-time, using motion detection and face tracking for security systems for example. However there are still many challenges including the ability to recognize and track objects at arbitrary rotations.

Haar-like features have been used successfully in image sensors for face tracking and classification problems [Konstantinos, 2008, Duda, 2001], however other problems such as hand tracking [Shan, 2004] have not been so successful. Historically, working with only image intensities ((i.e., the RGB pixel values and every pixel of image) made the task of feature calculation computationally expensive. In [Papageorgiou, 1998] discussed working with an alternate feature set based on Haar wavelets instead of the usual image intensities. Viola and Jones [Viola and Jones, 2001] adapted the idea of using Haar wavelets and developed the so called Haar-like features. A Haar-like feature considers adjacent rectangular regions at a specific location in a detection window, sums up the pixel intensities in these regions and calculates the difference between them. This difference is then used to categorize subsections of an image. For example, let us say we have an image database with human faces. It is a common observation that among all faces the region of the eyes is darker than the region of the cheeks. Therefore a common Haar feature for face detection is a set of two adjacent rectangles that lie above the eye and the cheek region. The position of these rectangles is defined relative to a detection window that acts like a bounding box to the target object (the face in this case).

In the detection phase of the Viola-Jones object detection framework, a window of the target size is moved over the input image, and for each subsection of the image the Haar-like feature is calculated. This difference is then compared to a learned threshold that separates non-objects from objects. Because such a Haar-like feature is only a weak learner or classifier (its detection quality is slightly better than random guessing) a large number of Haar-like features are necessary to describe an object with sufficient accuracy. In the Viola-Jones object detection framework, the Haar-like features are therefore organized in something called a classifier cascade to form a strong learner or classifier.

The key advantage of a Haar-like feature over most other features is its calculation speed. Due to the use of integral images, a Haar-like feature of any size can be calculated in constant time (approximately 60 microprocessor instructions for a 2-rectangle feature).

Several researchers have studied the impact of in plane rotations for image sensors with the use of twisted Haar-like feature 45° [Mita, 2005] or diagonal features fairly good performance has been achieved. These techniques will have little benefit for problems that are sensitive to rotations, such as hand identification [Shan, 2004] which are not aligned to fixed angles (0° , 45° , 90° , etc).

Haar-like feature based classifiers like the Jones and Viola, face detector work in almost real time using the integral image (or summed area table) data structure that allows features to be calculated at any scale with only 8 operations. The integral image at location x, y contains the sum of the pixels above and to the left of x, y , inclusive:

$$II(i, j) = \sum_{x' \leq x, y' \leq y} I(x', y'), \quad (1)$$

where $II(i, j)$ is the integral image and $I(i, j)$ is the input (original) image (see Fig. 2 (a)). Using the following pair of recurrences the integral image can be computed in one pass over the original image:

$$\begin{aligned} S(x, y) &= S(x, y-1) + I(x, y), \\ II(x, y) &= II(x-1, y) + S(x, y), \end{aligned} \quad (2)$$

where $S(x, -1) = 0, II(-1, y) = 0$.

Using the integral image any rectangular sum can be computed in four array references (see, Fig.2b). Clearly the difference between two rectangular sums can be computed in eight references. Since the two-rectangle features defined above involve adjacent rectangular sums they can be computed in six array references, eight in the case of the three-rectangle features, and nine for four-rectangle features. The sum of the pixels within rectangle D can

be computed with four array references. The value of the integral image at location 1 is the sum of the pixels in rectangle A. The value at location 2 is $A + B$, at location 3 is $A + C$, and at location 4 is $A + B + C + D$. The sum within D can be computed as $4 + 1 - (2 + 3)$.

However standard Haar-like features are strongly aligned to the vertical/ horizontal or 45° (see, Fig. 3.) and so are most suited to classifying objects that are strongly aligned as well, such as faces, buildings etc.

Standard Haar-like features consist of a class of local features that are calculated by subtracting the sum of a sub region of the feature from the sum of the remaining region of the feature.

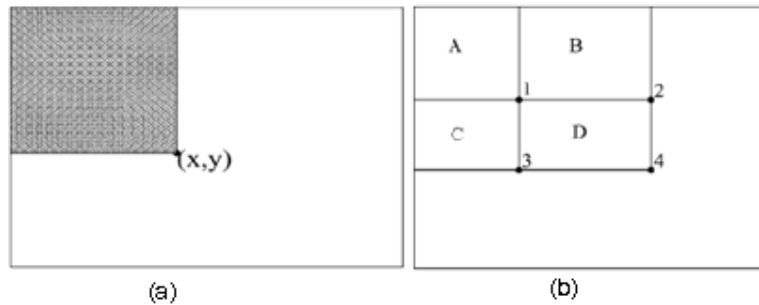


Figure 2. (a) Sum of the integral image at point (x, y) and (b) integral image array references

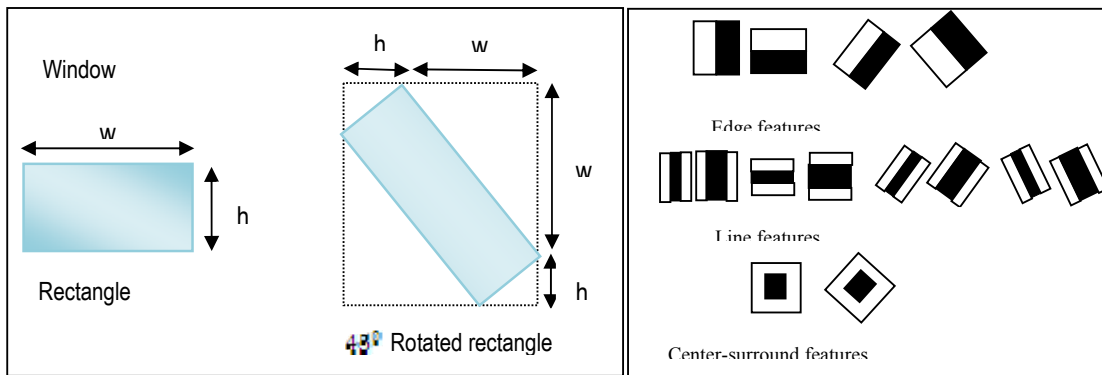


Figure 3. Upright and 45° rotated rectangle, features prototypes of simple Haar-like

Decreasing volume of face images database using LEM

Edge information is a useful object representation feature that is insensitive to illumination changes to certain extent. If the edge detection step is successful, the subsequent task of interpreting the information contents in the original image may therefore be substantially simplified. However, it is not always possible to obtain such ideal edges from real life images of moderate complexity.

In this section we are using $n \times n$ rectangular mask for getting LEM of image (Fig. 3). We are dividing all image into $n \times n$ size of rectangles (in this work $n=8$) and these rectangles must be smaller than the main features of the image details (nose, mouth, eyes in this case). It helps us to observe all brightness points and avoid from not important pixels of image.

We are using equation (3) for calculating brightness of horizontal or vertical pixels and their opposite side pixels (see, Fig. 4).

$$V = \sum_{i=1}^8 [f(i,1) - f(i,8)] \quad H = \sum_{j=1}^8 [f(1,j) - f(8,j)] \quad (3)$$

We could develop function having brightness values of horizontal and vertical sides on current rectangle, which is drawing lines according to brightness values (see, Fig.5).

In order to explore the feasibility of using image LEM in face detection and recognition system we reconstructed all image database (as we mentioned in introduction quantity of images is 40) and get their LEMs.

After that we used OpenCV 2.1 version (Open Source Computer Vision) for detecting and recognizing human faces. We used Haar classifier face detection algorithms functions in which we used 8 futures prototype in Fig. 3. In Fig. 6 given reconstructed images data flow for Haar classifier face detection and recognition algorithm.

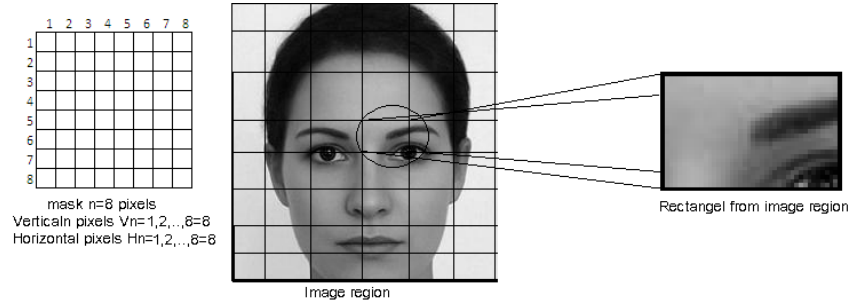


Figure 4. 8x8 mask and image divided with 8x8 rectangles.



Figure 5. Getting LEM of image using 8x8 mask

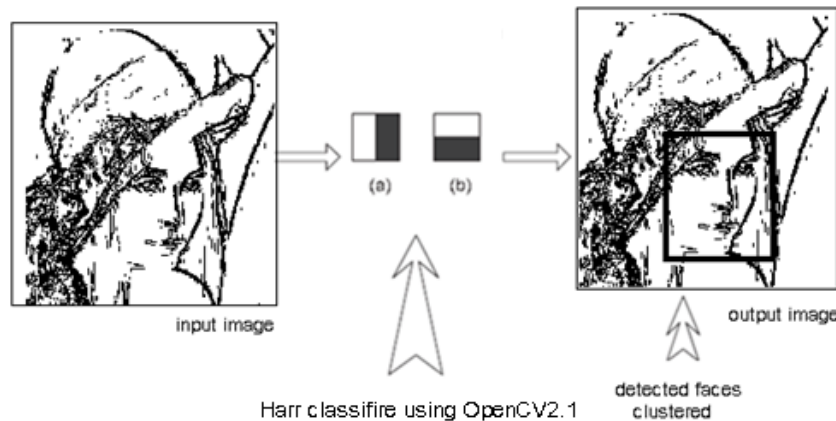


Figure 6. Reconstructed images data flow for Haar classifier

We used Haar classifier face detection algorithms and developed Face detection and recognition software tolls (FDRT) which is using our images LEM database. Comparison results with OpenCV given in table bellow, where we used 40 images of 250×250 pixel sizes.

Training database type	Method/Tools	Detection and recognition time	Training database size
Color (RGB)	OpenCV2.1	2.02msec	2Mb
Image LEM	OpenCV2.1	2.02msec	1.2Mb
Image LEM	Proposed	1.01msec	1.2Mb

From this table we can say that training database volume reduced ~40 % and time decreased for face detection and recognition. So we get image optimization and face recognition tools which can help us to optimize and reduce the volume of the face images database and recognition time.

Conclusion and future work

In a future work we will try to increase percentage of correctly recognition for real time frame moving face discovering and identifying automation system, which will use result of this work and will try identifying and recognizing faces using database with LEM of images.

Bibliography

- [Tolba, 2006] A. S. Tolba, A.H. El-Baz, and A.A. El-Harby Face Recognition: A Literature Review International Journal of Signal Processing, 2, 2006
- [Face Database] Face Database, <http://vis-www.cs.umass.edu/lfw/>
- [Takacs, 1998] B. Takacs, "Comparing face images using the modified hausdorff distance," Pattern Recognition, vol. 31, pp. 1873-1881, 1998.
- [Gao, 2002] Y. Gao and K.H. Leung, "Face recognition using line edge map," IEEE Transactions on Pattern Analysis and Machine Intelligence, vol. 24, No. 6, 2002.
- [Leung, 1990] M.K.H. Leung and Y.H. Yang, "Dynamic two-strip algorithm in curve fitting," Pattern Recognition, vol. 23, pp. 69-79, 1990.
- [Bern, 2002] Bern Univ. Face Database, <ftp://iamftp.unibe.ch/pub/Images/FaceImages/>, 2002.
- [Purdue Univ. Face Database] Purdue Univ. Face Database, http://rvl1.ecn.purdue.edu/~aleix/aleix_face_DB.html, 2002.
- [Konstantinos, 2008] Konstantinos Koutroumbas and Sergios Theodoridis. Pattern Recognition (4th ed.). Boston: Academic Press. 2008
- [Duda, 2001] R. O. Duda, P. E. Hart, and D. G. Stork. Pattern Classification. Wiley, 2001
- [Shan, 2004] C. Shan, Y. Wei, T. Tan, F.Ojardias, "Real time hand tracking by combining particle filtering and mean shift", Proc. Sixth IEEE Automatic Face and Gesture Recognition, FG04, pp: 229-674, 2004.
- [Papageorgiou, 1998] C. Papageorgiou, M. Oren, and T. Poggio, "A general framework for object detection", International Conference on Computer Vision, 1998.
- [Viola and Jones, 2001] P. Viola and M. Jones, "Rapid object detection using a boosted cascade of simple features," IEEE Computer Society Conference on Computer Vision and Pattern Recognition, vol.1, pp. 511-518, 2001.
- [Mita, 2005] T. Mita, T. Kaneko, and O. Hori, "Joint Haar-like features for face detection," Tenth IEEE International Conference on Computer Vision: ICCV 2005. Vol. 2, pp. 1619-1626, 2005.
- [Yang, 1996] Jie Yang, A. Waibel, "A real-time face tracker", Proceedings of the 3rd IEEE Workshop on Applications of Computer Vision (WACV '96), p.142, Dec., 1996
- [Raul, 1996] Raul Rojas, Neural Networks - A Systematic Introduction, Springer-Verlag, Berlin, New-York, 1996, 502p.

Authors' Information



Grigor Poghosyan – PHD student, Institute for Informatics and Automation Problems of NAS of RA; e-mail: grigor.poghosyan@mail.ru
Major Fields of Scientific Research: Digital Signal and Image Processing



Hakob G. Sarukhanyan – Head of Digital Signal and Image Processing Laboratory, Institute for Informatics and Automation Problems of NAS of RA; e-mail: hakop@ipia.sci.am
Major Fields of Scientific Research: Digital Signal and Image Processing, Fast Orthogonal Transforms, Parallel Computing

MODELING OF TRANSCUTANEOUS ENERGY TRANSFER SYSTEM FOR AN IMPLANTABLE GASTROINTESTINAL STIMULATION DEVICE

Joanna Liu C. Wu, Martin P. Mintchev

Abstract: This study models a transcutaneous energy transmission system which can supply DC power to an implanted device without an external battery. The goals of the study are to: (1) develop a model to describe the transcutaneous energy transmission system; and (2) use the developed model to design a transcutaneous energy transmission system for an implantable gastrointestinal neurostimulator. The complete transcutaneous energy system includes a power amplifier, a highly inductive coupling structure, and an ac-to-dc rectifying circuit in the receiver. Power amplification is based on the single-ended class E amplifier concept. The power amplification stage is self-oscillating, and the oscillation frequency is influenced by the coupling of the coils. The highly inductive coupling structure employs the stage tuning concept. Design methods and detailed analysis are provided. The proposed model is verified through the implementation of the design.

Keywords: computer modeling, neurostimulation, gastrointestinal disorders

1. Introduction

1.1 Brief Introduction to the Gastrointestinal System

The gastrointestinal (GI) tract is essentially a long tube stretching from the mouth to the anus as shown in Figure . It includes the esophagus, the stomach, the duodenum, the small intestine, the colon, and the rectum. The functions of GI organs include digestion, absorption, secretion and motility. The GI system is capable of digesting orally accepted material and extracting any useful components from it, then expelling the waste products at the bottom end.

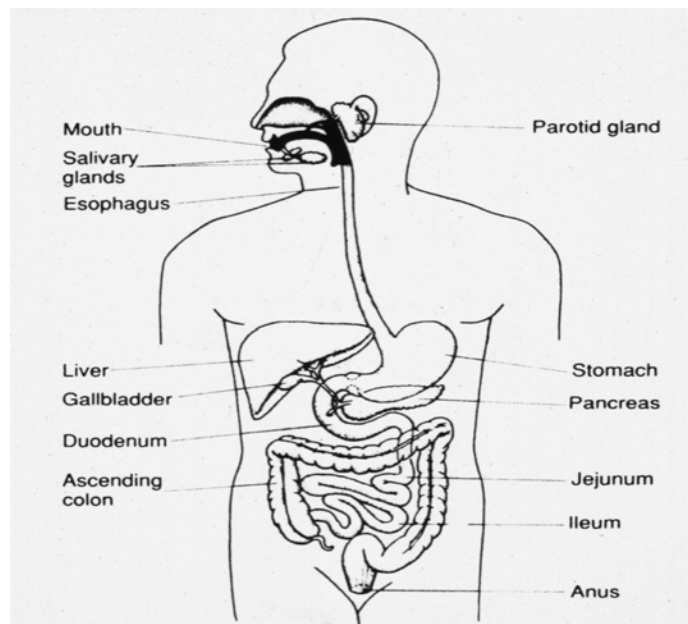


Figure 1: The gastrointestinal tract

1.2 Gastrointestinal Motility

Gastrointestinal motility is defined by the movements of the organs in the digestive system, related to the transit of content in them. For example, on the basis of its motility patterns, the stomach can be divided into two regions. The upper stomach is composed of the fundus and upper corpus. It shows sustained tonic contractions that create basal pressure within the stomach. The lower stomach is composed of the lower corpus and the antrum. It develops strong peristaltic waves of powerful distally propagating contractions that increase in amplitude as they migrate towards the pylorus. Contractions in the distal two-thirds of the stomach occur as a result of the rhythmic depolarization of the gastric smooth muscle cells in annular bands, originating in a region of the proximal corpus usually defined as the gastric pacemaker. Control of gastric contractile activity is mediated through the interaction between both sympathetic and parasympathetic nervous system and the intrinsic electrical activity of the gastric smooth muscle [1]. These gastric slow waves propagate caudally by entraining depolarization in adjacent distal areas of less frequent intrinsic activity. Stronger electrical signals may be superimposed on these slow waves, which are known as spike activity, and have been associated with gastric contractility.

1.3 Gastrointestinal Motility Disorders

Digestive diseases and disorders related to abnormal GI motility patterns occur primarily in the esophagus, the stomach and the colon. The symptoms related to such motility problems may range from gastroesophageal reflux to gastroparesis to constipation. GI disorders are the most common gastrointestinal problems seen by physicians in primary care, and affect millions of people of different ages, including men, women, and children.

Except for the gastroesophageal reflux, which will not be in the focus of the present study, the predominant motility disorders are gastroparesis and constipation, which are explained below in more details.

Gastroparesis is a disease in which the stomach takes too long to empty its contents. It is suggested to be a disorder of the nerves and the smooth muscles of the stomach. The most common symptoms include nausea, vomiting, bloating, feeling full after small meals, and regurgitation. The reasons that cause such a disorder are not fully understood, but diabetic gastroparesis has been clearly identified, and viral causes have been suggested. About 10-20% of gastroparetic cases are of unknown origin and etiology, and are usually labelled as idiopathic gastroparesis. The most common treatment of gastroparesis includes diet changes, medications, and in the most severe cases, parenteral nutrition and partial or total gastrectomy.

Constipation typically refers to dry, difficult, and painful bowel movements related to abnormally delayed colonic transit. The symptoms of constipation include feeling bloated, uncomfortable, and sluggish. Constipation is one of the most common GI complaints in the United States. The data from the 1996 National Health Interview Survey show that about 3 million people in the United States have frequent constipation. Constipation occurs when the colon absorbs too much water or if the colon muscle contractions are slow or sluggish. The main reasons that cause constipation include lack of fiber and liquid intake, lack of exercise, medications, ignoring the urge of bowel movement, problems with the colon and the rectum, etc. Because of the large population suffering from constipation, alternative treatments of this disorder are being investigated [26, 27, 28]. However, in severe cases of idiopathic constipation, partial or total colectomies remain the only presently feasible treatment providing long-term improvements of symptoms.

In the recent years, more and more scientific groups are interested in applying functional electrical stimulation to restore impaired motility in the gastrointestinal tract. There are four distinct methods for GI electrical stimulation. The first method is to entrain slow wave activity in both animals [4] and humans [3] by "pacing" the organ at a frequency slightly higher than the intrinsic slow wave frequency, and approach similar to cardiac pacing. The second method applies current stimulation at 4-40 times the intrinsic slow wave frequency and has been reported to have some antiemetic effect. The most recent stimulation technique is known as neural gastrointestinal

electrical stimulation (NGES) [12, 13]. This approach involves voltage stimulation at 50 Hz delivered through matched pairs of electrodes implanted in the smooth muscle of the stomach wall. The effect of this approach has been shown by accelerated microprocessor-controlled gastric emptying of both solids [10] and liquids [11] in the stomach, as well as by increased colonic transit in both acute and chronic canine models.

The success in the implementation of an NGES system is intimately and directly related to the development of a fully implantable but externally controllable multichannel device. Powering such implanted device becomes a principle challenge. There are four widely accepted techniques for powering an implanted device: (1) Conventional wire cord (focusing on the biocompatibility of the shielding materials), (2) stand-alone implantable battery, (3) radio frequency (RF, transcutaneous inductive) link technologies, and (4) a combination of (2) and (3) using implantable stand-alone rechargeable batteries.

1.4 Aim of the Present Study

The purpose of this feasibility study is to design a transcutaneous power transfer system for a neurostimulator design aiming at restoring impaired gastrointestinal motility. The first mention of powering an implanted device through a transcutaneous inductive coupling link was in 1934 [5]. The practical attempts appeared in the late 1970s [13]. There are two distinct paradigms for designing such a system. One paradigm is known as a loosely coupled link [14] which has a low degree of coupling between the transmitting and the receiving coils, while the other one is highly coupled inductive link, which has a relatively high degree of coupling between the coils. The highly coupled inductive link assumes transmitting and receiving coils of approximately the same size [15] and is the design aim of this project.

2. Methods

2.1 Methods of Power Supply of Implanted Devices

In general, there are four approaches to supply the power to an implanted device: (1) conventional wire cord; (2) battery technologies; (3) RF technologies; and (4) a combination of (2) and (3) using rechargeable batteries. The major advantage of the wire cord approach is technical simplicity. Similar to regular devices, this approach employs power cords and data lines that supply all necessary electrical energy and command signals to the implanted device. Problems of infection, maintenance, and cosmetics hinder the applicability of wired power and data transfer, and therefore, battery-based technologies have been preferred.

Recently developed high energy density batteries increase the life-span of implantable functional devices, making battery-based implants preferable from commercial point of view. However, unlike the technologies of the wired or RF links, which supply both power, and data transmission, the single function of supplying power limits the applicability of battery technologies in implantable devices, since the addition of a separate power-consuming RF link providing device programmability would be necessary. Furthermore, batteries cannot be replaced once they have been implanted, and the patients need to undergo another surgery to replace the batteries. Thus, an implant lasting more than 3 years on a single battery could be reasonably acceptable, but designs with a lower lifespan would be difficult to justify.

The RF approach is believed to be the most promising technique for implantable devices. Its advantages include continuous availability of high levels of power to an implanted device, and the ability to control it with the external device using the same RF link. In addition, the lifetime and shelf life of the implanted devices are not restricted by the life of the battery [16]. The major disadvantage of this approach is the inconvenience for the patient having to permanently wear and external setup providing the transcutaneous link. A combination of having the RF link to recharge an implanted battery converts this permanent inconvenience into an intermittent nuisance. This

approach is typically utilized in cases where the implanted device requires power for a longer period of time than the time that is practical to wear an external transmitter.

2.2 An Overview of Highly Coupling Inductive Link

It has been discussed already that in order to avoid the possibility of infection from piercing the skin and the undesirable replacement of implantable power sources, transcutaneous power transfer is a preferred modality for implantable devices which cannot operate with implantable batteries for more than 3-4 years. This report is concerned with the investigation of the feasibility of utilizing a transcutaneous inductive link for an implanted gastrointestinal stimulation system.

The development of the transcutaneous power technology has been ongoing for several decades. The first attempts to use RF telemetry for providing power to an implanted device took place in 1934 [5]. In late 1970s and early 1980s, practical implantable systems for functional electrical stimulation (FES) applications first appeared [13, 14]. The inductive link employed was called highly coupled stagger-tuned inductive link [15]. The link is a radio-frequency coil system consisting of two same-sized pancake-shaped coils, oriented face-to-face. The primary coil is outside the body and driven by an external circuit. The secondary coil is implanted with the device and connected to a receiver circuit. The coupled coils can move relative to one another as shown in Figure . As they move, their link voltage gain changes. Hence, good tolerance to axial and angular misalignment and coil separation is desired. Furthermore, to obtain large stimulating output voltage for the stomach and colonic stimulation, link voltage gain should be maximized for the required inductive link. Therefore, several factors should be taken into account when designing such an inductive link system. These factors include: (1) size of the transmitting and receiving coils, (2) link efficiency, (3) link voltage gain, (4) misalignment and separation tolerance, (5) communication bandwidth, and (6) overall size and complexity of the both transmitter and receiver.

According to Zierhofer and Hochkai [30], and Galbraith et al. [15], there are several advantages of developing a highly coupled inductive link which are applicable when designing a multi-channel gastrointestinal stimulation system.

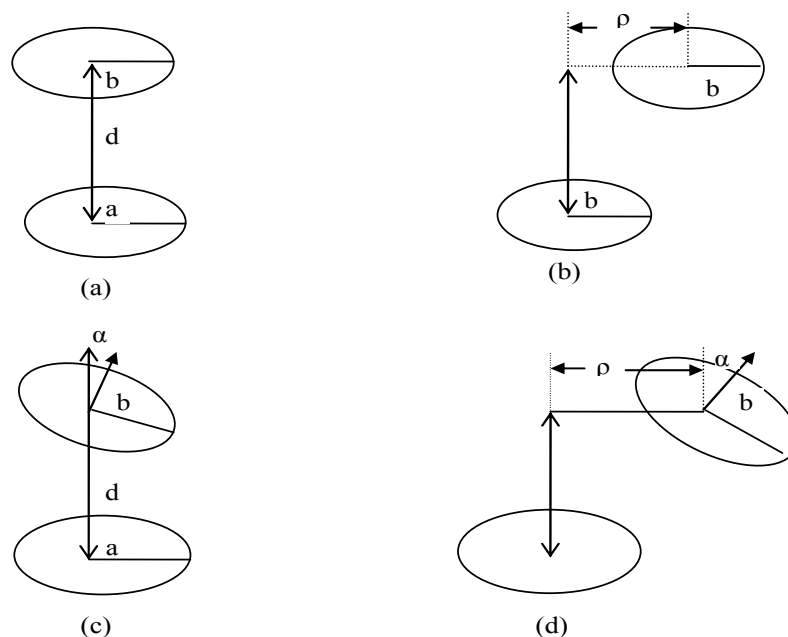


Figure 2: Coil alignments.

(a) Ideal alignment. (b) Lateral misalignment.
(c) Angular misalignment. (d) General misalignment.

1. The overall voltage gain is insensitive to variations of the relative position of the coupling coils.
2. The high coupling coefficient between the transmitter and the receiver reduces the current in the primary coil. This reduces the power dissipation in the primary side due to I^2R -losses. Thus the overall power transmission efficiency is enhanced.
3. The high coupling coefficient between the transmitter and the receiver reduces the magnitude of the required electromagnetic field, which in turn diminishes tissue heating.

2.3 Modeling the Highly Coupled Inductive Link

Galbraith et al (1987) [15] introduced four different combinations of highly coupled stagger-tuned inductive link. They were: (1) voltage in - voltage out, (2) voltage in - current out, (3) current in - current out, and (4) current in - voltage out. The "voltage in - voltage out" link is an approach which can control the output gain. This approach is based on coupling, not geometry. It not only corrects for lateral displacement, but also handles coil separation. The frequency response of such a link for various coupling coefficients k , in a frequency range of 0.5 - 3 MHz, is illustrated on Error! Reference source not found.. At a frequency of approximately 1.60 MHz, the variation in the gain is minimized, even though the coupling coefficient between the transmitter and the receiver varies from 0.26 to 0.54.

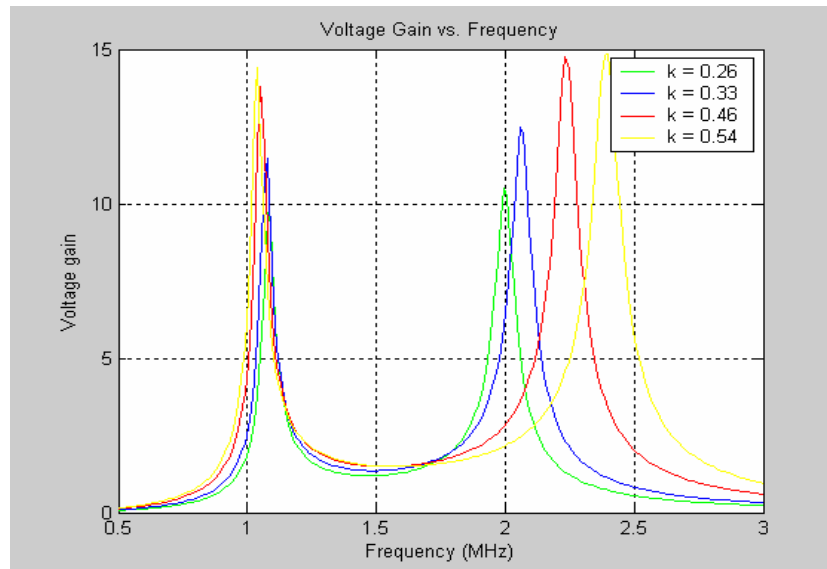


Figure 3: Voltage Gain of Stagger Tuned Inductive Link

In gastrointestinal electrical stimulation the properties of the stimulated tissue are dynamically different, and therefore the current consumption and loading of the inductive link would vary widely. This means that the gain of a transcutaneous inductive link should be stable over a wide range of coupling and loading impedances. A highly coupled link of the type "voltage in - voltage out" is to be preferred, because it can control the overall gain. The design procedure for such a link will be described in Section 2.5. A model of the highly coupled inductive link is depicted on Figure . On the primary side, the transmitter coil is tuned into a serial resonance with a capacitor C_t , so that appreciable coil current can be achieved from a sinusoidal voltage source. The receiver coil is tuned into a parallel resonance with a shunt capacitor C_r in order to obtain a high voltage output.

The expressions used to calculate the magnitudes of the unregulated DC load voltage and the DC power delivered to the load for the circuit model of Figure are described in [20].

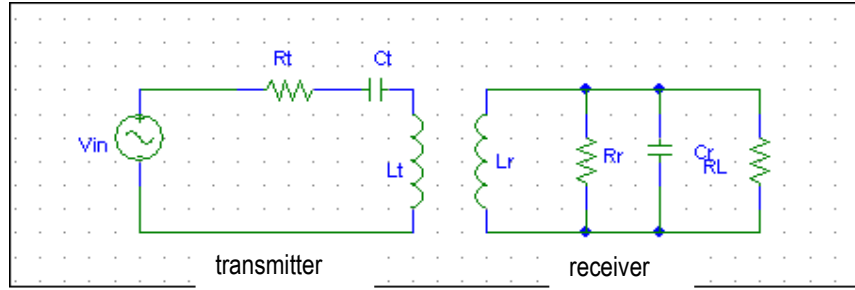


Figure 4: Simplified "Voltage in: Voltage out" circuit model of the stagger-tuned link

The impedance of the receiver is: $Z_{receiver} = Z_{real} + jZ_{imag}$. The equations used for this calculation are presented as follows:

$$P_{dc} = \frac{|V_{load}|^2}{R_{load}} \quad (2.3.1)$$

where P_{dc} is the DC power deliver to the load, R_{load} is impedance of the load in the receiver, and

$$|V_{load}| = |I_r| \sqrt{\left(\frac{2R_{load}}{4 + \omega^2 C_r^2 R_{load}^2} \right)^2 + \left(\frac{\omega C_r R_{load}^2}{4 + \omega^2 C_r^2 R_{load}^2} \right)^2} \quad (2.3.2)$$

where ω is the operating frequency, C_r is the shunt capacitor in the receiver, and

$$|I_r| = \frac{(|I_t| \omega R)}{\sqrt{\left(R_r + \frac{2R_{load}}{4 + \omega^2 C_r^2 R_{load}^2} \right)^2 + \left(\omega L_r - \frac{\omega C_r + R_{load}^2}{\omega^2 C_r^2 R_{load}^2} \right)^2}} \quad (2.3.3)$$

where R_r is the equivalent series resistance of the receiver coil

$$|I_t| = \sqrt{\frac{(V_{in} Z_{real_total})^2 + (V_{in} Z_{imag_total})^2}{(Z_{real_total}^2 + Z_{imag_total}^2)}} \quad (2.3.4)$$

where

$$Z_{real_total} = Z_{reflected_real} + R_t \quad (2.3.5)$$

$$Z_{imag_total} = Z_{reflected_imag} + \left(\omega L_t - \frac{1}{\omega C_t} \right) \quad (2.3.6)$$

where R_t is the equivalent series resistance of the transmitter coil, C_t is the capacitor in the transmitter, and

$$Z_{reflected_real} = \frac{\omega^2 M^2 Z_{real}}{Z_{real}^2 + Z_{imag}^2} \quad (2.3.7)$$

$$Z_{reflected_imag} = \frac{-\omega^2 M^2 Z_{imag}}{Z_{real}^2 + Z_{imag}^2} \quad (2.3.8)$$

where M is the mutual inductance between the transmitter and receiver coils, and

$$Z_{real} = R_r - \frac{R_{load}/2}{1 + \omega^2 C_r^2 (R_{load}/2)^2} \quad (2.3.9)$$

$$Z_{imag} = \omega L_r - \frac{\omega C_r (R_{load}/2)^2}{1 + \omega^2 C_r^2 (R_{load}/2)^2} \quad (2.3.10)$$

In the above circuit model, the transmitter is usually powered by batteries utilizing a power amplifier. In order to power the transmitter and to avoid frequent battery replacements, it is required to be relatively efficient in converting DC to AC (RF) power. Class E power amplifier boasts a theoretical DC to AC conversion efficiency up to 95%, and is the most widely used transmitter topology used in transcutaneous power transformers. Therefore, Class E topology is routinely employed for powering the transmitter.

2.4 Class E Power Amplifier

Converters represent the primary portion of a power system. There are many types of converters such as (1) dc to ac, (2) ac to dc, (3) dc to dc, and (4) ac to ac.

The Class E power amplifier is an inverter which converts dc to ac voltage. It consists of a choke inductor L_{choke} , a power MOSFET utilized as a switch, a parallel capacitor C_p , and an LC resonant circuit (Figure 2.4). The switch turns on and off by a driver at a designated operating frequency f_o , and the LC resonant circuit oscillates at a frequency f_t . If f_o is equal to the resonant frequency f_t , the efficiency of Class E inverter is maximal. The choke inductor should have a high enough inductance to assure the ac ripple on the dc supply, I_{cc} (shown in Figure 5: Class E power amplifier) can be neglected [17]. In this case, the current through the choke inductor can be regarded as a steady current. When the switch is on, C_t and L_t function as a resonant circuit due to C_p being

short-circuited by the switch, where f_t equals to $\frac{1}{(2\pi\sqrt{(L_t C_t)})}$. When the switch turns off, C_p , C_t , and L_t form a

resonant circuit, where f_t equals to $\frac{1}{\left[2\pi\sqrt{L_t C_t \frac{L_t C_t C_r}{(C_t + C_r)}}\right]}$. The advantages of Class E amplifier are zero

power loss during the switching and high efficiency (about 95%) during the dc-to-ac power conversion. The capacitance C_t and the inductance L_t can be utilized to adjust the resonant frequency f_o . There are two important components, C_p and L_{choke} , which need to be determined. The capacitance C_p can be calculated by:

$$C_p = \frac{1}{(2\pi \times f_o \times R_t \times 5.477)} \quad (2.4.1)$$

where R_t is the resistance in the transmitter coil.

The choke inductor, L_{choke} , shown in Figure 5: Class E power amplifier is usually 3 – 10 times greater than the inductance of the transmitter coil [18].

Finally, the magnitude of the AC source of the transmitter, V_{in} (shown in Figure) is a function of DC supply powering the class E topology, and is calculated according to Eq. (2.4.2) [18, 19]

$$V_{in} = \frac{2V_{dc}}{\sqrt{1 + \left(\frac{\pi^2}{4}\right)}} \quad (2.4.2)$$

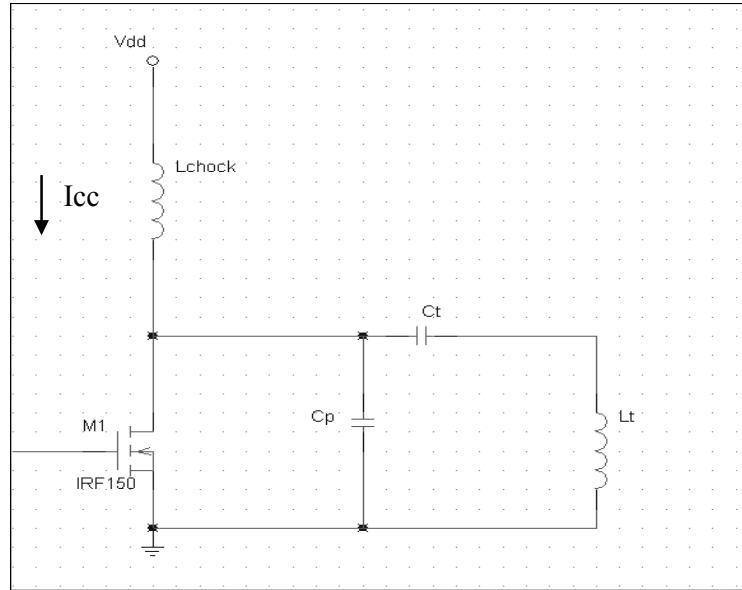


Figure 5: Class E power amplifier

2.5 Design of the Highly Coupled Inductive Link

2.5.1 Design Requirements

The voltage to be delivered to the implanted device would be in the range of 10 to 20 V DC for implanted stimulator current drawing between 0 and 50 mA [22]. The minimum and maximum equivalent loads are 200 Ω and 100 k Ω respectively [20]. The design requirements are presented in Table 1.

Design Requirement	Value
Minimum load voltage, V_{load}	10 V
Maximum load current, I_{load}	50 mA
Minimum value of load, $R_{loadmin}$	200 Ω
Maximum value of load, $R_{loadmax}$	100 k Ω
Power delivered to R_{load}	500 mW

Table 1: Highly coupled inductive link design requirement

2.5.2 Design Procedure

The design procedure of a stagger-tuned inductive link is outlined in [15] and is briefly described below.

Error! Reference source not found. shows that the minimum variation of gain of the inductive link occurs at 1.6 MHz. In the following procedure, it is assumed that the inductive link operates at an operating frequency of $f_o = 1.6$ MHz and the DC supply of the link is 9V.

2.5.2.1 Spiral Coil Design

In this project, the transmitter and receiver coils are both spiral coils and approximately of the same size. The methods used in calculating the self-inductance of such coils and the mutual inductance between the two coils have been previously reported [23, 13]. The calculation of the self-inductance of the spiral coils is based on the assumption that the spiral coils can be modeled as coaxial circular loops of wire.

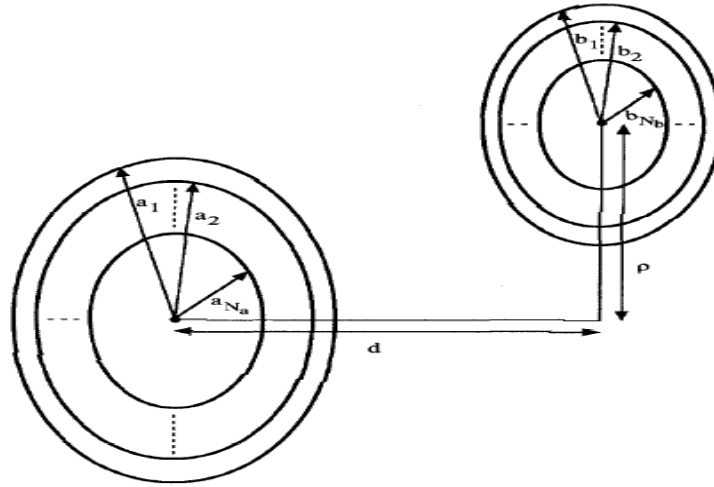


Figure 6: Geometric arrangement and notation for transmitter and receiver coils composed of circular concentric loops.

I. Calculation of the self-inductance of a spiral coil

The self-inductance of a single loop of wire can be calculated by:

$$L(a, w) = \mu_0 a \left(\ln \left(\frac{8a}{w} \right) - 2 \right) \quad (2.5.1)$$

where a is the radius of the single loop, w is the radius of the wire, and μ_0 is the magnetic permeability of the free space.

The mutual inductance of two spiral coils whose axes are parallel can be presented by:

$$M(a, b, \rho, d) = \mu_0 \sqrt{ab} \left[\left(\frac{2}{k} - k \right) K(k) - \frac{2}{k} E(k) \right] \quad (2.5.2)$$

where

$$k \equiv \left(\frac{4ab}{(a+b)^2 + d^2} \right)^{\frac{1}{2}}$$

and where a and b are the radii of the two loops, d is the distance between the two loops, ρ is the axial misalignment, and K and E are the complete elliptic integrals of the first and second kind, respectively.

The self-inductance of such a coil is approximately equal to the summation of self-inductances of single loops, and with wire-radius w , the overall self-inductance is represented by:

$$L_a = \sum_{i=1}^{N_a} L(a_i, w) + \sum_{i=1}^{N_s} \sum_{j=1}^{N_a} M(a_i, a_j, \rho = 0, d = 0) (1 - \delta_{i,j}) \quad (2.5.3)$$

where $\delta_{ij} = 1$ for $i = j$, and $\delta_{ij} = 0$ otherwise.

II. Calculation of mutual inductance between two spiral coils

The mutual inductance between primary and secondary coils can be calculated by:

$$M_{ab} = \sum_{i=1}^{N_z} \sum_{j=1}^{N_a} M(a_i, b_j, \rho, d) \quad (2.5.4)$$

However, Eq. (2.5.4) is valid for the case with axial misalignment only. To calculate the exact mutual inductance between two coils with simultaneous axial and angular misalignments, an approximation is provided in [29]:

$$M(a, b, \rho, d, \alpha) = \frac{M(a, b, \rho, d)}{\sqrt{\cos \alpha}} \quad (2.5.5)$$

where α is the angular misalignment. Once the calculation method of self-inductance of a spiral coil and mutual inductance of two spiral coils is introduced, the parameters of transmitter and receiver coil orientations need to be determined. The constraints of the design are listed in Table 2.

Coil Separation	0.5 cm - 2.0 cm
Axial Misalignment	0 cm - ± 1.0 cm
Angular Misalignment	0° - 20°
Diameter of transmitter and receiver coil	5 cm

Table 2: Highly coupled inductive link coupling constraints

Matlab code was developed for calculating the self-inductances and the mutual inductance of the transmitter (L_t) and the receiver (L_r) coils, based on the outlined constraints. The maximum and minimum coupling coefficients, k_{max} and k_{min} , are then calculated according to Eq. (2.5.6) and (2.5.7), respectively.

$$k_{max} = \frac{M_{max}}{\sqrt{L_t L_r}} \quad (2.5.6)$$

$$k_{min} = \frac{M_{min}}{\sqrt{L_t L_r}} \quad (2.5.7)$$

Furthermore, in order to determine the optimal number of turns, the Matlab Design Tool was used to vary the number of turns in the transmitter and receiver coils, and to compare the performance of the resulting links. In general, increasing the number of turns in the two coils reduced the variation in the load voltage, and enhanced the overall efficiency of the link. For this design, 10-turn spiral coils were chosen for the transmitter (n_t) and the receiver (n_r) coils. When the space between concentric turns of the coils is approximately 1.18 mm, the geometry of these coils results in a self-inductance $L_t, L_r = 4.07 \mu\text{H}$, with coupling coefficients $k_{min} = 0.26$ and $k_{max} = 0.82$.

2.5.2.2 Choosing the Operating Frequency fo

In order to minimize the amount of magnetic field absorbed by the abdominal tissue, the frequency should be chosen to be as low as possible, since the absorption increases exponentially with frequency [25]. However, the power transfer capability of the inductive link improves with increasing operating frequency. In addition, Error! Reference source not found. shows that at a frequency of approximately 1.60 MHz, the variation in the gain is minimized. Therefore, the frequency of $f_o = 1.6$ MHz was chosen as an operating frequency of the link.

2.5.2.3 Choosing the Resonant Frequency of the Receiver, fr

The resonant frequency of the receiver was chosen such that $f_r / f_o > 1$. The trade off is that as f_r / f_o increases, the overall voltage output gain increases. In other words, if the overall gain is too small, the ratio of f_r / f_o should be

moved away from unity. However, if the ratio of f_r / f_o increases, the overall gain variation also increases. To determine the optimal ratio of f_r / f_o , Matlab Design Tool was used to vary f_r / f_o and to compare the performance of the resulting links. Figure 7 shows different performances of the links with different ratios of f_r / f_o . After examining the magnitude and the variation of the load voltage for a set of values of f_r / f_o , it became apparent that for $f_r / f_o = 1.2$, the load voltage variation was minimized. This means the resonant frequency of the receiver was $f_r = 1.92$ MHz. The value of the shunt capacitor C_r can be calculated as follows:

$$C_r = \frac{1}{\omega^2 L_r} \tag{2.5.8}$$

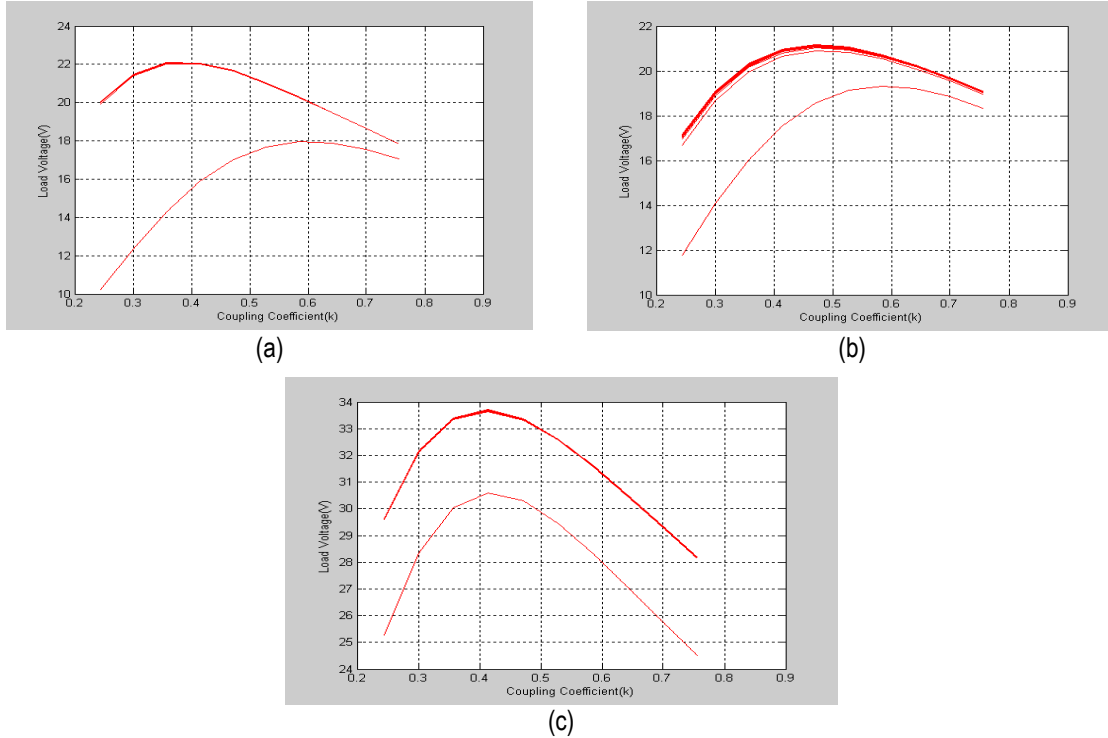


Figure 7: Load voltage over entire design space. (a) $f_r / f_o = 1.1$. (b) $f_r / f_o = 1.2$. (c) $f_r / f_o = 1.4$.

2.5.2.4 Choosing Resonant Frequency of Transmitter, f_t

Next, the resonant frequency of transmitter, f_t , is calculated by Eq. (2.5.9) [11].

$$\omega_t = \sqrt{\frac{(\omega^2) \left(1 - H + \frac{1}{Q_t^2}\right)}{1 + \sqrt{H - \frac{1}{Q_r^2}}}} \tag{2.5.9}$$

Where

$$H = \frac{k_{opt}^4 \left[\left(\frac{\omega^2}{\omega_r^2}\right)^2 + \frac{1}{Q_r^2} \right]}{\left(1 - \frac{\omega^2}{\omega_r^2}\right) + \frac{1}{Q_r^2}} \tag{2.5.10}$$

and

$$k_{opt} = \sqrt{k_{min}k_{max}} \quad (2.5.11)$$

and

$$Q_t = \frac{\omega L_t}{R_t}, \quad Q_r = \frac{R_r}{\omega L_r} \quad (2.5.12)$$

With the determined tuning ratio, f_r/f_o , the receiver resonant frequency was determined with Eq. (2.5.13), and the transmitter resonant frequency was calculated as $f_t = 1.12$ MHz. The tuning capacitor of the transmitter is

$$C_t = \frac{1}{\omega^2 L_t} \quad (2.5.13)$$

Finally, Matlab Design Tool was used to determine the maximum and the minimum DC load voltages from the highly inductive link in order to specify the tolerance for the voltage regulation and other components for the rest of the transcutaneous energy transfer system. The plot of the maximum and the minimum load voltages for the inductive link is presented in Figure 8.

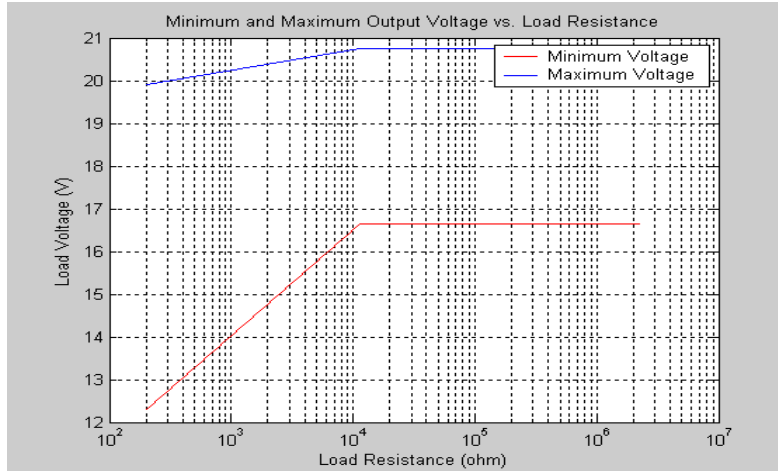


Figure 8: The maximum and minimum load voltage for the highly coupled inductive link.

3. Results

3.1 Spiral Coil Characterization

In order to reduce the power losses in the transmission load, Litz wire was used to make the spiral coils. Both the transmitter and the receiver coils were constructed using 270/46, 22 Gauge equivalent Litz wire (New England Electric Wire Corp., Lisbon, NH, USA). The number of turns in both coils was 10, and space between concentric turns of the coils was approximately 1.18 mm. There are two methods employed to validate the coil models, as described in Section 2.5.2.1. The first method is to use an LCR meter to extract the self-inductance and the equivalent series resistance (ESR) values from the coils. The values extracted from RLC meter for frequencies of 120 Hz, 1 KHz, and 10 KHz are presented in Tables 3, 4, and 5 respectively.

	Measured Self-inductance (μH)	Calculated Self-inductance (μH)	Percent Difference (%)	ESR ($\text{m}\Omega$)
Transmitter coil	4.0	4.07	1.72	170
Receiver coil	4.05	4.07	0.49	170

Table 3: Self-inductance and ESR values extracted from RLC meter in 120 Hz

	Measured Self-inductance (μH)	Calculated Self-inductance (μH)	Percent Difference (%)	ESR ($\text{m}\Omega$)
Transmitter coil	3.58	4.07	12.01	168
Receiver coil	3.77	4.07	7.37	168

Table 4: Self-inductance and ESR values extracted from RLC meter in 1 kHz

	Measured Self-inductance (μH)	Calculated Self-inductance (μH)	Percent Difference (%)	ESR ($\text{m}\Omega$)
Transmitter coil	3.53	4.07	13.26	168
Receiver coil	3.71	4.07	8.85	168

Table 5: Self-inductance and ESR values extracted from RLC meter in 10 kHz

Measured values of self-inductance from the RLC meter at a low frequency (120 Hz in this case) agreed with the calculated values, while the percent difference between measured and calculated values increased with the increment of the operating frequency. This means that the self-inductance value of a spiral coil changes when the operating frequency changes. Alternatively, a testing circuit, depicted in Figure , was implemented to extract these same values. In the circuit, R was 10 Ohm and C was 1.78 nF. An *HP 33120A* function generator was used to drive the circuit. An *Agilent 54621D* oscilloscope measured the output voltage of the coils V_{out} . If the resistance of the circuit was small, the resonant frequency occurred at $\omega L = \frac{1}{\omega C}$. Also, the resonant frequency occurred when the impedance reaches maximum. The frequencies used for characterizing the circuit varied from 100 Hz to 3 MHz. Matlab Design Tool was used to plot the output voltages of the coil at various frequencies (Figure).

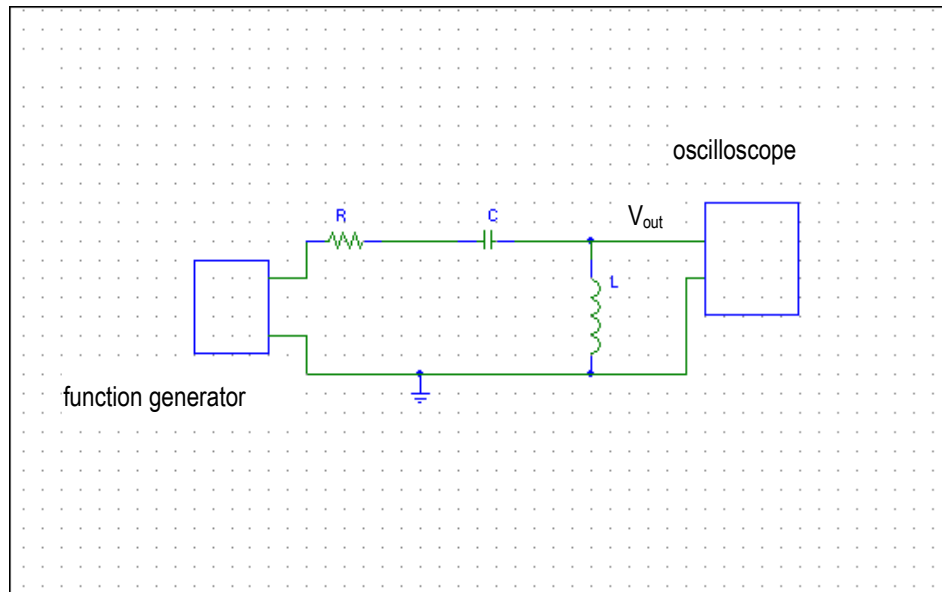
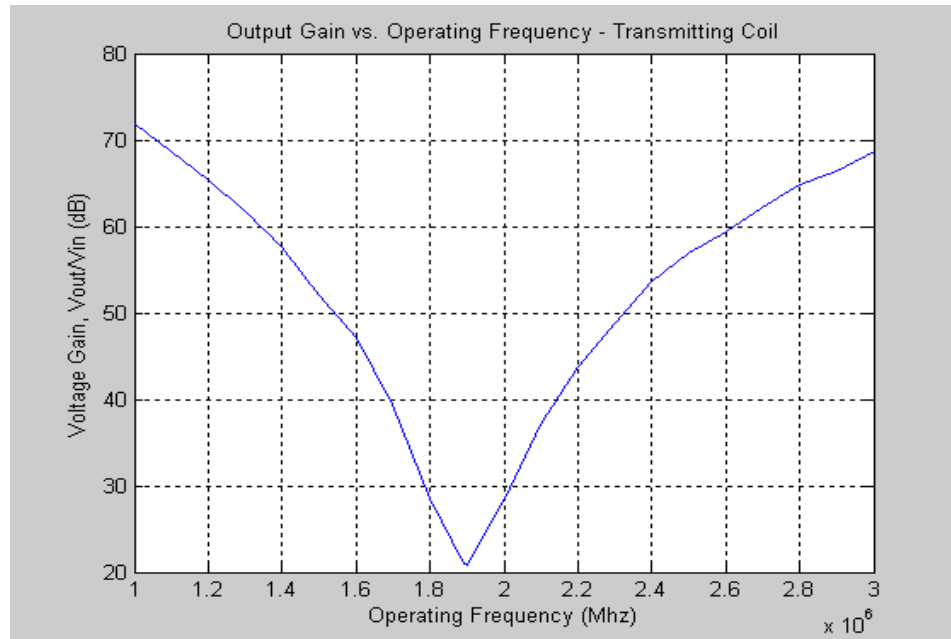
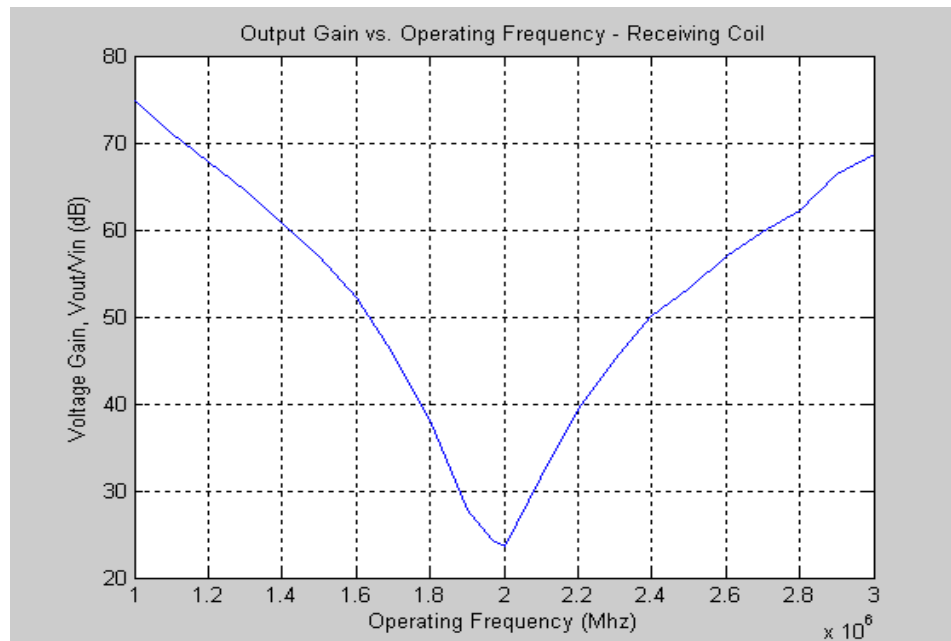


Figure 9: Serial resonant circuit for calculating the self-inductance of each coil



(a)



(b)

Figure 10: Frequency response of spiral coils. (a) transmitter coil; and (b) receiver coils.

Observing Figure , the resonant frequencies of the transmitter and the receiver coils were 1.9 MHz and 2.0 MHz, respectively. According to $L = \frac{1}{(2\pi f)^2 C}$, the self-inductance of the transmitter and the receiver coils can be calculated. The values of the self-inductance of the coils are shown in Table 6.

	Measured Self-inductance from resonant circuit (μH)	Calculated Self-inductance (μH)	Percent Difference (%)
Transmitter coil	3.52	4.07	13.5
Receiver coil	3.50	4.07	14.0

Table 6: Self-inductance values extracted from parallel resonant circuit

Comparison between the data from Tables 3, 4, and 5 shows that there is a gap greater than 10% between the measured and calculated values when frequency is higher than 1 kHz. The values in Table 6 were extracted from the frequency response of the resonant circuit. The circuit was built on a breadboard. The breadboard might affect the performance of the circuit. As a result, the difference between measured and calculated values in the above tables is reasonable, since the value of calculated inductance is frequency independent and the measured values of the self-inductance decrease with increasing the operating frequency. To obtain a more accurate result at the operating frequency of 1.6 MHz, a network analyzer is recommended.

3.2 Implementing the Highly Coupled Inductive Link

The implementation of the highly coupled inductive link is based on the coils characterized in the previous section. First, the implementation of the transmitter begins with the calculation of the component values of class E power amplifier according to the methodology described in Section 2.4. The values of the choke inductor, the parallel capacitor, and the series capacitor are listed in Table 7 below.

Component name	Value
Chock inductor, L_{chock}	33 μH
Parallel capacitor, C_p	12 nF
Series capacitor, C_t	3.3 nF

Table 7: Calculated values of the components in the transmitter

Second, the shunt capacitor and the filter capacitor in the receiver need to be determined. The value of the filter capacitor C_f can be calculated according to the voltage rise time required by the stimulator unit described in [21]. The values of both components, C_r and C_f , are presented in Table 8.

Component name	Value
Filter capacitor, C_f	15 nF
Shunt capacitor, C_t	1.2 nF

Table 8: Calculated values of component in the receiver

3.3 Highly Coupled Inductive Link Testing

3.3.1 DC Output Voltage with Various Load Resistance

The measurement of the DC output voltage with various load resistances was based on a coil separation of 1.8 cm with an axial misalignment of 0° and an angular misalignment of 0° . The values of the resistive load varied from 100 Ω to 3.3 k Ω . The measured and calculated results are present on Figure 8.

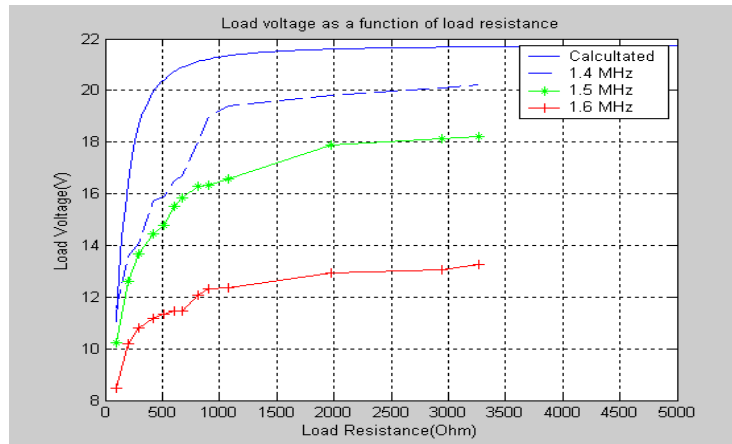


Figure 11: Measured and calculated values of the highly transcutaneous inductive link with various load resistances.

Figure 1 depicts the difference between the measured maximum and minimum load voltages, which is minimized when the operating frequency is 1.6 MHz. However, the difference between the calculated (ideal case) and measured load voltages is maximized at the same frequency. It is observed that the maximum variation between the measured maximum and minimum load voltages occurs at 1.4 MHz. To optimize the transcutaneous inductive link, 1.5 MHz is chosen as the operating frequency for the link, instead of 1.6 MHz, which was discussed in Section 2.5.

3.3.2 Coil Tolerance

All measured and calculated results presented in this section were based on a DC power supply of 9 V in the transmitter, with a 1 k Ω load in the receiver. The operating frequency of the transcutaneous inductive link was 1.5 MHz. The voltage drop across two Schottky diodes (about 0.8 V) of the full-wave bridge in the receiver was also subtracted from the model.

I. Separation Tolerance

The transmitter and the receiver coils in the highly inductive link operate at separation range of 5 – 25mm. Both calculated and measured values are plotted in Figure 12.

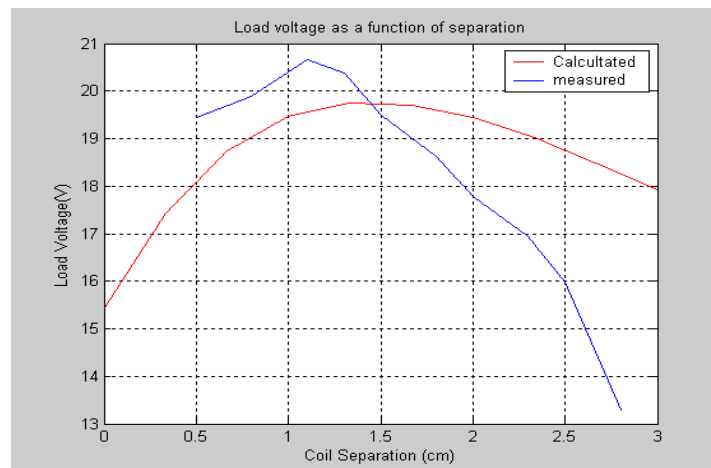


Figure 12: Comparison between calculated and measured coil separation tolerances in the highly coupled transcutaneous inductive link

The maximum measured and calculated values were observed when the coil separation was about 1.5 cm. The variation of measured and modeled values was greater than 10%. However, the minimum measured value was 16 V which was within the range of desired DC load voltage (10 V – 20 V).

Angular tolerance

The measurement of the angular tolerance was based on the coil separation of the transmitter and the receiver coils of 1.5 cm. The range of the angular misalignment was between 0° and 20°. Measured and calculated results are depicted on Figure 13.

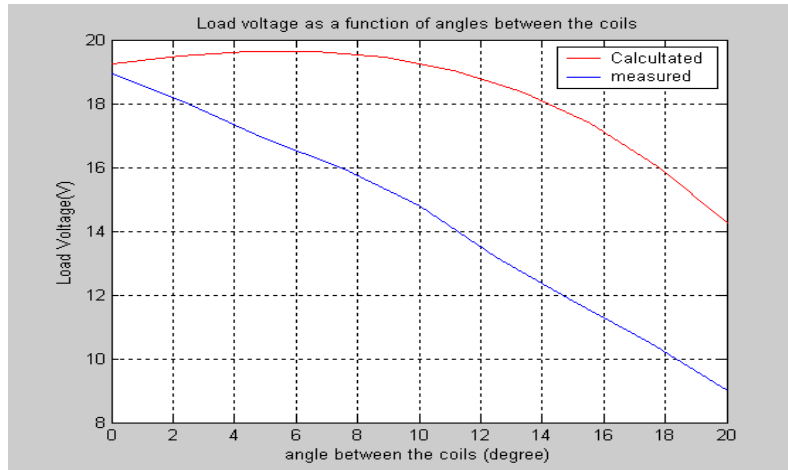


Figure 13: Comparison of calculated and measured angular misalignment tolerance in the highly coupled transcutaneous inductive link.

The slope of the measured values is much higher than the slope of the calculated values. However, the measured value at 18° is still within the desired DC load voltage (10 V – 20 V).

Axial misalignment tolerance

The measurement of the axial misalignment tolerance was based on a load resistance of 200Ω and 1.5 cm separation between the transmitter coil and the receiver coil. The range of the axial misalignment was between 0 and 1cm. The measured and calculated results are plotted on Figure 3.5, which shows that the difference between the measured and the modeled values of axial misalignment is within 12%.

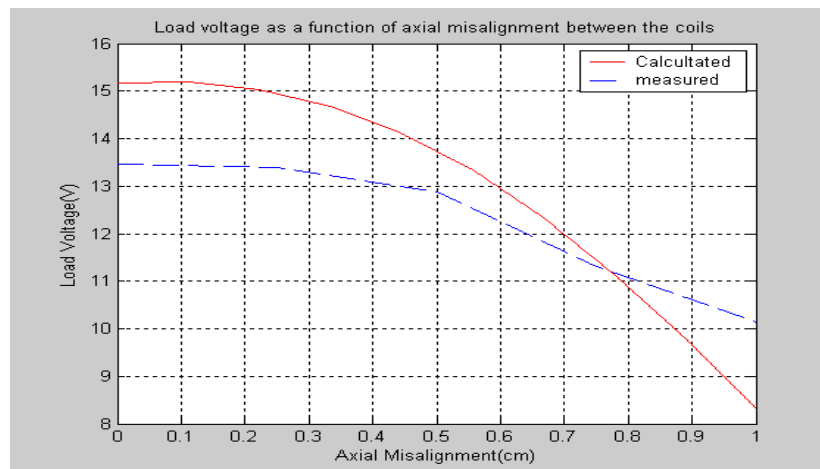


Figure 14: Comparison of the calculated and measured axial misalignment tolerance in the highly coupled transcutaneous inductive link

Power Transfer Efficiency

One may be interested in the overall power transfer efficiency η of a highly coupled transcutaneous inductive link. Under a typical coupling condition, with a coil separation of 15 mm, and 5 mm of axial misalignment, the overall DC power from the transmitter was delivered to a DC load ranging from 100Ω to 3200Ω , as presented in Figure 14. The overall energy transfer efficiency of the transcutaneous energy transformer is presented in Figure 15.

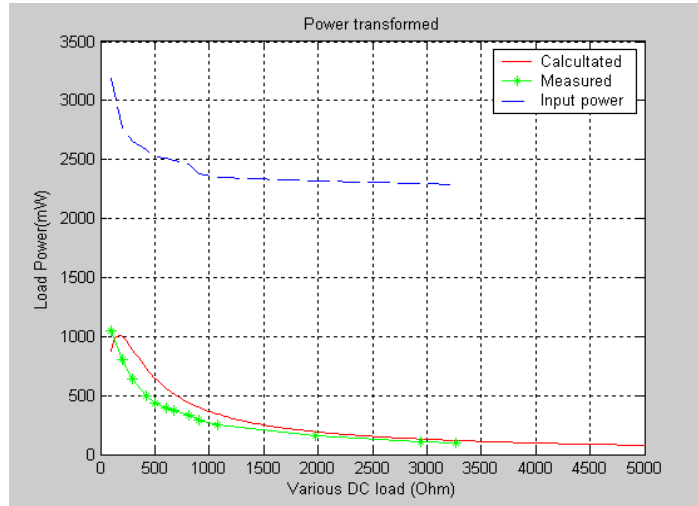


Figure 15: Input power from the transmitter, calculated and measured power to the implanted load

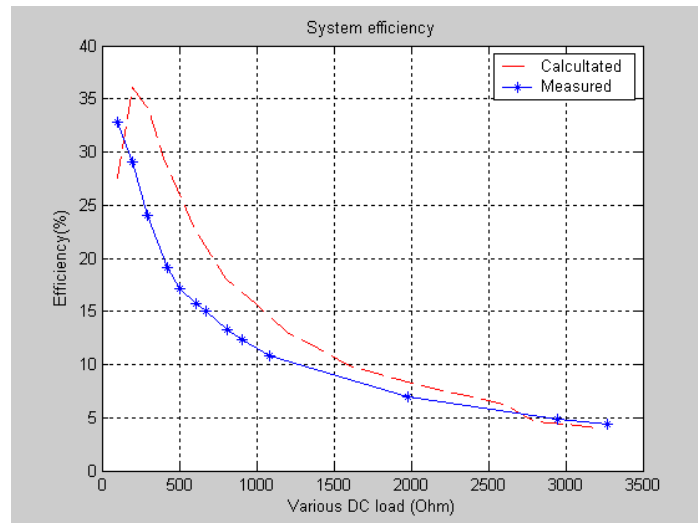


Figure 16: Overall power transfer efficiency of the highly transcutaneous inductive link.

Figure 15 reveals that the overall energy transfer efficiency is maximized at 33% when the DC load, R_{load} , is 100Ω . When R_{load} is 200Ω , the efficiency reaches 28%.

Conclusion

In this report a comprehensive design and testing of a transcutaneous energy transfer system for an implanted system is provided, specifically targeted for gastrointestinal stimulation. The robust modeling of the transcutaneous transformer has been validated through the design, implementation, and testing stages. The measured results for the transformer are in a good agreement with the predicted values.

Bibliography

- [1] J.E. Everhart (Ed). Digestive Diseases in the United States: Epidemiology and Impact. National Institutes of Health Publication No. 94-1447, 1994
- [2] A. M. Bilgutay, R. Wingrove, W. O. Grifen, R. C. Bonnabeau, C.W. Lillehei. Gastro-intestinal pacing: a new concept in the treatment of ileus. *Annals of Surgery*, 158(3), 139-144, 1963.
- [3] J.D. Huizinga. Electrophysiology of human colon motility in health and disease. *Clinics in Gastroenterology*, 15(4), 879-901. 1986.
- [4] S. Grundfest-Bronialowski, A. Moritz, E. Olsen, J. Kasick, L. Ilyes, G. Jacobs, and U. Nose. Electrical control of intestinal reservoirs in a chronic dog model. *ASAIO Transactions*, 34:664-668, 1988.
- [5] E.L. Chaffee and R.E. Light. A method for remote control of electrical stimulation of the nervous system. *Yale J. Biol. Med.*, 7, 1934.
- [6] T. Cameron, G.E. Leob, R.A. Peck, J.H. Schulman, P. Strojnik, and P.R. Troyk. Micro modular implants to provide electrical stimulation of paralyzed muscles and limbs. *IEEE Trans. Biomed. Eng.*, 44(9):781-790, September 1987.
- [7] K. Bruninga, L. Reidy, A. Keshaveersian, et al. The effect of electrical stimulation on colonic transit following spinal cord injury in cats. *Spinal cord*. 36:847-53, 1998.
- [8] S. Grundfest-Broniakowski, A. Moritz, L. Ilyes, et al. voluntary control of an ideal pouch by coordinated electrical stimulation, a pilot study in the dog. *Dis Colon Rectum*. 31:261-7, 1998
- [9] S.F. Hughes, S.M. Scott, MA Pilot, et al. electrically stimulated smooth muscle neosphincter. *Br J Surg*. 82:1321-61, 1996.
- [10] M. P. Mintchev, C. P. Sanmiguel, M. Amaris, K. L. Bowes. Microprocessor controlled movement of solid gastric content using sequential neural electrical stimulation. *Gastroenterology*, 118, 258-263. 2000.
- [11] M. P. Mintchev, C. P. Sanmiguel, S. G. Otto, K. L. Bowes. Microprocessor controlled movement of liquid gastric content using sequential neural electrical stimulation. *Gut*, 43, 607-611, 1998.
- [12] M.P. Mintchev and K.L. Bowes. Computer model of gastric electrical stimulation. *Ann. Biomed. Eng.*, 25:726-730, April 1997.
- [13] W.H. Ko, S.P. Liang, and C.D.F. Fung. Design of radio-frequency powered coils for implant instruments. *Med. & Biol. Eng. & Comput.*, 15:634-640, 1977.
- [14] N. de N. Donaldson and T.A. Perkins. Analysis of resonant coupled coils in the design of radio frequency transcutaneous links. *Med. & Biol. Eng. & Comput.*, 21:612-627, 1983.
- [15] D.C. Galbraith, M. Soma, and R.L. White. A wide-band efficient inductive transdermal power and data link with coupling insensitive gain. *IEEE Trans. Biomed. Eng.*, 34(4):265-275, April 1987.
- [16] O. Soykan, Power sources for implantable medical devices, *Device Technology & Application ELECTRONICS*. 2002.
- [17] M. K. Kazimierzuk, D. Czarkowski. Resonant power converters. Wiley-Interscience Publication, 1995, ISBN 0-471-04706-6.
- [18] Nathan O. Sokal, Alan D. Sokal. Class E – A new class of high-efficiency tuned single-ended switching power amplifiers. *IEEE Journal of solid-state circuits*, vol. SC-10, No. 3, June 1975
- [19] F.H. Raab. Idealized operation of the class E tuned power amplifier. *IEEE Trans. Cir. Sys.*, CAS-24(12):725-735, December 1977.
- [20] J.A. Doherty, G.A. Julien, M.P. Mintchev. Transcutaneous powering of implantable micro-stimulators for functional restoration of impaired gastrointestinal motility. In proceeding of the 25th Annual International Conference of the IEEE EMBS of the IEEE Engineering in Medicine and Biology Society, Cancun, Mexico, 2003, pages 1575-1578, 2003.
- [21] J. Doherty. Implantable, transcutaneously powered neurostimulator system to restore gastrointestinal motility. M.Sc. Thesis, University of Calgary, Calgary, Alberta, Canada, 2005.
- [22] D. Onen. Implantable, transcutaneously powered neurostimulator system to restore gastrointestinal motility. M.Sc. Thesis, University of Calgary, Calgary, Alberta, Canada, 2005.
- [23] C. M. Zierhofer, E. S. Hochmair. Geometric approach for coupling enhancement of magnetically coupled coils. *IEEE Trans. Biom. Eng.*, 43(7):708-714, July, 1996.
- [25] T. Akin. An integrated telemetric multi-channel sieve electrode for nerve regeneration applications. Ph.D. dissertation, University of Michigan, Ann, Arbor, MI, USA, 1994

Authors' Information

Joanna Liu C. Wu – undergraduate Student, Department of Electrical and Computer Engineering, University of Calgary, Calgary, Alberta, Canada T2N1N4; e-mail: joannawu@enel.ucalgary.ca
Major Fields of Scientific Research: Embedded Systems, Electronic Instrumentation

Martin P. Mintchev – Professor, Department of Electrical and Computer Engineering, University of Calgary, Calgary, Alberta, Canada T2N1N4; Fellow, American Institute for Medical and Biological Engineering, Washington, DC, USA; e-mail: mintchev@ucalgary.ca
Major Fields of Scientific Research: Biomedical Instrumentation, Navigation, Information Systems in Medicine

THE PROBLEM OF SCIENTIFIC RESEARCH EFFECTIVENESS

Alexander F. Kurgaev, Alexander V. Palagin

Abstract: *The paper enlightens the following aspects of the problem of scientific research effectiveness: it formulates the main problem of growth of the scientific research efficiency; reveals the most essential attributes of scientific knowledge limiting the area of optimum existence for professional scientists' work efficiency; reveals the hierarchy of problem situations on a way to growth of scientists' work efficiency; defines and grounds the solution of the above-mentioned problem situations. As well the given paper investigates efficiency of the chosen way.*

Keywords: *scientific researches, the canonical form of knowledge, integral knowledge, cognition, knowledge processing system.*

ACM Classification Keywords: *A.0 General Literature; J.4 Social and Behavioral Sciences; M.4 Intelligence Metasynthesis and Knowledge Processing in Intelligent Systems*

Introduction

Development of the world community, a society of each state and all their components is constantly accompanied by uncountable set of problems, the solution of which is unknown, is inadmissibly difficult or poorly effective for practical embodiment. Only the part of problems of civilization's evolution receives social recognition, is formulated in the obvious form and consolidates scientific, organizational, material and financial effort of society to their solution in the form of scientific and technical program (STP).

The program-target method of problems' solution is generally accepted for the world community, the separate states and their components. Numerous generally positive experience of STP formation and performance for solution of many problems is saved up, (Kuhn 1962). However together with significant positive experience of STP formation and performance the certain lacks in *organization*, as well as in actual *carrying out* of scientific research take place.

Lacks of working *organizational* processes consist in some subjectivity when defining priority for scientific research problems and interrelation between them, as well as when managing each STP. These lacks are consequences of absence of the objective control mechanism for essence coordination in different documents (and coordination of their components among themselves) of each STP and, finally, conformity of essence of the received results with the planned ones. The main of the existing lacks of working processes for *carrying out* the research in STP framework is impossibility to use directly already extracted knowledge for statement and solution of the current and new problems in scientific and social evolution.

The specified lacks are inherent in all researches, but they acquire special acuteness for solving problems of society development practice necessarily demanding interdisciplinary research. This research is complicating work of scientists up to almost insuperable barrier in connection with ultrahigh complexity of their specific content. Consequence of these lacks is loss of a part of economic effect from performance of each STP and all their set.

Research tasks of the paper are revealing attributes of the scientific knowledge limiting area of existence for an efficiency optimum of the scientists' professional work; revealing problem situations on a way of scientific research progress and the most essential attributes of information technologies adequate to natural processes of problem solving.

2 The characteristic of an essence for interdisciplinary research

Extracted knowledge of the set of scientific disciplines is represented in the form of corresponding set of hierarchical scientific theories' networks (theories with different level of development, formality, content-richness and reality coverage), elements of which are probably connected through common objects of validity.

Theoretical knowledge functions and develops as a complex system inside disciplinary and interdisciplinary interactions, directed at the solution of actual problems in social science and practice's evolution. It is well known, that evolutionary development of science is periodically interrupted by revolutionary changes in the scheme (*paradigm*) of cognition's activity embodying a progressive system of ideals and norms of research (Kuhn 1962).

Any cognitive process of problem solving has a bidirectional nature – from less to more substantial and from less to more general knowledge. Aspiration to the unity of knowledge at the maximal breadth of reality coverage is caused by the unity of the world, to the display of which in science the given knowledge is directed. Growth of content-richness is caused by incessant penetration of science into more and more deep essence of the reality, defining its more and more adequate model (Popper 1984).

In the most general view disciplinary genesis of science includes two components: from particular theories solving specific problems concerning a part of the discipline's objects – to the fundamental theory fixing the most general knowledge concerning all the area of a discipline, and from the fundamental theory – to particular theories deepening knowledge of the fundamental theory.

Any interdisciplinary research includes: reveal of new relations between terms of original disciplines, establishment of the new system of laws connecting them, and synthesis of the solution pragmatics for new and more complicated tasks. Thus the knowledge of original disciplines may remain constant (an elementary, *linear* case of interdisciplinary interaction) and included entirely (or selectively) in a new hierarchical structure. The knowledge may as well undergo modification, or development due to the processes of exchange in paradigm installations, concepts and methods between different sciences (*nonlinear* interdisciplinary interaction) dictated by interdisciplinary character of a problem. But in all the cases there is a deepening of scientific knowledge and expansion or specification of the area of reality objects studied by initial disciplines.

Nonlinear interdisciplinary interaction combined with problem orientation has already become a conventional norm of global evolution in modern science (Stiopin 2003).

As a result of this process a new discipline, de facto, is formed and the iterative sequence of events repeats infinitely (from some disciplines through interdisciplinary research – to new disciplines with a new object of research) towards the approach to the integral scientific picture of the world.

The real state of affairs in science is characterized by the following: problem situations arising during the infinite process of cognition continuously become complicated and include the increasing area of reality phenomena. Thus the greater number of the problem situations demand interdisciplinary research for their solution.

On the basis of the stated above, it is possible to consider the following as the most essential attributes of interdisciplinary research:

- *Active possession* of the wide range of knowledge;
- *Unification of the form* of knowledge representation for different scientific disciplines with regard to the actual problem's solution;
- *Non-deterministic* creative process of substantial connection of insufficiently constructive scientific knowledge accumulated by diverse scientific disciplines into conceptually unified new knowledge (being the decision of some problem), creation of which is exactly the purpose of the corresponding STP.

3 Statement and general characteristic of the efficiency problem in scientific research

The current state of affairs cannot exist for a long time as it continuously complicates the scientific activity, which leads to constant decrease in efficiency of scientists work and which in its turn causes the reduce of new knowledge importance. Finally, the contribution of science into solution of urgent problems of social evolution decreases, threatening with the contribution's full loss.

On the basis of the stated, the essence of the problem of scientific research efficiency is finally reduced to the following problem of 0 levels:

Achievement of socially significant growth of the scientists' working efficiency by improvement of information technologies, directed at overcoming barriers on the way of scientific progress.

The solution of this problem is exactly the key that opens a door to acceleration of scientific development rates and progress of society as we will not exaggerate excessively by asserting that "*all components of a modern civilization are initially created in scientific laboratories*" and that is why we consider the given problem as the most important and most actual for development of science and a society.

4 Necessity of problem solving in the form of STP

4.1 The characteristic of the problem's complexity

The formulated **0-level** problem is fundamental, its solution depends on the whole complex of conditions (scientific, organizational, material, financial and personnel), among which specific knowledge's creativity of many scientific disciplines is determining.

In the world science there is no standard constructive scientific theory of statement and effective solution of any scientific problems not only concerning interdisciplinary research, but also research within the framework of the any separate unit of science. Moreover, even the obvious statement of this problem is absent. Main causes for such state of affairs consist in its ultrahigh complication and complex character. Remaining the basic subject of the methodology of science, cognition processes and their components are investigated when solving the specific problems in cybernetics and mathematics, the theory of complex systems, linguistics, logic and in all a spectrum of computer sciences: from computer engineering up to the systems of knowledge processing and an artificial intellect.

4.2 An unproductive component of the scientists' work

Still Aristotle was confident, that any doctrine and training are based on some earlier existed knowledge. The appeared or extracted knowledge is necessary for scientists and their professional work just as a pivot was necessary for Archimed to raise the Earth. Presence of volume of the extracted knowledge, sufficient to be a basis for some problem's solution, is the only (except for necessary and sufficient attributes of a learning subject and conditions of its work) and objectively necessary condition of success. In the most abstract form scientific activity is carried out according to the iterative structure (fig. 1), where 1 – extracted knowledge, 2 - the plural subject of science, in particular in structure of pairs: 3 - scientists, 4 - information technologies (IT), 5 - the reality.

This implies a direct dependence of the professional work efficiency of scientists on labor expenditures on *search, reveal and comprehension* of actually necessary fragment of extracted knowledge and *operating* it in the course of research. In its turn, the volume of all these four components of labor expenditures is determined by perfection of the form of representation of the becoming knowledge circulating in society, i.e. by the level of its most essential attributes:

- *Popularity* (a range: from well-known, professional up to indeterminate knowledge);
- *Openness* (a range: from obvious up to the implicit form);
- *Commonality* (it is measured by a variety of forms);

- *Constructivity* (a range: from suitability up to ineligibility for direct use in problem solving). According to a standard conception about duality of the world, knowledge acquires constructivity in two displays: *information* (algorithms, knowledge bases, databases etc.) and *material* (patents, projects of designs etc.).

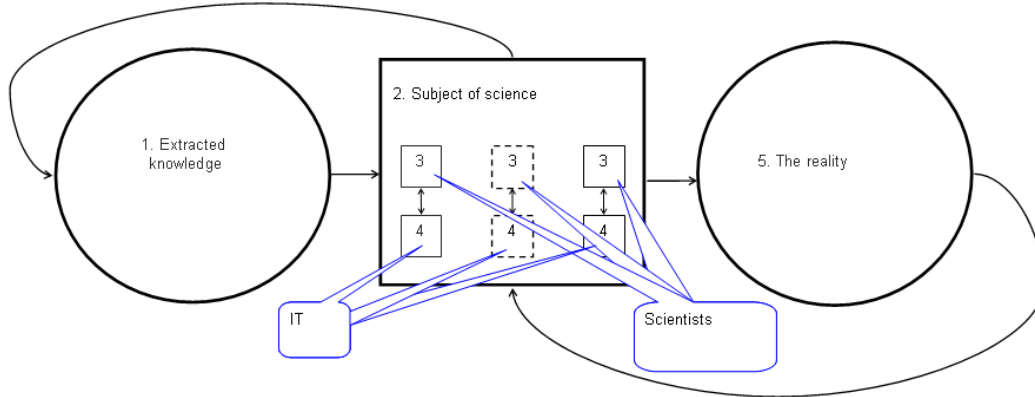
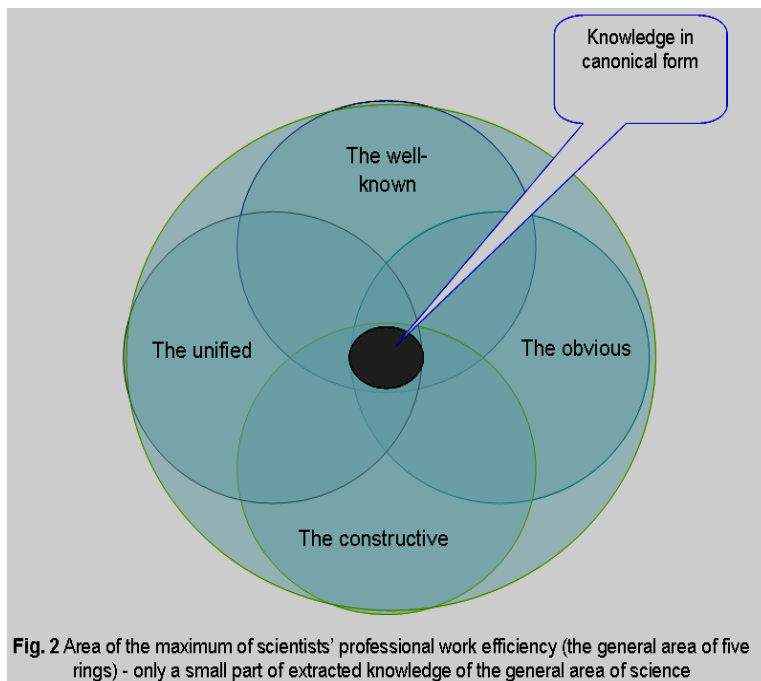


Fig. 1 Iterative structure of scientific activity

Obviously, the global minimum of labor expenditures or the maximum of the scientists' professional work efficiency exists only in a very small discrete subset (concerning cumulative extracted knowledge of all the area of science) of knowledge. It is represented in the single unified form, obvious, constructive and well-known concerning all the science (or well-known regarding disciplines to which the researched problem belongs). The form of knowledge meeting these conditions we shall name *canonical* (fig. 2).



Usually, *optimum conditions are absent* owing to many reasons and mainly some combination of negative attributes of knowledge takes place: *non-openness*, *uncertainty* (general or concerning some discipline), *non-constructivity* and *non-commonality*. In all these cases, instead of direct research of a current problem scientists apply efforts to *search* (with full or partial absence of guarantees of existence), *comprehension* and

transformation of the extracted knowledge from implicit into obvious, from unconstructive into constructive and from different forms into a single unified form with reference to conditions of the current problem.

All labor expenditures on *search*, *comprehension* and *transformation* of extracted knowledge, i.e. on its multiple reprocessing, are unproductive concerning the solution of each of many current problems; their volume reaches the lion's share of cumulative labor expenditures on separate problems' solution, and in general may considerably exceed labor expenditures on primary creativity of extracted knowledge. Moreover, this part of professional work of scientists is not only socially useless, but it even harms, as in each concrete research is carried out ad hoc (i.e. concerning specific conditions of the current problem), continuously increasing entropy of extracted knowledge in the general area of science.

4.3 Alternative ways of problem solving

In all the set of probable solutions of a 0-level problem there are two alternatives: evolutionary - gradual accumulation of positive effects and revolutionary - at the expense of paradigmatic innovations' introduction into the development of information technologies of processing and distributing scientific knowledge in society.

A number of lacks is inherent in the evolutionary way, namely:

- As the cognitive process *is not determined*, and *suitability* of the scientific results' content (in the modern form) *into the control is too low*, each research brings to the common coin box two parts of knowledge – the part that reduces entropy of awareness about reality, and another part that increases it, according to the two components of the scientists' work (productive and unproductive). At the same time the real state of development of a modern civilization does not add optimism for confidence in reduction of the common entropy of scientific knowledge while using available information technologies. Even if reduction takes place, it is quite obvious, that its *rates do not correspond to requirements of time*;
- Now, as a result of an informational "explosion" and continuous expansion of scientific space, *the volume* of extracted scientific *knowledge has already achieved critical point* in ability of scientists to receive actually necessary part of knowledge, its mastering and active use;
- *Indemnification* of an unproductive component of scientist's work at the expense of *extensive development* of science *is unacceptable in essence*!;
- It is allowable to assert, that the present *state of development* of science is close to *crisis*.

Thus the problem situation is obvious and it is unsolvable at the current state of affairs. As the acuteness of a problem situation induces to resolute actions for its solution, the specified lacks and difficulties of evolutionary succession of events compel to concentrate effort on development and realizations of an alternative way, especially as according to the general belief *about no time for delay in science!*

As a whole, the way of paradigmatic innovations is quite natural, it is certified by the indisputable facts of development of both separate scientific disciplines and all science, and it repeatedly justified itself. Its efficiency (even at presence of risk) is generally accepted, provided that a new paradigm has ripened enough within the current one, i.e. its suitability for solving available problems (unsolvable or difficult within the limits of a current paradigm) and an opportunity for realization of its constructive embodiment are grounded (Kuhn 1962).

4.4 The basic idea of the problem solving

It is offered to change cardinally the methods of extraction, representation and use of scientific knowledge, and as consequence - the attitude to knowledge on the part of a society, scientists themselves and finally to science as a whole (Palagin and Kurgaev 2009).

In a modern society there is a conventional belief, that *the scientific knowledge* (irrespective of its structure, level and place, time of creation and the subject-creator) is a *version of raw material* use of which is impossible without spending additional resource for its processing during new knowledge's creativity and/or creation of more or less

useful material or information product. There are quite enough bases for it, which can be proved by world scientific practice, and all scientists submissively accept it as inevitable evil or, on the contrary, as a public permission for imperfection of personal working results.

Obviously, such state of affairs does not satisfy anyone. In interaction of society and science everyone is interested in receiving the greatest contribution to one's development: society from science, and science from society. The exit of this problem situation is only one – meet each other instead of opposition, filling with the constructive contents and accepting for joint realization the well-known thesis: "*Science is a direct productive force of social progress*". It is offered to make a fundamental statement as a new paradigm's foundation.

The statement. *Extracted knowledge in a canonical form – is the most perfect version of a fixed capital of society which is providing development of science and progress of the civilization.*

It has own bases even now, as the common attributes (suitability for duplication, modification, development, improvement of safety and comfort of life and labor, growth of social progress rates, profit formation etc.) are inherent in its components. Regarding the quality of the listed attributes, there is no doubt that knowledge's attributes are essentially better, than attributes of material versions of a fixed capital, and only scientific knowledge may determine and continuously correct civilization's development towards its harmony with nature. In spite of this, it is obvious, that in relation to modernity the suggested statement is false, as the scientific knowledge still does not possess the following most essential attributes of the final commodity and condition for its existence in society:

- Suitability for *direct use*;
- *Measurability* of parameters of quantity and quality;
- *A market price and cost*;
- *Effective norms for the rights and duties* of the manufacturer and consumers.

The essence of the 0-level problem's solution consists in an embodiment of necessary and sufficient conditions for effective functioning of the extracted knowledge as a commodity and also in stimulation of this process. The main means for achievement of these conditions should be the solution of the scientific problems' set concerning creation of a system of new computer information technologies which are adequate to natural problem solving processes in science.

4.5 Hierarchy of problem situations

On a way of solving the 0-level problem appears a group of the 1-level problems the presence of which is proved by the 1-level problem situations confirmed by the facts of a modern state of science:

- *Inadequacy* of modern computer knowledge processing to natural process of scientific research;
- *Difference of the form* of the scientific knowledge used for the constructive problem solving and the form that circulates in an infrastructure of the knowledge distribution in society.

Each of the specified problem situations of the 1st level is complex in its turn and demands carrying out the research of different scientific disciplines for solving the problems of the 2nd level, the presence of which is proved by the problem situations, in particular:

- *Insufficient* constructivity of scientific knowledge, its *ineligibility* for direct use in solving the current and new problems and for practical implementation;
- *Variety* of the existing forms of extracted knowledge (i.e. structures and languages of theories), inherent in different scientific disciplines, in comparison with *the unified* form of conceptually single new knowledge, for creativity of which a corresponding STP is generated;
- *Complexity, variety and uncertainty* of natural creative processes for statement and solution of scientific problems, their versions and components;

- *Inadequacy* of computer information technologies, models and languages of knowledge representation to natural creative processes of statement and solution of scientific problems;
- *Inadequacy* of the working Internet-technology to needs of scientists concerning accuracy and relevance of search of actually necessary scientific knowledge;
- *Production* of new scientific knowledge is carried out by intensive work of creative persons who pay *the expensive price* for it, and *it is sold too cheaply*, almost at the price of the carrier spent for fixing this knowledge;
- *The level* of educational methods and technologies, preparation of experts in the higher school *does not correspond* to the modern state of science.

The stated items prove quite sufficiently the complexity, interdisciplinary character of research of the formulated **0-level problem**.

5 The characteristic of problem solving results

5.1 Expected results

As a result of research directed at the solution of the problem situations listed above, the following should be determined: a conceptually uniform area of extracted knowledge in canonical form and the totality of adequate and mutually coordinated information technologies for effective support of all components of scientific professional work in the sphere of any scientific problems' constructive solution and direct practical implementation of new scientific knowledge.

Analyzing the essence of causes and effects of paradigm innovations' introduction into computer systems' development, it is possible to make certain, based on many facts, that the whole evolution of computer science is connected with reception of precisely these results. At the time of computers' emergence the primary attention was concentrated on questions of practicability of constructive calculations and achievement of record values of quantity indicators. Eventually among the foreground questions appeared issues of adequacy of information-analytical support for all components of natural problem solving process in relation to scientific and practical problems. Nowadays the primary attention is focused on realizations of knowledge processing systems represented by various formal models with use of modern mathematical methods and architectural decisions, in particular, with hardware support of these methods.

5.2 The characteristic of the results' efficiency

Due to lending a combination of the most essential creative attributes to the extracted knowledge, under conditions of their overall effective support by means of information technologies and rules of law, scientific knowledge will acquire the abovementioned but absent now attributes of a final commodity:

- Suitability for *direct use*;
- *Measurability* of parameters of quantity and quality;
- *A market price and cost*.

Efficiency of the solution for the abovementioned problem situations is defined by the sum of effects (different quality as a whole) from purchase of these and other attributes.

5.2.1 The effect from direct use of the extracted knowledge

This effect is formed due to the change in structure (fig. 3) of the scientists' professional work in new (II) information technology in comparison with traditional (I), where labor inputs on: 1 - search, 2 - comprehension and transformation of the extracted knowledge in an canonical form; 3 - creativity of new knowledge (operation

with knowledge, theoretical and empirical knowledge, examination of hypotheses and test of results); 4 - embodiment in the final information product.

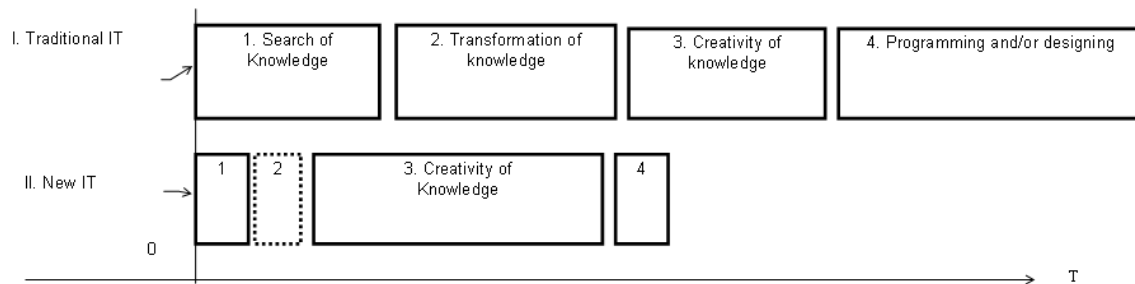


Fig. 3 Comparison of structure of scientists' professional labor inputs in two information technologies, where T – time

In new information technology:

- Labor inputs 1 for search of actually necessary knowledge are essentially smaller than in traditional informational technology, due to restriction of search space by knowledge in a canonical form;
- Labor inputs 2 are optional (any benefit is possible only from their part connected to the knowledge comprehension, though, mainly we are not interested in some artifact's functioning, if only it is known which problem it solves and also norms of its use);
- Labor inputs 4 are essentially reduced due to the use of technology opportunities in operating information in the form of knowledge.

Granting scientists an opportunity to use knowledge directly in a canonical form creates the *base* that will allow scientists either to find time for the new problem solving, or to concentrate all their creative abilities and efforts on improvement (validity, deepening and generalization) of the new knowledge being the constructive solution of certain actual problem. That is, the new opportunity creates necessary and sufficient conditions for essential *growth of the scientists' professional work efficiency, rates and quality* of scientific development.

5.2.2 Effects of the knowledge parameters' measurability – such as quantity and quality

Quality of the extracted knowledge acquired as a result of any scientific research, is exhaustively determined in four-dimensional space of the most essential attributes:

- *A problem*, solution of which is a new knowledge;
- *The content* of knowledge;
- *The form* of knowledge;
- *A fragment of the reality* to which the knowledge is distributed.

Specific characteristics are inherent in each of these attributes:

- *The problem* is determined by a closed logic formula (or its natural language equivalent) validity of which is a consequence of scientific research, and also by a place among other problems of science (or its separate discipline) in the form of structure of connections between them;
- *The contents of knowledge* is determined by a cortege of $\langle A, KB, K, X, C \rangle$ sets (where *A* - axioms, *KB* - basic concepts, *K* - derivative concepts, *X* - variables, *C* - constants) and *structure S* built on their generators;
- *The form of knowledge* is determined by volume (e.g. in quantity of definitions, formulas, text's or code's lines etc.) and some set of quality indicators (in particular, productivity of task solution, volume of testing, tasks' examples etc.);

- *The fragment of the reality* – is a cortege of sets of objects or phenomena, to which knowledge is distributed, i.e. domains of X – variables, and C – constants .

For example, on the basis of the logic formulas being the statement for different problems, it is possible to define some set of relations between them, in particular, the relation of following, and on the basis of structure of some problem's connections with other problems – their affinity to *the base* or *periphery* (to a special, individual branch) of corresponding discipline and other problems' dependence on it.

Only for the canonical form of extracted knowledge there is an opportunity to measure indicators of quantity and quality of scientific results and, accordingly, *assess objectively, compare and supervise* scientific research results. In particular, due to this it becomes possible to measure *the certain researches' level of fundamentality*, completely *exclude* attempts of bureaucratic *dichotomy of science* (for example, its division into the fundamental and applied) and criteria of research *results' dichotomy into* obvious or implicit, constructive or unconstructive acquire an obvious form.

5.2.3 Effects of adequacy

Effects of *adequacy* of information technology to natural problem solving processes consist in comfort improvement in the scientists' professional work at the expense of granting qualitatively new opportunities for individual use:

- Direct operating with knowledge;
- Supports of intellectually difficult processes of theoretical and empirical cognition, transformation of implicit knowledge into obvious, etc.;
- Establishments of mutual understanding, partner interaction with a computer directed at problem solving.

In its turn, a new quality of comfort comes back to scientific development as an additional (related to fig.3) decrease in the scientists' labor inputs exactly into the creative component, as a more complete display of the deepest components of scientists' personality intelligence concerning *quality perfection* of problem solving results, and also as a growth of *appeal* and *prestige* of scientific work in society.

Due to structural change in the creative component of scientists' work, in new (II) information technology we will obtain essential *social effect* (Kurgaev 2008), in comparison with traditional (I) technology (fig. 4), where 1 - programming and/or designing; 2 - task solving; 3 - knowledge in a canonical form (accumulated at the beginning of the current problem's solution), 4 - the new knowledge acquired during the current problem' solution.

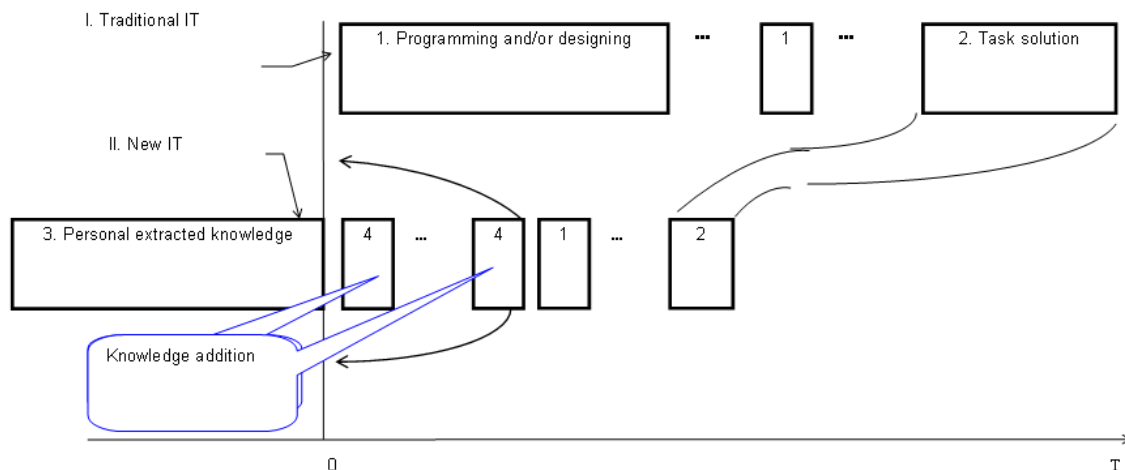


Fig. 4 Comparison of structure of individual professional scientists' work in two information technologies, where T – time

Social effect is generated from two components; the first one consists in change of attitude to evaluation of the researchers' work:

- Information products created by using traditional technologies, do not accept secondary use for task solving, and the tasks' statement differs from the primary one. Therefore these informational products are valued as quickly worn means of labor, and accordingly the labor applied to them is qualified as not valuable and quickly losing its utility;
- The new information technology is based on accumulation of knowledge in a canonical form – knowledge entered and verified is suitable for multiple reuses, irrespective of the specific tasks' statement up to moment of change of reality or our idea about it. The labor applied for knowledge extraction, accumulates and acquires the quality of an intellectual capital, and the character of labor update coincides with the character of update of capital's means.

This component is estimated as the difference between total cost of the past labor applied to the extracted knowledge which is a basis for the current problem's solution, and the cost of the labor applied to the knowledge adjustment and update.

The second component of social effect is defined by saving social labor for problem solving by new technology application.

5.2.4 Effects of attaching a market price and cost to the knowledge

The knowledge received as a result of any of scientific research, acquires the objective price and cost only within market relations between manufacturers and consumers of knowledge and with strict observance of legal relations between them.

Primary cost of *the C-knowledge* in a canonical form can be defined on the basis of different fact sheets. In particular, the assessment will be quite objective in the following range:

$$C_0 \cdot (1 + k) \leq C \leq k \cdot P,$$

where C_0 – the cost price of knowledge, k – average profit rate for information branch, P – the average consumers' profit on the use of knowledge, cost of which is assessed. Market cost is determined by conditions of supply and demands.

Obviously, that *the main effect* from adding a *market price and cost* to knowledge consists in involving science in *direct participation* in economic activity of society with all its positive attributes and consequences, the essence of which leads to more effective (in comparison with modern) use of powerful regulating mechanisms of market relations as *additional stimulus* for scientific development.

5.2.5 Effects of assistance to positive tendencies of social development

The abovementioned effects prove the expediency of the considered way for the specified problem situations' solution and prove it more than sufficiently.

However *the main effects* are seen in realization of the optimum new conditions for evolution of the positive civilization phenomena observed at present. These positive phenomena consist in *development* (in structure of type fig. 1) *population* of individual man-machine intellectual systems (IMMIS) where information technologies play the role of a catalyst, an amplifier of individual intelligence. Due to the possibility of continuous knowledge accumulation (according to fig. 4) new information technologies are means of encouragement for development of human creative abilities, realization of personal ambitions concerning the intellectual capital's accumulation for social status improvement at the expense of it, and also are the guarantor of rights and freedoms for each scientist.

In its turn, the development of IMMIS population capable of knowledge creativity in the form of end product is optimum for existence and development of *creative IMMIS groups* in which necessity of administration is

completely eliminated (bureaucracy is out of the question) and a basis for trust and cooperation is displaced from moral to professional qualities of colleagues. Due to this there appear *new opportunities* for socially significant growth of scientists' professional work efficiency in problem solving, because owing to *creative interaction* in a working team total result of work of each creative team (measured by collective volume of knowledge) is essentially higher than the sum of those results for team members, which they are capable of outside of the team. This additional effect, under condition of efficient protection of the employees' rights for its part, serves as a cementing stimulus for a creative working team, and its existence – as competitiveness in *the creative society*, which is determined by the total effect of realization for the created non-material product.

The structure of effective knowledge and problems' functioning in society (fig. 5) includes: 1 – extracted knowledge; 2, 3 – an information and material embodiment of knowledge in a canonical form; 4 – current problems of science and society; 5 – problems in the obvious form; 6 – set of structures built of creative IMMIS groups; 7 – creative IMMIS groups; 8 – administrative structure for the managing subjects of society; 9 – managing subjects; 10 – educational structures; 11 – examination of the produced knowledge in novelty, perfection, utility; certification of knowledge, their distribution according to these features and allocation of knowledge in a canonical form; 12 – realization of market relations concerning knowledge; 13 – examination of problems in novelty, importance, urgency, and certification of problems.

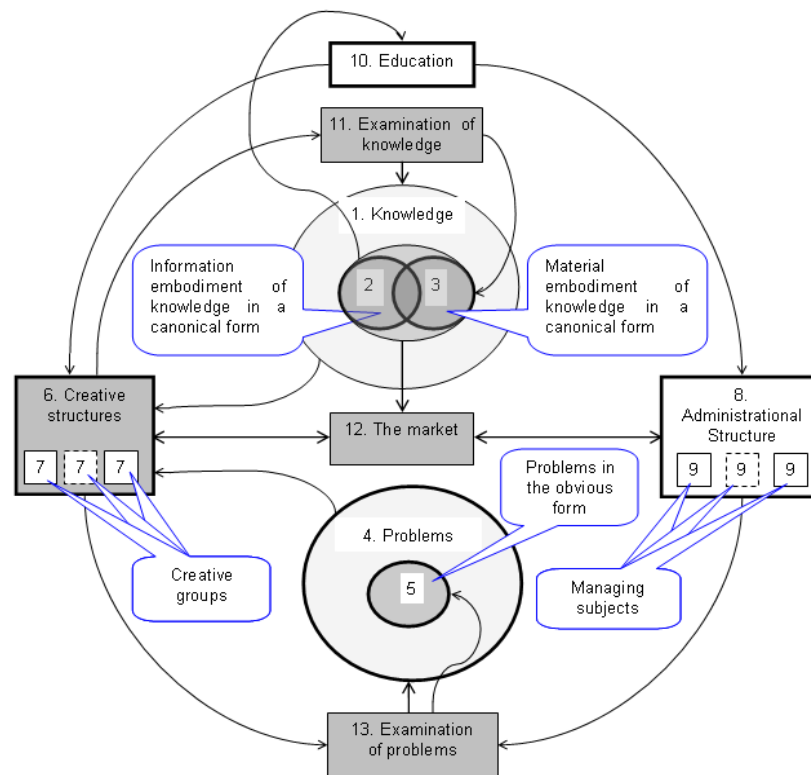


Fig. 5 Structure of information space of the effective process of the knowledge and problems' functioning in society

At fig. 5 new or essentially updated components of a (modern) information infrastructure for spread of knowledge are selected with blackout. The presented structure shows the interaction of its components which due to mutually coordinated combination of positive effects of several feedback contours creates optimum conditions for stimulating informational development of all society's components – science, education and manufacture (Palagin and Kurgaev 2009).

6 Summary and Concluding Remarks

It is proved, that:

- The area of a maximum of scientists work efficiency is limited by extracted knowledge in a canonical form, i.e. obvious, constructive and presented in the unified form;
- Paradigm innovations are expedient for development of information technologies of processing and distribution of scientific knowledge in society.

It is offered to accept for implementation the new attitude to scientific knowledge (as to *the most perfect version of a fixed capital of society*) by providing the knowledge with the most essential attributes of the final commodity which are absent at present and creating the most favorable conditions for its existence and development in scientific and public practice.

It is proved, that efficiency of results for creation of new information technologies' system is defined by the sum of effects, in particular:

- *Unproductive labor expenditures* of scientists are extremely reduced due to *the direct use* of extracted knowledge in a canonical form;
- Only the canonical form of knowledge enables objective *assessment* (in particular, in money equivalent), *comparison and supervision of* scientific research results;
- *Comfort* of scientists' work essentially improves due to use of the information technologies *adequate* to natural creative processes in problem solving;
- *Quality* of problem solving results *will be improved* and *appeal and prestige* of scientific job in society grows;
- The extracted knowledge acquires attributes of *the intellectual capital* owing to the realization of functions of *knowledge accumulation* in a canonical form;
- With the receipt of a *market price* and *cost* by knowledge, science becomes a *direct participant* of the economic activities of society, which serves as an additional stimulus for scientific development;
- The updated information infrastructure of knowledge functioning in society technologically provides productive interaction of all its components, which create the most favorable conditions for progress of both the science and a creative society.

Bibliography

- Kuhn T.S (1962) The Structure of Scientific Revolutions, Chicago
- Kurgaev A (2008) Problem orientation of computer systems architecture. Stal, Kiev
- Palagin A. and Kurgaev A (2009) Interdisciplinary scientific research: optimization of system-information support. Visnik. *National Academy of Sciences of Ukraine*. 3, pp. 14-25.
- Popper K. R (1984) Evolutionary Epistemology. In: Pollard J. W (ed) Evolutionary Theory: Paths into the Future, John Wiley & Sons, Chichester and New York, ch. 10, pp. 239-255.
- Stiopin V. S (2003) Theoretical knowledge. Progress-Tradiciya, Moscow

Authors' Information



Alexander F. Kurgaev - Leading Researcher, Doctor of Technical Science, Ukraine, Kiev, 03187, Akademika Glushkova ave., 40, Institute of Cybernetics V.M. Glushkov National Academy of Sciences of Ukraine, E-mail: afkurgaev@ukr.net



Alexander V. Palagin – Prof., Member of National Academy of Science of Ukraine, Deputy Director Ukraine, Kiev, 03187, Akademika Glushkova ave., 40, Institute of Cybernetics V.M. Glushkov National Academy of Sciences of Ukraine, E-mail: palagin_a@ukr.net

TABLE OF CONTENT

On Structural Recognition with Logic and Discrete Analysis

Levon Aslanyan, Hasmik Sahakyan..... 3

Representing Tree Structures by Natural Numbers

Carmen Luengo, Luis Fernández, Fernando Arroyo..... 10

Mathematical Model of the Cloud for RAY Tracing

Andrii Ostroushko, Nataliya Bilous, Andrii Bugriy, Yaroslav Chagovets..... 18

The Algorithm Based on Metric Regularities

Maria Dedovets, Oleg Senko 27

Adaptive Coding Scheme for Rapidly Changing Communication Channels

Gurgen Khachatryan 31

A Mamdani-type Fuzzy Inference System to Automatically Assess Dijkstra's Algorithm Simulation

Gloria Sánchez-Torrubia, Carmen Torres-Blanc..... 35

A Survey of Nonparametric Tests for the Statistical Analysis of Evolutionary Computational Experiments

Rafael Lahoz-Beltra, Carlos Perales-Gravan..... 49

Decreasing Volume of Face Images Database and Efficient Face Detection Algorithm

Grigor A. Poghosyan and Hakob G. Sarukhanyan..... 62

Modeling of Transcutaneous Energy Transfer System for an Implantable Gastrointestinal Stimulation Device

Joanna Liu C. Wu, Martin P. Mintchev..... 69

The Problem of Scientific Research Effectiveness

Alexander F. Kurgaev, Alexander V. Palagin 88

Table of content 100